พฤติกรรมของโครงสร้างอุโมงค์หน้าตัดกลมเนื่องจากอิทธิพลของวัสดุยึดจับชิ้นส่วนอุโมงค์

นายธนันท์ ชุบอุปการ

INFLUENCE OF SEGMENTAL JOINTS ON TUNNEL LINING BEHAVIOR

Mr. Tanan Chub-uppakarn

Thesis Title   Influence of Segmental Joints on Tunnel Lining Behavior

By   Mr. Tanan Chub-uppakarn

Field of Study   Civil Engineering

Thesis Advisor   Associate Professor Supot Teachavorasinskun, D.Eng.

Accepted by the Faculty of Engineering, Chulalongkorn University in Partial Fulfillment of the Requirements for the Doctoral Degree

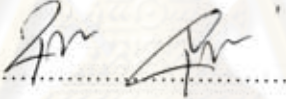.. Dean of the Faculty of Engineering

(Associate Professor Boonsom Lerdhirunwong, Dr.Ing.)

THESIS COMMITTEE

.... Chairman

(Associate Professor Boonchai Ukritchon, Sc.D.)

.... Thesis Advisor

(Associate Professor Supot Teachavorasinskun, D.Eng.)

.... Examiner

(Assistant Professor Suched Likitlersuang, D.Phi.)
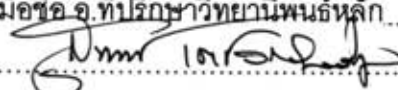
.... External Examiner

(Assistant Professor Siam Yimsiri, Ph.D.)

.... External Examiner

(Pipat Thongchim, Ph.D.)

ธนันท์ ชุบอุปการ :พฤติกรรมของโครงสร้างอุโมงค์หน้าตัดกลมเนื่องจากอิทธิพลของวัสดุ
ยึดจับชิ้นส่วนอุโมงค์. (Influence of Segmental Joints on Tunnel Lining Behavior)
อ.ที่ปรึกษาวิทยานิพนธ์หลัก : รศ. ดร.สุพจน์ เตชวรสินสกุล, 140 หน้า.

การดำเนินงานก่อสร้างโครงสร้างใต้ดิน จำเป็นต้องกำหนดมาตรฐานการก่อสร้างและ
ระบบความปลอดภัยไว้ในระดับสูง ในหลายโครงการจึงมีการนำหัวเจาะอุโมงค์มาใช้ในการ
ก่อสร้าง เพื่อช่วยลดระยะเวลาในการก่อสร้างและช่วยลดจำนวนค้ำยัน ส่งผลให้ลดอุบัติเหตุในการ
ก่อสร้าง แต่ด้วยข้อจำกัดทางด้านพื้นที่ระว่างการก่อสร้าง ทำให้ต้องใช้สลักเกลียวในการยึดดาด
อุโมงค์เข้าด้วยกัน วิธีการนี้ทำให้รอยต่อของดาดอุโมงค์กลายเป็นจุดวิกฤตของโครงสร้าง
การศึกษาพฤติกรรมของโครงสร้างใต้ดินจึงมีความจำเป็น โดยเฉพาะตำแหน่งที่คาดว่าจะเป็นจุด
วิกฤต เพื่อที่จะลดค่าใช้จ่ายในการก่อสร้างและการซ่อมแซม พฤติกรรมของดาดอุโมงค์ขึ้นกับตัว
แปรหลายตัว เช่น แรงดันดิน รูปร่างชิ้นส่วนโครงสร้าง และความแข็งแรงของวัสดุที่ใช้ในการ
ก่อสร้าง ดังนั้นการศึกษาจะแยกพิจารณาตัวแปรที่ส่งผลกระทบต่อพฤติกรรมของดาดอุโมงค์ ได้แก่
จำนวนรอยต่อในโครงสร้าง เส้นผ่านศูนย์กลางของโครงสร้าง แรงดันดิน และความแข็งแรงของ
รอยต่อดาดอุโมงค์ โดยกำหนดขอบเขตไว้ในช่วงพฤติกรรมอิลาสติก ซึ่งการศึกษาประกอบด้วย 1.
การใช้โปรแกรมไฟ-ไนต์ เอลีเมนต์ ในการทำนายพฤติกรรมของโครงสร้าง 2. การทดสอบรอยต่อ
ของดาดอุโมงค์ในโครงสร้างจริง ที่ดาดอุโมงค์สองชิ้นยึดติดกันด้วยสลักเกลียวเหล็ก ด้วยวิธีการ
ทดสอบแบบแรงกระทำสองจุด 3. การทดสอบแบบจำลองโครงสร้างขนาด 1:40 ด้วยวิธีการ
ทดสอบแบบแรงกระทำสองจุด โดยรูปแบบจำลองโครงสร้างเป็นทั้งแบบสองชิ้นยึดติด และเต็มวง
หน้าตัด ซึ่งผลจากการทดสอบพบว่าความแข็งแรงของรอยต่อยึดดาดอุโมงค์ จำนวนรอยต่อดาด
อุโมงค์ แรงดันดิน และเส้นผ่านศูนย์กลางของโครงสร้าง มีผลกระทบโดยตรงต่อความแข็งแรงของ
โครงสร้างดาดอุโมงค์ ดังนั้นข้อสรุปที่ได้จะนำไปใช้ปรับปรุงแนวทางในการออกแบบอุโมงค์ใต้ดิน

ภาควิชาวิศวกรรมโยธา   ลายมือชื่อนิสิต ธนันท์ ชุบอุปการ
สาขาวิชาวิศวกรรมโยธา   ลายมือชื่อ อ.ที่ปรึกษาวิทยานิพนธ์หลัก
ปีการศึกษา 2551

4871864421   : MAJOR CIVIL ENGINEERING

KEYWORDS: SEGMENTAL LINING / TUNNEL / BENDING MOMENT

TANAN CHUB-UPPAKARN: INFLUENCE OF SEGMENTAL JOINTS ON TUNNEL LINING BEHAVIOR. ADVISOR: ASSOC. PROF. SUPOT TEACHAVORSINSKUN, D. Eng, 140pp.

Underground Construction has to higher standards and regulations for safety designs than others. To reduce construction time and number of supports, tunneling shield could be applied to many underground construction projects especially in soft ground area. Because of limitation of working space, segments lining must be assembled on site by steel bolts. Segmental joints, weak point on lining, will be occurred by this method. Because the lost due to collapse of structure is very high, it is necessary to investigate the capacity and behavior of underground tunnel. However, lining behavior depends on many parameters such as earth pressure, geometry and stiffness of structure. Therefore, this study tries to separately consider individual parameters list like number of segmental joint, diameter of lining, earth pressure and stiffness of segmental joint. In practice, evaluation of the structure capacity should be limited in elastic range to maintain a value of safety factor. In this study is composed of three programs: 1. Numerical method, Finite element, to predict behavior of structure 2. Full-scale testing of two segments which are connected by steel bolts 3. Plastic models are one-fortieth in size of the full-scale structure. The models are composed of full section and half section. Both the full-scale and plastic models are tested by two point load method. The results show stiffness of segmental joint, number of segmental joint, earth pressure and diameter of lining directly effect to rigidity of lining structure. Finally, information is used to develop adaptive design code of underground structure.

Department: Civil Engineering   Student's signature. *Tanan Chub-uppakarn*

Field of study: Civil Engineering   Advisor's signature.

Academic Year: 2008

ACKNOWLEDGEMENT

CONTENTS

LIST OF TABLES

LIST OF FIGURES

CHAPTER I

INTRODUCTION

1.1 Introduction

Metropolitan areas today have very high populations and continue to expand because of their improved amenities, convenient lifestyles and job opportunities. To support these cities, high-rise buildings and public utilities are continuously being built. However, cities with limited space and growing economic activities need to be well planned and managed to provide sufficient infrastructure and services. Hence, once ground areas are fully developed, social problems are difficult to solve and problems are continuously increasing. This is why the development and management of underground space is needed, even though structure costs are more expensive than ground structures. Currently, underground space is utilized to satisfy a number of objectives such as electric power lines, telecommunication networks, water supply systems, sewerage, railways and roadways. However, underground construction projects require higher levels of technology and knowledge than ground construction, thus, increasing construction costs. Due to limited budget, we face many uncertain design parameters and unpredictable construction accidents. Engineers in many fields involved in such construction must gain an understanding of underground tunnel structures, the categories and soil behavior. As a result, many tunnel design lining methods are now being studied. Finally, currently, the main assumptions of tunnel design methods are based on elastic and homogenous materials.

With a large underground space and project objectives, the design method can be divided into two types. The first is the shallow tunnels constructed by a cut and cover method, or thrusting method, at one to five meter depths. This type of tunnel is very close to many design assumptions because the tunnel is pre-cast during manufacturing

and soil-structure interaction of the tunnel is not complicated. The second type are the deep underground tunnels, which are used in mega-projects. The technology for deep tunnel construction is very complex and has been improving very quickly to ensure the safety of people around the construction site. Most deep tunnels today are constructed using shield tunneling methods, which reduce construction time and cost, surface damage and accidents. Today, these tunnels are constructed in a variety of sizes and shapes, depending on their use. However, deep tunnel construction has main technical problems because shield tunneling mechanics requires a lot of space for an entire tunnel section. Therefore, tunnel sections are separated into many segments. Each segment lining is connected with long steel bolts in shield tunneling mechanics. It should also be noted that the sizes of shield tunnels are growing. Thus, joint bolts diameter have become larger as have the bolting tools. Construction time has a tendency to be long, which affects soil behavior around tunnels. Therefore, the design for deep tunnels must consider a number of different conditions.

The sequence of the design methods comprises two main parts. First is the construction design method that requires detailed field data. Construction companies record the data for structure behavior to improve construction designs and methods, primarily to reduce costs and increase safety. Still, long-term tunnel behavior data for after construction is currently not enough to analyze and improve design methods. Engineers assumed that effects of segmental joint lining for a whole tunnel structure were negligible because its internal location, which remains stable because of soil pressure. Moreover, the underground tunnel is composed of two tunnel segment layers, pre-cast concrete (primary lining) and post-cast concrete (secondary lining). Most engineers do not adequately consider the effects on segmental joints because these would conflict with design assumptions. The results are stiff segment joints because of incorrect calculation (Yukinori, 2003). Fortunately, serious tunnel structure problems do not occur. Up till now, some design methods try to consider this parameter problem but still without a successful conclusion.

Although, predictions of tunnel and soil behavior are difficult to perform, solving each parameter is possible. Therefore, engineers in related fields study the effects of segmental joints on entire tunnel structure sections. With such studies, it is possible to identify the typical types, forms, and reinforcement details of the segmental lining and steel rods in respect to structure behavior. Then, the capacity and performance of such vulnerable structures can be improved and design assumptions can be closer real behavior. To understand structure failure, the behavior of segmental joints of underground structures must first be considered. However, the behavior of the structure is very complicated, and so it is difficult to find an exact behavior solution with a mathematical model. Therefore, the limitations of results must be considered in any case problem by setting assumptions. These methods can provide overestimated solutions. On the other hand, in order to understand the real behavior of tunnel segment connections, an experimental method must be employed to explain the behavior of the structure.

1.2 Purpose

Tunnel segmental joint behavior is dependant on many parameters such as soil properties, soil pressure, properties of the segmental structure and steel bar, rubber gaskets or seals between segments, tunnel segment sizes, steel bar pre-tension force. These properties cause the behavior of a segmental joint of a whole tunnel structure to be more complex and difficult to explain. Therefore, most engineers try to deal to consider each parameter separately. A study on the effects of segmental joints on circular tunnel structure has been conducted, but this study was based on the elastic behavior of sealing cushioning (Zhong, 2006), one other property of segmental joint behavior. Still research that looks at segmental joints as well as the properties of joint material is still very limited. This is why intensive studies in segmental joint behavior of underground structures and designs is so vital. However, it is impossible to find optimal solutions or solutions for segmental joint behavior because the problems are very

complicated. Therefore, the evaluation of the segmental joint capacity of a given structure should be limited in scope such as Liner Static Procedure (LSP) or Nonlinear Static Procedure (NSP). Based on design method and safety specifications, elastic behavior is considered sufficient for analyzing the behavior of segmental joints.. To carry out such evaluations, it is necessary to have accurate knowledge of structures and soil behavior in many conditions.

Studies of structure behavior can conducted following two main approaches: analytical and experimental. One important and popular analytical approach, the finite element method, has been increasingly developed in recent years. Employing this approach provides many advantages such as easy analysis of complicated phenomena as well as expense and time reduction. However, the drawbacks and limitations of the finite element method include potential difficulties in the task of mesh generation and in dealing with bodies undergoing large deformation or crack propagation. Elements of the original mesh may become over-stiff due to conflict among multiple fields, high distortion or cracks segmentation. In addition, finite elements must be determined by researchers who also require an extensive database for good assumptions and equations when employing the finite element method. However, this method cannot provide completely reliable results without verification of results obtained using experimental approach, especially for non-homogenous material structures. This is due to the fact that structures now contain many complex behaviors. Moreover, in Thailand, experimental results are still not sufficient to serve as a database for creating a reliable analytical model. Thus, for Thailand, the experimental approach seems to be more suitable at this time.

1.3 Problem Statement

Investigation reveals that the segmental joints of underground tunnels are effected much more compared to the entire tunnel structure than one ever expected. The vulnerability of underground structures and segmental joint structure will be studied to predict behavior and modify design assumptions to be close to real tunnel behavior.

Because of the amount of time, money and labor required to repair tunnel collapse under heavy loads, underground tunnel structures require investigation of capacities and behaviors in resisting structural failure. Most popular underground tunnel structures are circular because this homogenous shape is assumed to offer high stability and strong structure while requiring the cheapest construction equipment and cost. These tunnels are constructed on soft deposit to stiff deposit clay at depths of 5 to 20 meters. In the event of underground earth pressure, the structures will respond to the surrounding soil in two ways: one, they will move with the soil or two, the clay will resist of the structure because of inertia interaction. This movement of the structures creates moment, shear and torsion of an unstable structure. If the moment, shear and torsion resistance under load is above the expected structure material capacity, the structure will change some properties to non-ductile or collapse or change its original shape when that material is elastic. Tunnel shape is mainly affected by the stiffness of segmental joint structures because these and the holes for steel bolts located on each segment are not strong enough when compared to the main segments of a tunnel structure. These behaviors are difficult to analyze with analytical methods, so the response of these segmental joint structures during underground loading is a requirement for analysis of behaviors.

1.4 Objectives

The uncertain real behavior of segmental joints that affect a whole tunnel structure under surrounding soil pressure is a problem in analysis and the modification of design assumptions of underground tunnel structures. As the problem is very complicated, this is difficult to evaluate. Because assumptions conflict with real states and drawbacks in the analytical method, the most popular method for solving highly complex problems is a combination of experimental and finite elements.

The main objective of this research is to investigate the segmental joint behavior of circular underground tunnel structures, which are generally used in Thailand, by employing an experimental and analytical approach. This includes the evaluation of the relationship between force-displacement behavior and different soil densities and moment-transfer capacity. Finally, this research focuses on investigating the performance of a simple numerical method in predicting the behavior of structure models through a comparison of results with analytical models from other research and experimental results.

1.5 Scope

This study focuses on the evaluation of segmental joint behavior of circular underground tunnel structures typically used for electric power lines, telecommunication networks, water supply systems, sewerage, railways, and roadways. To demonstrate the essential factor of segmental joints that affect whole tunnel behavior under surrounding soil pressure, many different sized tunnels models and segmental joint inertias were selected and tested. In addition, replica external force was limited to the vertical direction. The structural performance was evaluated on the basis of moment transfer capacity against deformation of the underground tunnel structures. The vulnerability of underground tunnel structure models was conducted by experimental testing and an analytical method. Furthermore, development of moment transfer in segmental joints was studied in detail. Finally, experimental results were compared with predictions based on analytical methods for simple behavior and adapted to the design process.

To properly determine the effective bending rigidity ratio of jointed, shield-driven tunnels for both tunnel design and numerical modeling purposes, especially for tunnels constructed in soft ground, further studies should be carried out. Thus, the objectives of this study are as follows: (i) to propose a field-observed, long-term earth pressure distribution pattern developed around shallow tunnels constructed in soft clays; (ii) to

develop a technique to estimate the effective bending rigidity of an equivalent continuous tunnel lining based on a matching scheme with the internal force of a jointed segmental tunnel predicted by the analytical solution; in this model, the effects of joint stiffness, number of joints, and tunnel geometry on the internal force of a circular jointed segmental tunnel lining can be considered; (iii) to propose simplified design equations for the estimation of the effective bending rigidity ratio (η); and (iv) to validate the proposed model by comparing the result with those from the model tunnel tests.

CHAPTER II

LITERATURE REVIEW

2.1 Primary information to analyze and tunnel design

Because of the restrictions in developing infrastructure and utilities in densely populated areas, underground tunnels are a good solution, especially for mega-cities. However, tunnel construction is difficult to set up because most construction sites are located in congested areas and have an impact on the environment, people and buildings. In additional, a high budget will be required. Hence, giant tunnel projects must be considered as a final solution to urban problems, but before undertaking such projects, many factors must be considered.

Tunnel design comes first. Engineers must first study soil behavior to determine the optimal structure. However, this is difficult because of uncertain factors such as soil behavior and soil-structure interaction. Therefore, the designer should increase safety factors for the structure, which will increase project budgets even further. To reduce safety factors while optimizing structure design, it is necessary to understand tunnel construction in detail.

Peck (1969) stated that a liner is said to be flexible if it interacts with the surrounding ground in such a way that the pressure distribution on the liner and the corresponding deflected shape results in negligible bending moments at all points in the lining, and a liner is said to be rigid if it deflects insignificantly under the loads imposed by the ground with very little ground-structure interaction. Whether a liner is flexible or rigid depends on the relative stiffness between ground and liner and a tunnel diameter. For example, a liner may be said to be flexible with a stiff surrounding ground and a large diameter, but the same liner may be said to be rigid with a soft surrounding ground and a small diameter.

Peck et al. (1972) introduced the definition of stiffness ratios, which are the flexibility ratio and the compressibility ratio, for tunnel liners with analytic works by Burns and Richard (1964) and Hoeg (1968).

The flexibility ratio is the flexural stiffness ratio between the ground and the liner with flexural stiffness defined as the resistance of a change in shape under a state of pure shear as show in Figure 2.1. The flexural stiffness of the ground can be obtained by measuring the diametrical change ($\Delta D/D$) under a state of pure shear with a uniform external pressure, P, as shown in Figure 2.1(a). The diametrical strain of the imaginary circle in ground (Figure 2.1(a)) is given by

$$\frac{\Delta D}{D} = \frac{P}{E}(1+\upsilon)$$

(2.1)

and the flexural stiffness of the ground is defined as follows:

$$\frac{P}{\Delta D/D} = \frac{E}{(1+\upsilon)}$$

(2.2)

where D is the diameter of the imaginary circle, E is the Young's modulus of the ground, and υ is the Poission's ratio of the ground.

Under a state of pure shear with a uniform external pressure, P, the diametrical strain of the circular tunnel liner (Figure 2.1(b)) is given by

$$\frac{\Delta D}{D} = \frac{PR^3}{6E_1 I_1}$$

(2.3)

and the flexural stiffness of the liner to consider the plane strain effect is defined as follows:

$$\frac{P}{\Delta D/D} = \frac{6E_1 I_1}{R^3 \left(1 - \upsilon_1^2\right)}$$

(2.4)

where E_1 is the elastic modulus of the liner, I_1 is the moment of inertia of the liner of the cross section per unit length along the tunnel axis of the liner, and R is the radius of the liner. The flexibility ratio (F) is obtained by dividing the flexural stiffness of ground by that of the liner and is defined as follows:

$$F = \frac{\dfrac{E}{\left(1 + \upsilon\right)}}{\dfrac{6E_1 I_1}{R^3 \left(1 - \upsilon_1^2\right)}}$$

(2.5)

The compressibility is the extensional stiffness ratio between the ground and the liner, and the extensional stiffness of the ground and the liner can be obtained by measuring the diametrical change ($\Delta D/D$) for a uniform external pressure, P, as shown in Figure 2.2. The diametrical strain of the imaginary circular tunnel (Figure. 2.2(a)) is given by

$$\frac{\Delta D}{D} = \frac{P}{E}(1 + \upsilon)(1 - 2\upsilon)$$

(2.6)

and the extensional stiffness is defined as follows:

$$\frac{P}{\Delta D/D} = \frac{E}{(1 + \upsilon)(1 - 2\upsilon)}$$

(2.7)

where D is the tunnel diameter, E is the Young's Modulus of the ground, and υ is the Poission's ratio of the ground.

For the uniform external pressure, P, the diametrical strain of the circular tunnel liner (Figure 2.2(b)) is given by

$$\frac{\Delta D}{D} = \frac{PR}{E_1 t}$$

(2.8)

and the extensional stiffness of the liner in plane strain is defined as follows:

$$\frac{P}{\Delta D/D} = \frac{E_1 t}{R\left(1 - \upsilon_1^2\right)}$$

(2.9)

where E_1 is the elastic modulus of the liner and R and t are, respectively, the radius and the thickness of the liner. The compressibility ratio (C) is obtained by dividing the extensional stiffness of ground by that of the liner and is defined as follows:

$$C = \frac{\dfrac{E}{(1+\upsilon)(1-2\upsilon)}}{\dfrac{E_1 t}{R\left(1 - \upsilon_1^2\right)}}$$

(2.10)

For preliminary design, a tunnel liner should be designed safe and stable for the thrust and moment induced by the external load. Because of the interaction between the ground and the liner, the thrust and moment in the liner are affected by the flexibility and compressibility ratios as Burns and Richard (1964) have shown. For example, for a given condition, the measure of measure of moment and thrust in the homogenous liner can be theoretically obtained as follows:

$$\text{Moment } (M) = \frac{PR^2}{2}\left\{(1 + K_0)\left[\frac{(1 - 2\upsilon)C}{6F}\right][1 - L_n]\right\}$$

(2.11)

$$\text{Thrust } (T) = \frac{PR^2}{2}\left\{(1+K_0)[1-L_n]+(1-K_0)[1+J_n]\cos 2\theta\right\}$$ (2.12)

where K_0 is the earth pressure coefficient at rest, θ is the angle measured in counterclockwise from horizontal plane, F is the flexibility ratio and C is the compressibility ratio.

$$L_n = \frac{(1-2\upsilon)(C-1)}{1+(1-2\upsilon)C}$$ (2.13)

$$J_n = \frac{[(1-2\upsilon)(1-C)]F - 0.5(1-2\upsilon)^2 C + 2}{[(3-2\upsilon)+(1-2\upsilon)C]F + 0.5(5-6\upsilon)(1-2\upsilon)C + (6-8\upsilon)}$$ (2.14)

$$N_n = \frac{[1+(1-2\upsilon)C]F - 0.5(1-2\upsilon)C - 2}{[(3-2\upsilon)+(1-2\upsilon)C]F + 0.5(5-6\upsilon)(1-2\upsilon)C + (6-8\upsilon)}$$ (2.15)

The moment and thrust that are theoretically determined are based on the assumption that the liner has a uniform thickness along the tunnel perimeter and there is no slippage at the contact between the ground and the liner.

For the overview design method, underground tunnel design methods can be divided into main three groups: analytical, numerical, and empirical. The above examples offal under the analytical method. However, because of limitations of knowledge of ground and structure behavior, engineers who establish soil and structure design models must set up assumptions to simplify behavior to make it easier to calculate. In addition, the engineers should consider economic benefits in underground tunnel construction as well. Due to varying assumptions in each design method, every method has some advantages and disadvantages. Therefore, a designer must understand assumptions and basic design concepts for each method before a tunnel should be designed. Figure 2.3 summarizes a model in a systematic approach for evaluating the internal force of underground structures.

2.2 Analytical approach for evaluation of tunnel behavior

Analytical methods for tunnel design involve the analysis of stress and deformation around an opening. They are a favorite design methodology for tunnels with common shapes such as circular because of their high stability and behavior predictability. Most assumptions of material characterization in analytical method are limited to isotropic, homogeneous, and linear elastic material (LEM). Unfortunately, the assumptions are not according to in-situ behavior such as non-homogenous soil and tunnel structure, unpredictable soil behavior, and soil-structure interaction problems, which are major obstacles of underground tunnel structure design. Therefore, analytical methods generally require a set of simple assumptions that may lead to discrepancies between the structural behavior of the model and that of the actual structure. In conceptual tunnel design, essential analytical method steps are: conceptual modeling of the boundary values of the tunnel to describe the problem in terms of geometry, rock mass classification, boundary conditions and in-situ stresses. It is therefore an appropriate technique to analyze problems in terms of stress concentrations and deformations as well as failure and support mechanisms.

In structural design, behavior of surface structure is closely examined and recorded to acquire useful information over the long term. In addition, most loads which are applied to the structure must be accurately forecasted. This information then serves as guidelines for engineers to design economically viable structures. In contrast, underground structure designs such as tunnels are more complicated than top ground structures due to multi-phase soil composition including soil, water and air, which are never constant and will change continually because of circumferential environmental components. This behavior leads into time dependent soil behavior, which is unpredictable. Moreover, the underground structures are constrained by the surrounding medium (soil or rock). This will influence soil-structure interface, leading to unclear behavior. Therefore, the proposed analytical method is to develop underground

structure knowledge and simplify the understanding of the behavior between soil and structure to improve designing process.

The behavior of underground structures such as tunnels requires an understanding of the stress-strain behavior of soil, soil properties and the deformation induced by disturbing the soil because of construction over the long term. This can be analyzed by either:

- Free-field deformation method
- Soil Structure interaction approach

Free-field deformation method

The free-filed deformation method, or uncoupled method, is a simple and effective design tool when ground distortions are small, i.e. the structure is built in very stiff ground conditions, or the structure is flexible relative to its surrounding medium. However, in many cases, especially in soft soils, the method gives overly conservative designs because free-field ground distortions in soft soils are generally large. For example, rectangular box structures in soft soils are typically designed with stiff configurations to resist static loads and are, therefore, less tolerant to racking distortions (Hwang and Lysmer, 1981; TARTS, 1989). Soil structure interaction effects have to be included for the design of such structures (Wang, 1993). A comparison of the free field deformation approach with other methods for design is given in Table 2.1.

In addition, the analytical advancements are aimed at case-specific analyses, while current design guidelines suggest the use of simpler approaches. Most current analytical methodologies are based on two basic assumptions. The first is that excited force and displacement of the circular underground tunnel structure should be elliptical in shape, while the second assumption states that inertia and kinematics interaction effects between the underground structure and the surrounding soil can be ignored. Theoretical arguments and numerical simulations plead for the general validity of the former statement regarding inertia effects, while the importance of kinematics interaction

effects can be checked on a case-by-case basis via the flexibility index (This is not the same as flexibility ratio of Peck (1972)).

$$F = \frac{2E_m\left(1 - v_l^2\right)(D/2)^3}{E_l\left(1 + v_m\right)t_s^3}$$

(2.16)

Where E_m, E_l is Young's modulus of the surrounding soil and the structure material, respectively,

v_m, v_l is Poisson's ratio of the surrounding soil and the structure material respectively

t_s is the thickness of the cross-section

D   is the structure diameter.

The flexibility index is related to the ability of the lining to resist distortion from the ground. Values of the flexibility index, higher than 20, are calculated for most common tunnels and pipelines, indicating that ignoring overall the soil-structure interaction is a sound engineering approach.

Soil-Structure interaction approach

Underground tunnel structure design is unique in several ways. The essential behavior of tunnel design is to resist a circumferential environment caused by soil-structure interaction. One problem is the inability of a tunnel to match the free-field deformation (kinematics interaction), while the second is the effect of an inertia force of the structure on the response of the surrounding soil (inertia interaction) which is analyzed separately. However, for most hollow underground structures such as tunnels, the inertia of the surrounding soil is large relative to the inertia of the structure. Some studies of tunnel behavior for immersed tube tunnels show that a tunnel's response is dominated by the surrounding ground response, and the soil-structure interaction behavior is strongly dominated when the excavation surface is rough. This behavior is not according to the free-filed deformation which is based on the assumption that the tunnel excavation surface is smooth. The focus of underground design in soft ground,

therefore, is on the free-field deformation of the ground and its interaction with the structure. The emphasis on displacement is in stark contrast to the design of surface structures, which focuses on inertial effects of the structure itself. This has led to the development of design methods such as the relative displacement of underground tunnel with original shape that explicitly considers the deformation of the ground and the underground structure together.

The ignored soil structure method is not adequate to solve underground structure problems when the flexibility index is lower than 20. More advanced, analytical methodologies simulate soil-structure interaction effects, by employing the beam-on-elastic foundation approach, Winkler-type soil springs to a tunnel, or modeling the underground structure as a cylindrical shell embedded in an elastic half-space and accounting for slippage at the soil-structure interface. These methods can explain some behavior of soil structure problems, but, at the same time, the methods are very complicated and employ multi-step processes to solve underground structure problems.

However, the Winkler model has several shortcomings; it assumes no interaction through the soil from location to location and no interaction through shear nor volumetric effects, and the model relies on a definition of soil pressure in terms of absolute displacement of the pipe, not displacement of the pipe relative to the soil. Nevertheless, given all uncertainties in modeling pipe-soil interaction, it is an acceptably simple model to permit the consideration of axial effects, longitudinal bending and radial effects associated with overburden pressure or internal pressure. Therefore, this model is mostly used in a preliminary design process.

Because the lengths of underground tunnels are very long when compared with cross sections, the general behavior of the lining may be simulated as a buried structure subject to ground deformations under a two-dimensional plane strain condition. To create more assumptions to simplify and solve the problem, the response of tunnels to underground forces is studied. In designing underground tunnel, one behavior value considered by a designer is the axial force from the jack force of tunneling mechanics. The second value, curvature bending is due to earth pressure and other loading.

Research has shown that curvature bending will affect the structure in the long term. The third value, shear force caused by components of earth pressure, affects loads and soil-structure interaction. However, because of technical construction in limited space in tunnel boring mechanics, segments of tunnel linings are usually made of reinforced concrete. The position of the maximum bending moment, which directly affects maximum stress in the structure, is not the same point for every deformation case. Thus, it is possible to superimpose the corresponding peak strain to obtain the overall maximum stress values.

From the above information, many closed form solutions in underground structure have been researched by analytical methods for specific cases. The study of the analytical method is a good lesson to understand the limitations of solutions used for preliminary experimentation. In addition, the solutions are used to determine estimates of stress and deformations of tunnels in various categories.

Most assumptions of analytical methods consider the plane pressure with a similar magnitude at all locations along the tunnel. The pressure scattering and complex three-dimensional pressure, which can lead to differences in pressure magnitude along the tunnel, are neglected, although soil category as incoherence tends to increase the strains and stresses in the longitudinal direction. However, the generic case of excited pressure at a random location relative to the structure is calculated separately. In soil-structure interaction case, the solutions are developed for both full-slip and no-slip conditions between the tunnel and the lining, although the conditions in real behavior are between full-slip and no-slip. Furthermore, other assumptions of analysis depend on other research cases' data. However, results of analyses based on the assumption should be interpreted in close conclusion.

This method has many advantages and disadvantages. For example, a linear elastic assumption, which is used in most models, states that soil and structure behavior can be independently examined in each factor and then integrated after acquiring the complete results of each behavior. However, the behavior is not likely to be the same linear elastic as the assumption. Results must have some faults when compared to real

behavior, and, thus. This method should include some excess budget in a project plan. Therefore, some designers use a plastic theory concept to develop their design process and approach to real behavior. Because the theory is difficult to use in analytical methods, the model will follow a numerical method.

A. M. Muir Wood, 1975, used a linear elastic analysis to develop a solution for bending moment and displacement of tunnel lining due to compression force, shear force and ground water affect. Because neither the ground around a tunnel behaves in an elastic manner, it is often difficult to determine the magnitude of force that affects a tunnel structure will dominate a design. The initial loading on the tunnel causing the deformation is shown in Figure 2.4. The assumption of external load as shown in Figure2.4 is a simplified load used in the analysis. In addition, the solution of the analysis does not consider the effect on cracks. Therefore, a solution using this method will be conservative and uneconomical. However, this is a convenient first design stage before using a computer method. The main factor in this design method, the bending moment on the lining produced by external forces, tends to affect behavior of both shallow and deep tunnel structures. As the radius of the tunnel increases, the contribution of curvature deformation to axial strain increases.

Various Notations used in the equation are given below:

c' : cohesion (in effective stress terms)

E : Young's modulus for lining (replaced by $E/\left(1-\upsilon_1^2\right)$ where lining is continuous along the tunnel)

E_c : Young's modulus for ground

F : Stress function

F_c : competence factor

G_c : modulus of rigidity of the ground

I : second moment of area of lining per unit length of tunnel

I_c : effective value of I for a jointed lining

I_j : effective values of I at a joint in a lining

K : constant

k : coefficient of permeability for water

K_0 : coefficient of earth pressure at rest

l : (as suffix) longitudinal direction

M : bending moment in lining per unit length of tunnel

N : ratio of horizontal to vertical pressures in the undisturbed ground

m : mode of distortion of lining

n : number of segments in a ring of lining

p : normal pressure between ground and lining

$\bar{p}$: mean value of p

$\hat{p}$: maximum value of $\pm(p-\bar{p})$

p_0 : excess of p on vertical axis over p on horizontal axis

p_v : value of p on vertical axis of tunnel

q : discharge of water per unit area of ground in unit time

r : radius (and as suffix in radial direction)

r_0 : radius to extrados of tunnel lining

R_c : compressibility factor

R_s : stiffness factor

T : shear stress between ground and lining

t : effective thickness of lining

u : redial movement of ground

u_0 : value of u at $r=r_0$

$\hat{u}_0$: maximum value of $\pm u_0$

$u_{0\theta}$: circumferential movement of ground at $r=r_0$

u_w : piezometric pressure at steady state of flow of ground water

Δr_0 : uniform radial deflection of lining

Δp : uniform variation in p

ε : strain in ground

η : ratio of radius of lining centroid to that of extrados

θ : angle (and as suffix in circumferential direction)

λ : coefficient of ground reaction

ν : Poisson's ratio for ground

ν_l : Poisson's ration for lining

σ : ground pressure

$\tau_{r\theta}$: shear stress in ground in r, θ plane

ϕ : Airy stress function

ϕ' : angle of friction (in effective stress terms)

In the simplest analytical method, shear stress between extrados and ground is neglected from consideration. The conservative and simplified solution is calculated by considering a circular lining deformed into the 'elliptical mode in elastic ground (typically under two-dimensional, plane-strain conditions) as Figure2.4. (Schmid, 1926; Engelbreth, 1961). From the assumption, the solution is solved by using the Airy stress function in polar co-ordinates. In the perforated ground, the radial movement of ground around the lining is a function as shown:

$$u = -\frac{2c(1+\nu)}{E_c}\left[r^{-3} - 6(1-\nu)r_0^{-2}r^{-1}\right]\cos 2\theta \tag{2.17}$$

Because of neglect of shear stress around the lining surface, displacement of lining is

$$u_0 = \frac{2cr_0^{-3}}{E_c}(1+\nu)(5-6\nu)\cos 2\theta \qquad \text{or} \qquad u_0 = \hat{u}_0 \cos 2\theta \tag{2.18}$$

where $\pm u_0$ represents the maximum displacements.

On the other hand, because of indefinable relaxation of the initial state of stress in the design method, p_v and $p_v - p_0$ would represent the initial conditions of vertical

and horizontal ground loading, which is maximum pressure and minimum pressure respectively. Taking into account the stiffness of the lining and the loading transmitted to the ground around the extrados, starting from an applied normal loading to the lining

$$p = p_v - \frac{p_0}{2}(1 - \cos 2\theta)$$

(2.19)

Consideration of a circular tunnel seen as a hole being drilled through an elastic solid suggests that the state of stress in the r, θ plane will be intermediate between the intact and the perforated condition, and the loads on the tunnel lining can be derived by considering such an initial value. From displacement and excited load around the lining, maximum bending moment on tunnel structure is responded to by change of curvature around the structure (Morgan, 1961)

$$M_{max} = \pm 3\hat{u}_0 \frac{EI}{\eta^2 r_0^2}$$

(2.20)

On the other hand, the corresponding maximum moment can be applied by the ground loading as

$$\pm \frac{p_0 \eta^2 r_0^2}{6}$$

(2.21)

note: that E should be replaced by $E/(1 - v_l^2)$ for a continuous lining.

The reduction of $\hat{u}_0$ resulting from the stiffness of the lining leads to the following relationship between M_{max} and p_0

$$M_{max} = \pm \frac{p_0 r_0^2 \eta^2 EI(1 + v)(5 - 6v)}{6EI(1 + v)(5 - 6v) + 2\eta^3 r_0^3 E_c}$$

(2.22)

The stiffness ratio, R_s (Muir Wood, 1970) represents the ratio of the stiffness of the tunnel lining (to deformation in the 'elliptical' mode) to that of the surrounding ground. Thus,

$$R_s = \frac{3EI(1+v)(5-6v)}{E_c \eta^3 r_0^3} = \frac{9EI}{\lambda \eta^3 r_0^4}$$

(2.23)

And the reduction in bending moment to be carried by the lining is immediately apparent in relation to its flexibility, since the equation may be written as

$$M_{max} \pm \frac{1}{6} p_0 r_0^2 \eta^2 [R_s /(1+R_s)]$$

(2.24)

Lyons and Reid (1974) provide some typical values for I and E_c.

A second coefficient very important to the design method is the coefficient of ground reaction. This coefficient explains the stiffness of ground around the tunnel with the coefficient is defined as

$$\lambda = \frac{\sigma_r(r = r_0)}{u_0} = \frac{3E_c}{(1+v)(5-6v)r_0}$$

(2.25)

However, studies have suggested that deformation and the bending moment on a structure is directly affected by the shear force between the ground and the lining. Therefore, Muir Wood tried to develop shear force on the surface lining. The theory is not that complicated if an explicit value for ground/lining shear stress is inserted and a means provided for establishing its compatibility with these criteria.

Its maximum frictional force value must not exceed permissible shear stress between a tunnel and surrounding soils. The criterion for stability of the ground, however, must always satisfy the Mohr-Coulomb condition.

$$T < c' + \overline{p} \tan \phi'$$

(2.26)

The related circumferential movement of the ground at $r = r_0$, assumed to be caused by drag as the ring deforms, must not exceed that of the corresponding point on the deformed ring. The introduction of shear stress between ground and lining implies that for $r = r_0$

$$\frac{\hat{u}_0}{2} < \frac{2(1+v)}{E_c}\left(4cr_0^{-3} + Tr_0\right)$$

(2.27)

From the assumption, the solution of displacement should be shown as:

$$u_0 = \frac{2cr_0^{-3}}{E_c}(1+v)\left[(5-6v)+\frac{1}{2c}Tr_0^4(1-v)\right]\cos 2\theta$$

(2.28)

The normal pressure on the extrados of the deformed tunnel may be represented as

$$p = \overline{p} + \frac{\hat{p}}{2}\cos 2\theta c$$

(2.29)

where $\hat{p} = p_0 R_s /(1+R_s)$

$c = \hat{p}/12r_0^{-4}$

And, the coefficient of ground reaction is defined as

$$\lambda = \frac{3(\hat{p}+5T)E_c}{r_0(1+v)[(5-6v)\hat{p}+2(13-15v)T]}$$

(2.30)

where $T < \frac{\hat{p}}{2}(6v-1)/(5-9v)$

In additional, the coefficient important to explain the type of lining and surrounding soil is the compressibility factor, R_c. This factor is defined as the compressibility of the tunnel in relation to that of the surrounding ground, which considers the cylinder of ground displaced by the tunnel.

$$R_c = \frac{r_0 E_c \left(1 - v_1^2\right)}{\eta t E \left(1 + v\right)}$$

(2.31)

In additional, Liu and Hou (1991) proposed an analysis expression to determine the reduction factor based on the assumptions that the mode of deformation of a circular tunnel is elliptical and the surrounding pressure can be expressed as an equation (2.19). Based on the elastic theory, the relationship of maximum bending moment (M_{max}) and the horizontal displacement (Δ_h) of a continuous lining ring can be expressed as

$$\Delta_h = \frac{M_{max} R^2}{3EI}$$

(2.32)

where R is the tunnel calculation radius, defined as the average of outer (R_0) radii. By applying equation (2.32) and the virtual work theory, the bending moment in a segmental tunnel ring composed of uniformly distributed segments can be derived as

$$M_{max} = \frac{3EI\Delta_h}{R^2 (1+b)} = \frac{3\eta EI\Delta_h}{R^2}$$

(2.33)

in which η is the effective bending rigidity ratio and is expressed as

$$\eta = \frac{1}{1+b}$$

(2.34)

where

$$b = \frac{3EI}{RK_\theta} \sum_{i=1}^{m} \cos\theta_i \cos 2\theta_i \qquad \left(0 < \theta_i < \frac{\pi}{2}\right) \qquad (2.35)$$

where EI is the bending rigidity of the tunnel lining per unit length; K_θ is the flexural stiffness of the joints, which is defined as the bending moment per unit length required to develop a unit rotation angle along a joint of the assembled segments; θ_i is the angle measured from the vertical direction around the tunnel of the i*th* joint in the range 0-90; and m is the number of joints in the range of 0-90. Equations (2.34) and (2.35) are usually adopted as the first approximation to determine the effective rigidity ratio for a uniformly distributed segmental lining. However, for most shallow tunnels constructed in soft ground, the earth pressure acting around the tunnel lining cannot be expressed by the equation (2.26).

Even when the problem is treated as an elastic one, in reality, for cohesive ground, it is known that a visco-elastic condition should be considered. The analytical method can calculate a conservative solution of the problem and give upper and lower limits in solution of the problem. This solution is postulated for particular circumstances to check the range of uncertainty in the numerical and experimental methods. It is generally far easier to control the stiffness ratio, R_s of the tunnel lining than it is compressibility factor, R_c. The ratio between stress and strain at acceptable working load limit cannot easily be varied but hinges can be introduced into the lining.

In early studies of ovaling, or racking deformation, Peck (1972), based on earlier work by Burns and Richard (1964) and Hoeg (1968), proposed closed-form solutions in terms of thrusts, bending moments, and displacements under external loading conditions. The response of a tunnel lining is a function of the compressibility and flexibility ratios of the structure, and the in-situ overburden pressure (γ, h) and at-rest coefficient of earth pressure K_0 of the soil. However, compressibility and flexibility ratios

of the structure are introduced by many scientists such as Muir Wood with each parameter has some advantages.

In another example of compressibility and flexibility ratios, the stiffness of a tunnel relative to the surrounding ground is quantified by the compressibility and flexibility ratios (C and F), which are measures of the extensional stiffness and the flexural stiffness resistance to ovaling, respectively, of the medium relative to the lining (Merritt, 1985):

$$C = \frac{E_m\left(1 - v_l^2\right)r}{E_l t\left(1 + v_m\right)\left(1 - 2v_m\right)}$$
(2.36)

$$F = \frac{E_m\left(1 - v_l^2\right)R^3}{6E_l I\left(1 + v_m\right)}$$
(2.37)

where E_m = modulus of elasticity of the medium

$\quad I$ = moment of inertia of the tunnel lining per unit width for circular R

$\quad t$ = radius and thickness of the tunnel lining

These forces and moment are illustrated in Figure 2.5. The relationship between the full-slip lining response coefficient (K_1) and flexibility ratio is shown in Figure2.6. According to various studies, slip at the interface is only possible for tunnels in soft soils or cases of severe seismic loading intensity. For most tunnels, the interface condition is between full-slip and no-slip, so both cases should be investigated for critical lining force and deformations. However, full-slip assumptions under simple shear may cause significant underestimation of the maximum thrust, so it has been recommended that the no-slip assumption of complete soil continuity be made in assessing the lining thrust response (Hoeg, 1968; Schwartz and Einstein, 1980):

$$T_{max} = \pm K_2 \tau_{max} r = \pm K_2 \frac{E_m}{2(1+\nu_m)} r \gamma_{max}$$

(2.38)

where

$$K_2 = 1 + \frac{F\left[(1-2\nu_m)-(1-2\nu_m)C\right]-\frac{1}{2}(1-2\nu_m)^2+2}{F\left[(3-2\nu_m)+(1-2\nu_m)C\right]+C\left[\frac{5}{2}-8\nu_m+6\nu_m{}^2\right]+6-8\nu_m}$$

(2.39)

The normalized lining deflection provides an indication of the importance of the flexibility ratio in lining response, and is defined as (Wang, 1993):

$$\frac{\Delta d_{lining}}{\Delta d_{free-field}} = \frac{2}{3} K_1 F$$

(2.40)

According to this equation and Figure 2.7, a tunnel lining will deform less than the free field when the flexibility ratio is less than one (i.e. stiff lining in soft soil). As the flexibility ratio increases, the lining deflects more than the free field and may reach an upper limit equal to the perforated ground deformations. This condition continues as the flexibility ratio becomes infinitely large (i.e. perfectly flexible lining).

Nowadays, a lining is composed of many concrete segments with each connected to the other by steel bolts. Therefore, segmental joints in a lining are very important to the main structure lining. For the Muir Wood design method, engineers must consider the stiffness at the joints, which are appreciably less than elsewhere and, for abutting joints, the effective will clearly increas as the ratio of hoop stress to bending stress increases. If the second moment of area at the joint is designated as I_j, the corresponding effective value of I for the ring, c, to be used in design equation for determining R_s, may be approximately calculated. For an increased number of equal segments, say n, we may assume as a first approximation a parabolic envelope to bending moment around a segment such that

$$I_e = I_j + \left(\frac{n}{4}\right)^2 I$$

where $I_e > I, n > 4$ (2.41)

and thus, where $I_j << I$ for an expanded and articulating lining of, say, eight segments, $I_e = I/4$. However, to closely examine the real behavior, a computer method will be the next step in the design process because a numerical method can solve more complicated problem than an analytical method.

In most analytical methods used in preliminary design, we assume the absence of the lining, therefore, ignoring tunnel ground interaction. In the free field, the perforated ground would yield a much greater distortion than the non-perforated, sometimes by a factor of two or three. This provides a reasonable distortion criterion for a lining with little stiffness relative to the surrounding soil, while the non-perforated deformation equation will be appropriate when the lining stiffness is equal to that of the medium. A lining with relative stiffness should experience distortions even less than those given by adopting an increase of the compressibility ratio (Wang, 1993).

Furthermore, soil-structure interaction is another method to be considered in underground structure problems. The solution from this method will show structural behavior that is close to real. However, the solution is limited for elastic behavior and a simple shape model such as a circular tunnel. In simple examples, the model will assume the tunnel and soil to be the beam of an elastic foundation approach while pressure loading is assumed to remain steady. Furthermore, the solutions ignore inertial interaction effects. Under load exciting, the cross-section of a tunnel will experience axial bending and shear strains due to free field axial, curvature, and shear deformations. The maximum axial strain is located at the crown and lining spring line. Finally, since both the liner and medium are assumed to be linear elastic, these lining strains and stresses may be superimposed to determine the maximum force on the lining in a structure design. Since pressure in ground is assumed to be static, both extremes must be evaluated. The maximum bending moment acting on a tunnel cross-section can be written as a function of maximum earth pressure.

A conservative estimate of the total axial strain and stress is obtained by combining the strains from the axial and bending forces modified from (Power, 1996):

$$\varepsilon^{ab} = \varepsilon_{max}^{a} + \varepsilon_{max}^{b}$$

(2.42)

Again, these equations are necessary only for structures built in soft ground, as structures in rock or stiff soils can be designed using free-field deformations. It should be further noted that increasing the structural stiffness and the strength capacity of the tunnel may not result in reduced forces; the structure may actually attract more force. Instead, a more flexible configuration with adequate ductile reinforcement or flexible joints may be more efficient (Wang, 1993).

Other expressions of maximum sectional force exist in the literature (Einsrein, 1979; JSCE), with the major differences involving the maximization of forces and displacements with respect to earth pressure. JSCE suggests the bending moment in a segmental joint directly affects a main segment structure. Therefore, stress in a main segmental lining must be added by a multiple factor to increase strength of the segment structure. However, the Einsrein method does not account for the affect of a segmental joint in the lining.

2.3 Numerical approach for evaluation of tunnel behavior

Compared analysis and designs of underground structures are not as extensive as for above ground structures. The study of the behavior of long underground structures, like tunnels, affected by many kinds of pressures is an important engineering problem. This is particularly true for the complex nature of soil-structure interaction and unpredictable and inconstant pressure problems as underground structures may require the use of complicated methods and multi-step procedures. The problems can be solved accurately, economically and under realistic conditions with the aid of numerical methods. The approximate methods for solving systems of complex problems

or partial differential equations have developed significantly and are used increasingly by engineers, physicists and mathematicians. Many methods for obtaining numerical solutions to problems have been well developed and possess much versatility in analyzing complicated phenomena whose behavior is governed by increasingly complex partial differential equations. However, the aforementioned numerical methods can be divided into several classes, which have some limitations in their processes. For example, the Finite Element Method (FEM) is one of the most popular approximate methods for solving problems. The FEM is relatively simple to solve systems of partial differential equations. The drawbacks and limitations of the FEM include potential difficulties in the task of mesh generation and in dealing with bodies undergoing large deformation or crack propagation. Elements of the original mesh may become over-stiff due to conflict among multiple fields, high distortion or segmentation by cracks. In geotechnical engineering problem solving, the use of the FDM requires, in addition to an interior discretization, artificial boundaries for the infinite or semi infinite soil medium and hence, an extensive and uneconomical mesh or extensive special absorbing boundaries. Thus, other methods are used to fix the limitations, such as Boundary Element (BEM) or meshless methods, to find solutions.

Numerical analysis methods for underground structures include lumped mass/stiffness, finite element and finite difference methods. To analyze axial and bending deformation, it is most appropriate to utilize three-dimensional models, as shown in Figure 2.8a. In the lumped mass method, the tunnel is divided into a number of segments (masses/stiffness), which are connected by springs representing the axial, shear, and bending stiffness of the tunnel. The soil reactions are represented by horizontal, vertical and axial springs (Hashash, 1998), and analysis is conducted as an equivalent static analysis, as shown in Figure 2.8b. These spring constants represent the ratio of pressure between the tunnel and the medium. On the other hand, the spring constants represent the reduced displacement of the medium when the tunnel is present. The springs differ from those of a conventional beam analysis on an elastic foundation. Not only must the coefficients be representative of the modulus of the

ground, but the derivation of these constants must consider excited loadingThe ends of the springs are represented by the soil-tunnel interaction. When using these equations to calculate the force and moments for tunnels located at shallow depths, the soil spring resistance values are limited by the depth of cover and lateral passive soil resistance. If a dynamic, time-history analysis is wanted, appropriate damping factors have to be incorporated into the springs and the structure.

In finite difference, or finite element models, the tunnel is discretized spatially, while the surrounding geologic medium is either discretized or represented by soil springs. Computer codes available for these models FLAC^{3D} include (Itasca, 1995), SASSI (Lysmer et al., 1991), FLUSH (Lysmer et al., 1975), ANSYS-III (Oughourlian and powell, 1982), ABAQUS (Hibbitt et al.,. 1999), and others. Two-dimensional and three-dimensional finite elements and finite difference models may be used to analyze the cross section of a bored tunnel or cut-and-cover tunnel. In cases of movement along weak plans in the geologic media shear zones, or bedding planes, joints may potentially cause local stress concentrations and failures in the tunnel; then, analyses using discrete element models may be considered. In these models, the soil rock mass is considered as an assemblage of distinct blocks, which may in turn be modeled as either rigid or deformable as an assemblage of distinct blocks, which may, in turn, be modeled as either rigid or deformable materials, each behaving according to a prescribed constitutive relationship. The relative movements of the blocks along weak planes are modeled using force-displacement relationships in both normal and shear directions (Power, 1996). UDEC (Itasca, 1992) and DDA (Shi, 1989) are two computer codes for this type of analysis.

The ability of numerical analyses to improve closed form solutions lies in the uncertainty of input data. If there is significant uncertainty in the input, refined analyses may not be of much value (St. John and Zahrah, 1987). A similar cautionary remark was made by Kuesel (1969), noting that 'mathematical elaboration of this complex subject does not necessarily lead to increased understanding of its nature', and placees high priority on developing 'a picture of the action of underground structures subjected to

earthquakes, with reasonable bounds on the problem'. Finally, both the analytical approach and the numerical approach lead to the same conclusions to solve specific problems and set assumptions to reduce problem complications. However, as analytical and numerical approaches reduce time and product costs, these methods remain popular.

2.4 Experimental approach for evaluation of tunnel behavior

This study focuses on the effect of lining segmental joints on an entire tunnel structure. In tunnel design, the parameters of ground motion and structure lining details are very important parameters. Segmental joint structure is one parameter of a tunnel that considers deformation and bending moment transfer between segments in the lining. Force response is a useful tool for engineers during design or analysis stages. However, it should not be used if the soil-structure system response is highly non-linear. Current tunnel design philosophy for many civil engineering structures will be explained in next chapter. First, though,, a structure should be designed with adequate strength capacity under static loading conditions. Generally speaking, if the members are to experience little to no damage during a lower level event, the inelastic deformations in the structure members should be kept low.

Reduced-scale structure models, or replica models, are defined as any physical representation of structure or portion of a structure, (ACI Committee 444). A second definition states that a structural model is any structural element or assembly of structural elements built to a reduced scale for testing and for which laws of similitude must be employed to interpret test results. Physical models are used by many researchers studying the behavior of structures in different environments. The models have evolved over the years in various categories, including education, design, research, and product and concept development in commercial companies. In research studies, the models are used when a solution cannot be found for structure behavior by analytical or numerical methods. Structural models can be defined and classified in a

variety of ways such as: Elastic, Indirect, Direct, Strength, Wind effects, Dynamic, Instructional, Research, and Design.

Scaled physical methods involve the study of small physical models of a structure to understand the behavior of its full-scale structure. In general, the size of a physical model is scaled down to the size of several meters in height and 10 meters or more in length. Equivalent materials with sufficiently low strength are used to build a model to ensure that it will fail at a relatively low load that can be applied in the laboratory. Scaled physical methods were a popular design approach between the 1950's and the early 1980's because the analytical methods available at that time were incapable of dealing with the effects of heterogeneity. However, the application of scaled physical models has declined significantly since then due to their high cost and the escalating capability of numerical methods that can handle complex tunnel design problems impressively. In addition, the advantage of a physical model over an analytical model is that it portrays behavior of a complete structure loaded to the collapse stage. Although substantial progress is continually made in computer-based procedures for analysis of structure, we still cannot predict analytically the failure capacity of many three-dimensional structural systems, especially under complex loadings.

In design codes in present time, there are numerous situations in which these code provisions might be applied in practice; in most cases it is where the analytical approach is not fully adequate. Basic doubts may arise in applying existing analytical techniques to new and complex structural forms. Analytical methods are not yet developed to handle the extremely complicated behavior of structures loaded to near-failure or certain other limit-state conditions. This is why modeling is often used by engineers studying the failure of structures. Types of structures suitable for possible structural model studies during the design phase include:

- Shell roof forms of complex configuration and boundary conditions
- Tall structures and other wind-sensitive structures for which wind tunnel modeling is indicated
- New building structural systems involving the interaction of many components

- Complex bridge configurations such as multi-cell pre-stressed concrete box girder highway bridges

- Nuclear reactor vessels and other reinforced and pre-stressed concrete pressure vessels

- Ordinary framed structures subjected to complex loads and load histories such as wind and earthquake forces

- Structural slabs with unusual boundary or loading conditions or with irregular geometry produced by cutouts and thickness changes

- Dams

- Undersea and offshore structures

- Detailing

Although, physical models are a good method to interpret complicated structure behavior, there is a problem with measurement accuracy. Thus, modeling development requires accurate instruments for measurement of strains, displacements and forces. Now the most-used measurements techniques of structural behavior include:

- Photo-elasticity for elastic stress analysis of complex geometries

- Deformeters developed by Beggs, Eney, Gottschalk, and others for introducing deformations into indirect models and then determining influence lines by use of the Muller-Bre-slau principle

- Mechanical and optical strain gages for measurement of surface strain

- Electrical resistance strain gages

- Linear variable differential transformers (LVDT), linear potentiometers, and similar devices for electrical recording of displacement

- Brittle coating, moiré and interference fringe methods, and photo-elastic coating for full-field strain measurements on the surface of a structure or model

- Automated data acquisition systems that use a minicomputer to control and process many channels of data

Furthermore, a successful modeling study is one that is characterized by careful planning of the many diverse steps in the physical modeling process. An experimental study of an engineering structure is a small engineering project in itself, and as in any engineering venture, a logical and careful sequencing of events is an absolute necessity. A typical modeling study can be broken into the following multi-step process: First of all, researchers should define the scope of the problem. They must select only the important properties for experimentation to help to find the solution. Second, researchers must consider similitude requirements such as geometry, material, and loading. Next, model size should be considered because it affects level of reliability or accuracy. If the model is very small when compared to the prototype structure, the experimental data is difficult to interpret because of large systematic model errors. Therefore, the above information can help when selecting model material. One of the more important processes is fabrication during which care must be taken in constructing the model. This can be a frustrating stage in modeling. After completing the model fabrication, instruments will be selected along with its installation in suitable positions to determine strain, displacement, force and other quantities. Furthermore, loading equipment must be designed to demonstrate intervals of behavior. Once the model and instruments are ready to start experiment, the researcher should examine behaviors of structure response and record the data to compare with approximate calculations, which should be done before the experiment. In addition, data analysis and report writing report should be completed as soon as possible, while the entire test is still fresh in the mind. The results will help engineers to understand structure behavior, which will be followed by mathematic or empirical models. However, most existing empirical models are event-specific and can not be reliably extrapolated to different sites and thus, their range of applicability in geotechnical engineering may be limited.

Table 2.1: Design approaches after Wang, 1993

Approaches	Advantages	Disadvantages	Applicability
Earth pressure method	Used with reasonable methods results in the past. Require minimal parameters and Computation error. Serve as additional safety measures against Loading.	Lack of rigorous theoretical basis. Resulting in excessive racking deformations for tunnels with significant burial. Use limited to certain types of ground properties.	For tunnels with minimal soil cover thickness.
Free-field racking deformation method	Conservative for tunnel structure stiffer than ground comparatively easy to formulate. Used with reasonable results in the past.	Non-conservative for tunnel structure more flexible than ground. Overly conservative for tunnel structures significantly stiffer than ground. Less precision with highly variable ground conditions.	For tunnel structures with equal stiffness to ground.
Soil structure interaction finite-element analysis	Best representation of soil structure system. Best accuracy in determining structure response Capable of solving problems with complicated tunnel geometry and ground conditions	Requires complex and time consuming computer analysis. Uncertainly of design seismic input parameters maybe several times the uncertainty of the analysis.	All conditions.
Simplified frame analysis model	good approximation of soil structure interaction. comparatively easy to formulate. Reasonable accuracy in determining structure response.	Less precision with highly variable ground.	All Conditions except for compacted subsurface ground profiles.
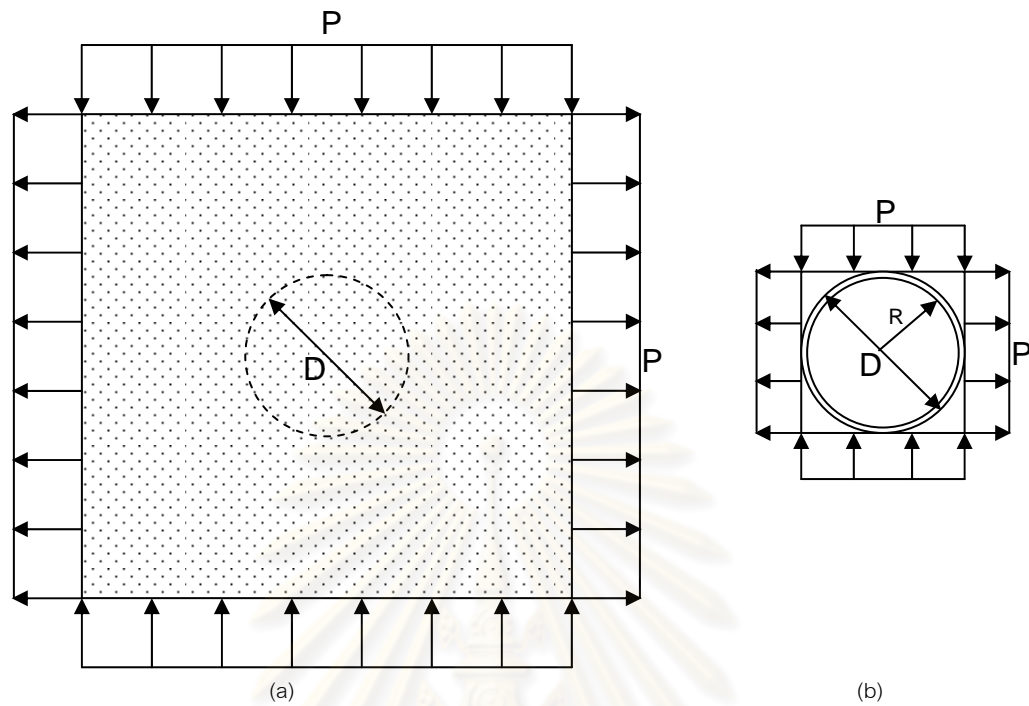
Figure 2.1: Ground and liner under a state of pure shear (after Peck et al., 1972)
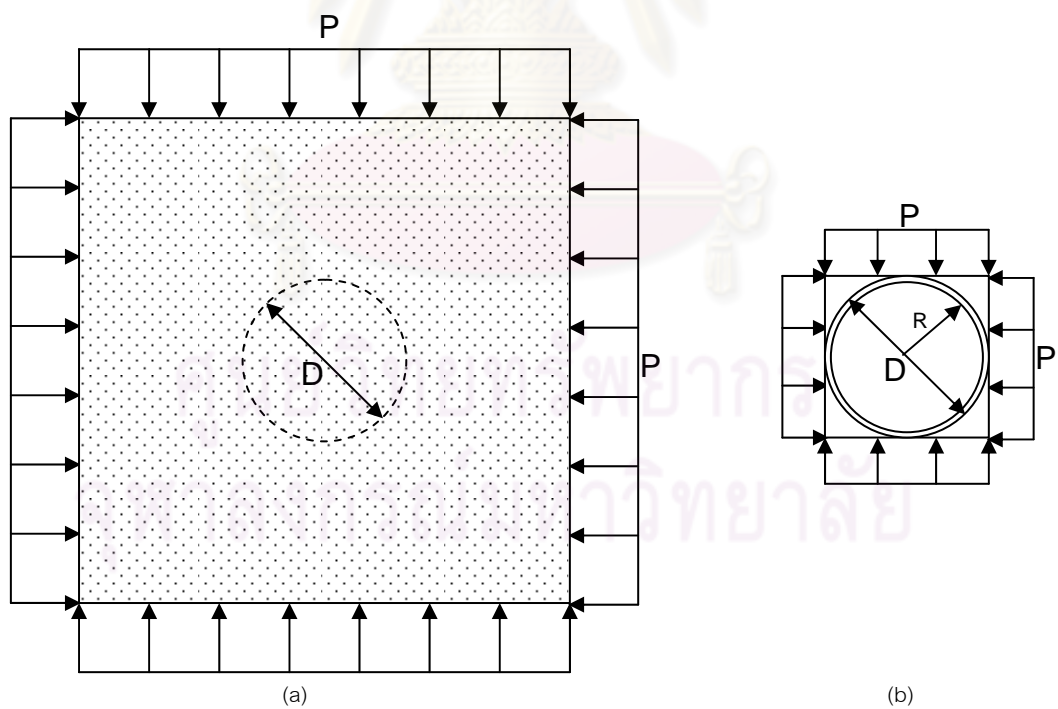
Figure 2.2: Ground and liner under a state of uniform compression (after Peck et al., 1972)

STRUCTURAL DESIGN MODELS FOR TUNNELS

Ground pressure (active load) is applied to the lining and determined with different methods (Terzaghi, Protodiaconov, Caqout)

UNIDIMENSIONAL MODEL

Based on Strength of Materials Theory

EMPIRICAL METHOD

CONTINUUM MODEL

Based on Theory of Elastic

Ground pressure on the lining
- is obtained at finish
- is set at beginning

Without ground – lining interaction

With ground – lining interaction

DEERE, 1969

Analytical solution

Numerical solution

Graphical Method

Free deformed ring

Continuum ring

Continuum ring partially bedded Continuum contact

Poligonal hinged beam on springs Discreet

Infinite plate with hole

Shallow tunnel

Finite Element Method

Boundary Element Method

Elastic medium

Elasto-plastic medium

Plastic medium

Reaction according to Winkler Theory

Arbitrary Reaction

Parabolic Reaction

Differential Ecuations

Winkler Reaction

Reaction according to Th. Of Elast.

Lined Opening

Unlined Opening

Convergence Confinement Method

Associated Fields Method

Figure 2.3: Structural models to compute member forces (Iftimie, 1994)
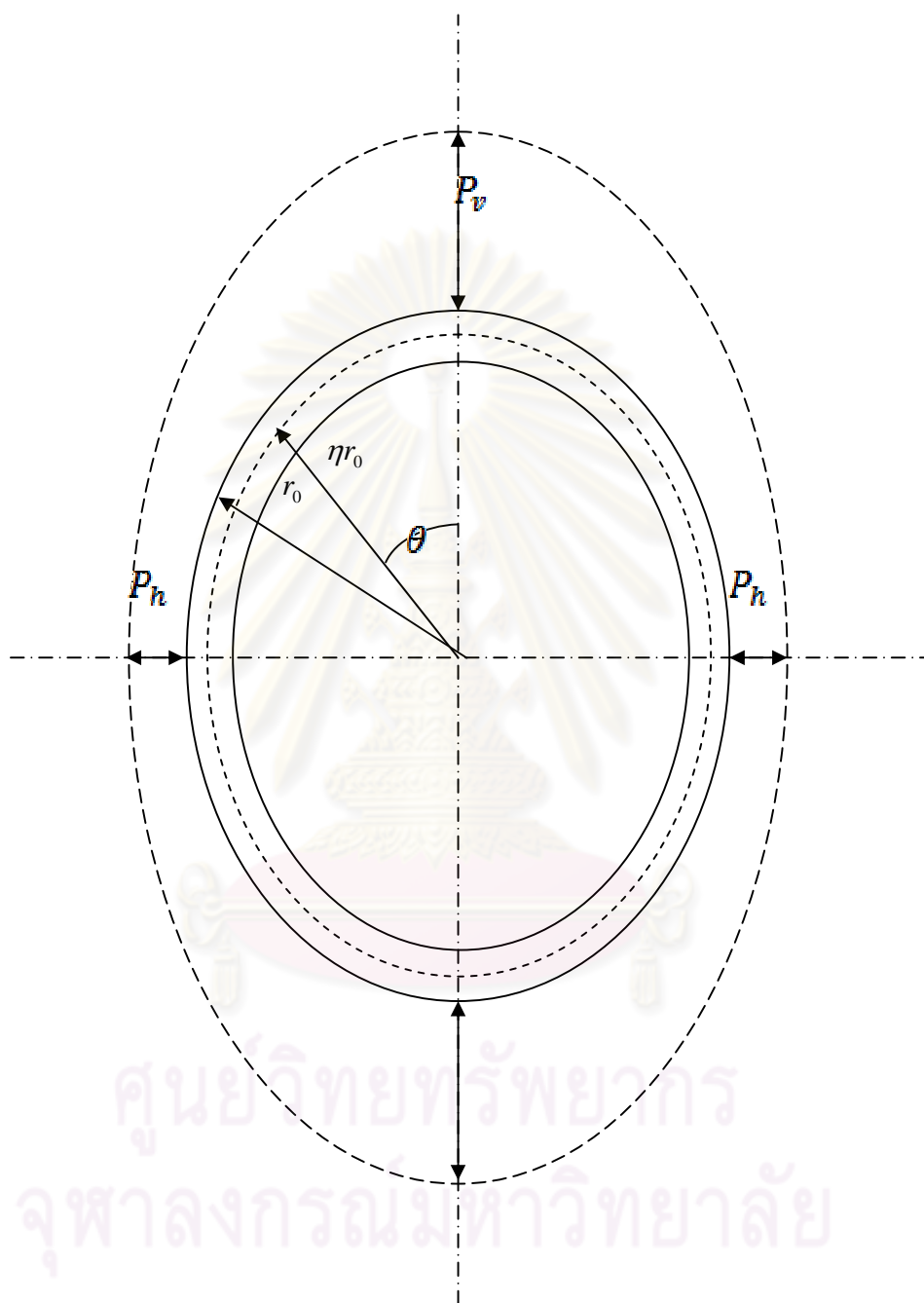
Figure2.4: Reference diagram for initial loading on tunnel prior to deformation (Wood, 1975)
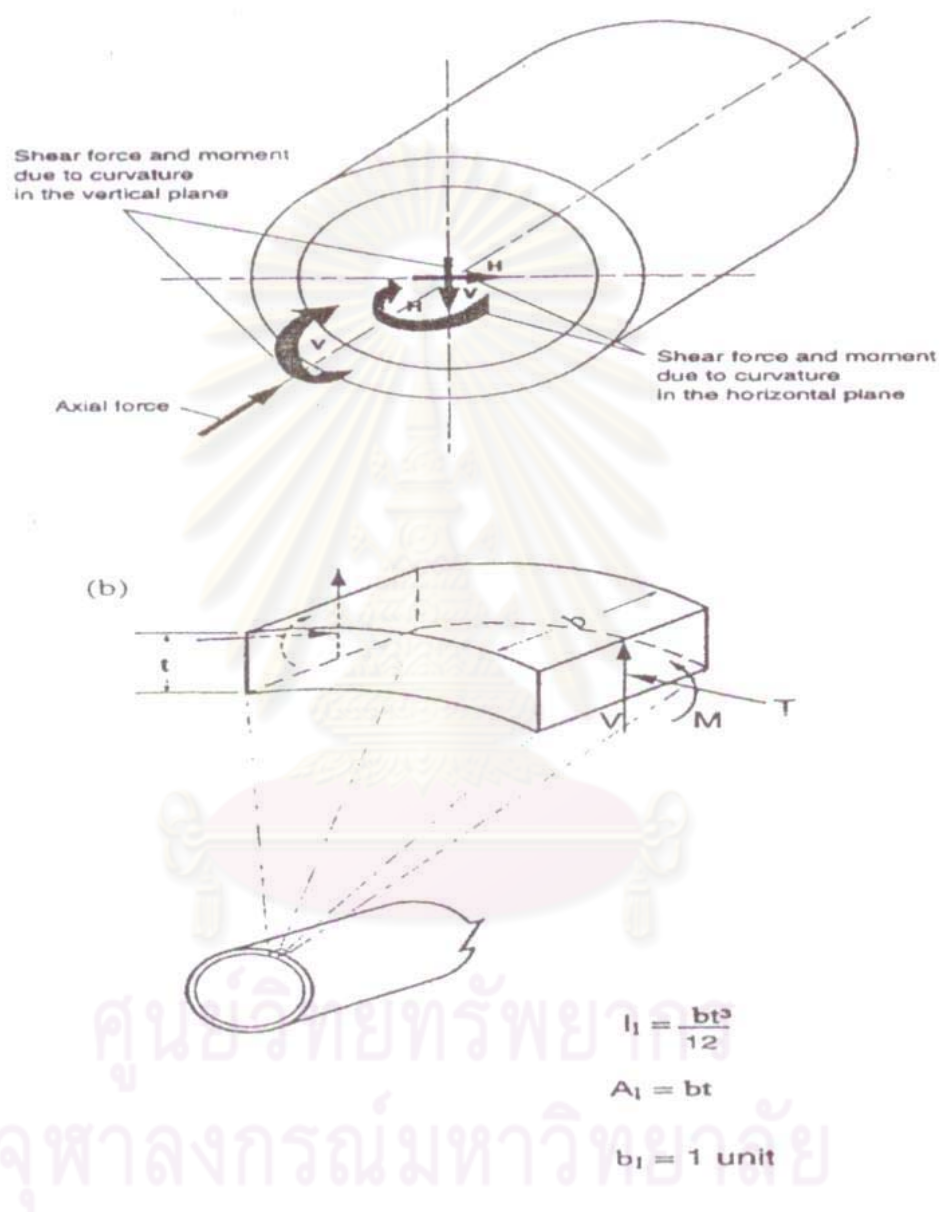
Figure 2.5: Induced forces and moments (Power. Et al., 1996), a) Induced forces and moments caused by waves propagating along tunnel axis, b) Induced circumferential forces and moments caused by waves propagating perpendicular to tunnel axis
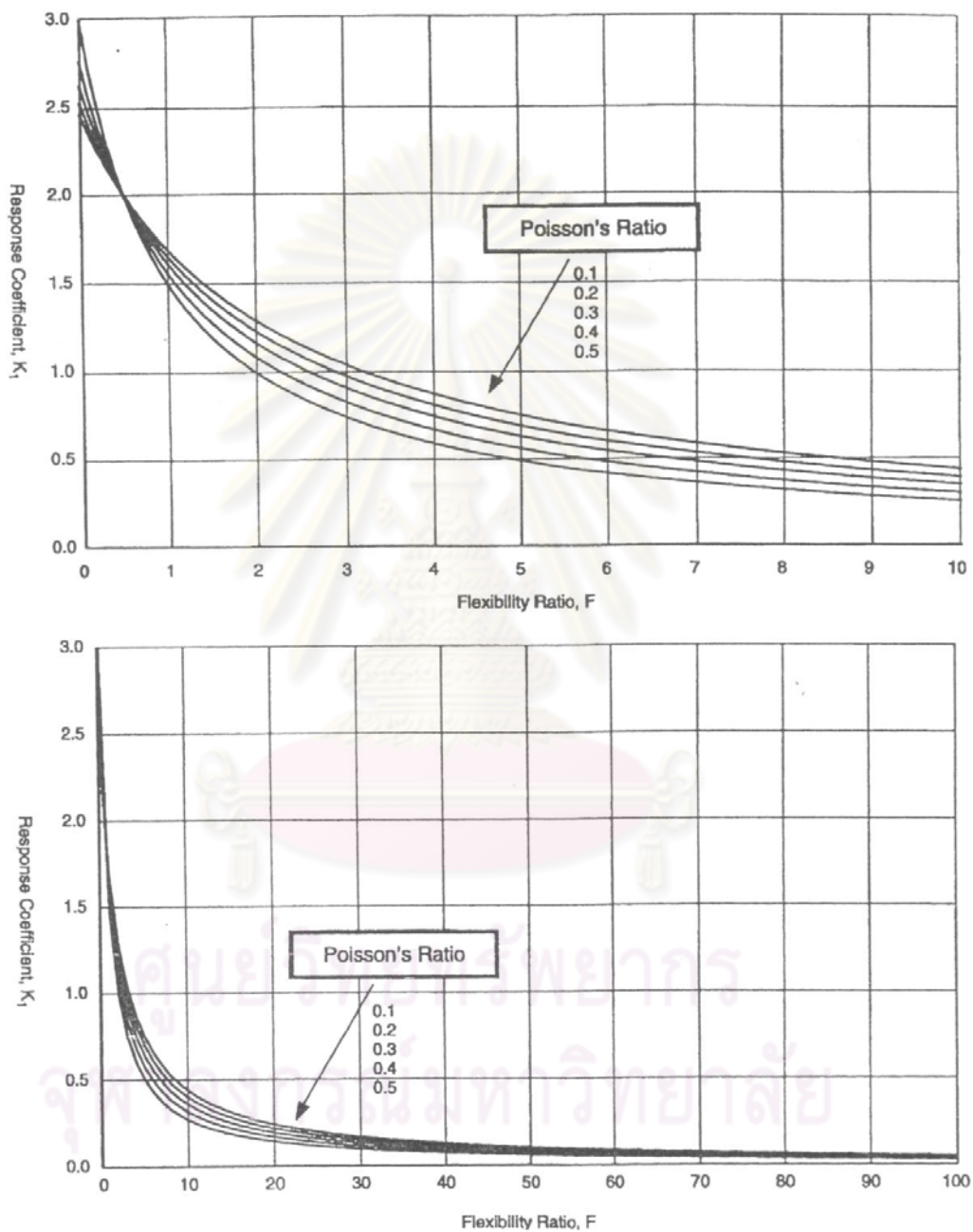
Figure 2.6: Lining response coefficient vs. flexibility ratio, full-slip interface, and circular tunnel (Wang, 1993)
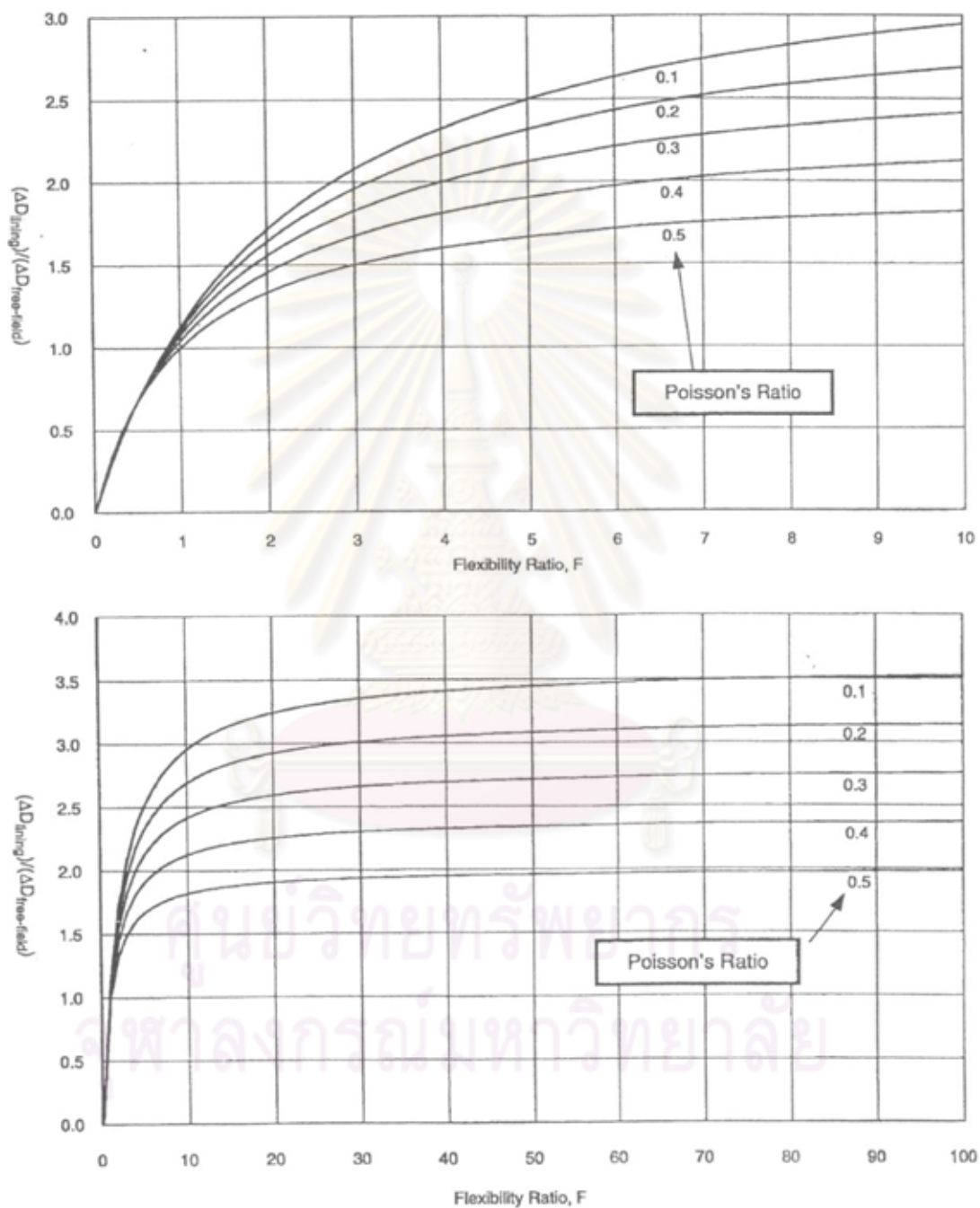
Figure 2.7: Normalized lining deflection vs. flexibility ratio, full-slip interface, and circular lining (Wang, 1993)

immersed tunnel

X
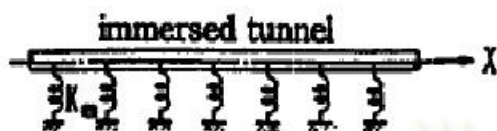
Figure a: Lumped mass method

CROSS-SECTION

t_s

$D=1.00m$

y

z

x

30m

1m

z_i
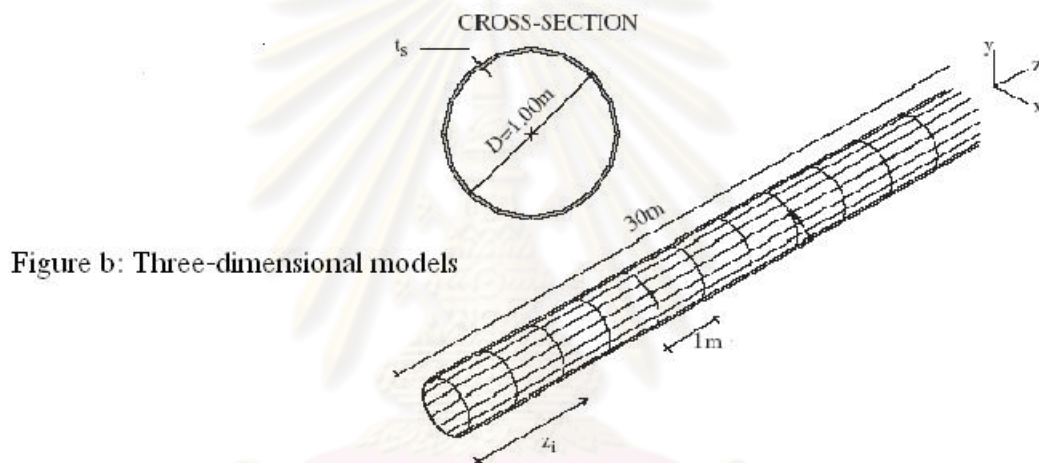
Figure b: Three-dimensional models

Figure 2.8: Tunnel structure models for numerical method

CHAPTER III

INVESTIGATION OF TYPICAL DESIGN
AND NUMERICAL ANALYSIS

3.1 Overview

Nowadays, circular shield tunnels are used in metropolitan transportation and infrastructure because this tunnel structure shape is very strong, stable and easier to construct than others based on homogenous material assumption. In additional, the earth pressure balance shield method (EPB) is very popular when constructing tunnels in soft soil because equipment can control soil movement on the construction site and, thus,decrease damage of surrounding structures such as bridges and buildings. Other benefits include a decrease in construction costs and time.

However, In Earth Pressure Balance machines, construction space is usually limited so a tunnel structure should be separated into many parts. Each segment should be connected by a steel rod as the lining of a shield tunnel is not a continuous ring structure since it has joints. Therefore, the behavior of an entire tunnel structure on external loading will not be according to design assumptions, and the effects of the segmental joints on internal member forces and displacements are not clear behavior. During construction and design processes, an engineer only tries to check the maximum force capacities of the shield tunnel structure by applying external loads to the completely assembled full-scale segmental structure. However, segmental joint behavior is not carefully observed in this design process. For more information, most designers try to ignore the effects of segmental joints on the whole tunnel structure.

Many researches have shown that segmental joints directly affect the whole structure. In conclusion, segmental joint structure effects on underground shield tunnel structure fall into two areas: (1) changing the original shape, which is the most popular research to consider effects to the structure and (2) maximum resistance force capacity of a shield tunnel under exciting load with maximum resistance force capacity, which is less popular because earth pressure behavior around the shield tunnel is not clear. The earth pressure is dependant on many environmental parameters and the soil micro-structure at specific times. However, many studies show that the average earth pressure in ground around a lining directly follows earth pressure theory. However, deformation of the lining measured inside a tunnel section is easy to calculate and will give reliable results. Therefore, this study compared the effects of the whole shield tunnel structure to segmental joint behavior based on displacement control. This work also only considered external force in a vertical direction to shield tunnel models.

To simulate the model, which represents the behavior of the real structure, the parameters with significant effects on the behavior of the model investigated had a segmental joint structure. Structural indices were defined as parameters that represent the behavior of the structure under external loading. The study of structure indices will be a mean to specify the configuration of the test specimens, which are expected to represent the typical behavior of tunnels. Therefore, a main objective of experimental application is to find the elastic behavior of segmental joints of a shield tunnel structure under external loading.

3.2 Typical design processes of underground tunnel lining

In tunnel design, there are many factors to be considered that cover all construction and working stages according to the following steps:

- First: Design of the inner tunnel dimension determined by space demand and functions such as railway, traffic lane, or water discharge

- Second: Engineers determine tunnel lining dependant on factors such as technical of construction and budget

- Third: Engineers determine soil properties such as specific gravity, cohesion, friction angle, and modulus of deformation

- Fourth, tunnel design must follow standards, or specification code, according to civil law

- Fifth: Design evaluation for critical forces acting on each tunnel section, including construction and working states, to select maximum possible excited loads.

- Sixth: Selection of construction material according to budget such This step considers both permanent and temporary structures. Material properties determine tunnel thickness, segment lining size, and construction method, process and time when using a shield tunnel machine because limited workspace.

- Seventh: Structure model created. Engineers will input maximum forces determined in above steps to calculate structural forces, computed using the following methods:

    - Bedded frame model method

    - Finite element method

    - Elastic equation method

    - Schultze and Duddeck model

    - Muir Wood model

- Eighth: Overall conceptual design is completed after structureal forces are calculated. Structure lining should be designed according to safety standard criteria. Safety of the most critical sections must be checked using the limit state

design or allowable stress design method. For example, a minimum thickness for the segments will be determined according to the bearing capacity to earth pressure and water pressure and proportion to tunnel outer diameter obtained by an analysis of damage records.

After the designers determine the lining is safe, economical and optimally designed, a design document of design must be approved by those in charge of the project. In Figure 3.1, these steps are shown on a flow chart for tunnel lining design.

However, tunnel lining design requires much experience as well as practical and theoretical knowledge. It is therefore not expected that these guidelines will cover every tunnel lining design point, but instead provide basic knowledge useful to design practitioners. In actual design and construction, lining makeup, segment shapes, joint and waterproofing details, and tolerances should be selected for effective, reliable and rapid erection, considering the following:

- Method and details of erection and erection equipment
- Functional requirements of the tunnel, including lifetime and water-tightness requirements
- Ground and groundwater conditions, including seismic conditions
- Usual construction practice in the location of the tunnel

3.3 Earth Pressure and other external loads distribution around a tunnel lining

Lining load conditions depend on the environment surrounding the construction site, including existing surface structures, underground geology and construction force as shown in Figure 3.2. To overcome natural conditions, designers must predict possible loads that will affect the lining. Load conditions include the following:

- Vertical earth pressure is assumed to be a uniform load, and the pressure will increase as you go deeper. A popular method to calculate the pressure is Terzaghi's formula. The upward earth pressure from the tunnel bottom is assumed to be the same as the downward earth pressure in magnitude and distribution. Soil unit weight for the calculation of earth pressure should use a wet unit weight above the groundwater table, and the submerged unit weight should be used for soil below the groundwater table.

- Horizontal earth pressure is assumed to be a uniformly varying load that increases with increasing depth, similar to vertical earth pressure. For calculation, horizontal earth pressure is the vertical earth pressure at same level multiplied by the coefficient of horizontal earth pressure as shown in Table 3.1. However, the coefficient value of lateral earth pressure varies according to ground conditions. In most cases, the interval of coefficient value is determined by the difference between the coefficient value of the passive lateral earth pressure and the coefficient value coefficient of the active lateral earth pressure. The designer should decide this value after considering passive and construction conditions.

- Water pressure is assumed to be a uniform load, and the pressure will increase according to the water depth at the ground water level. The pressure on the tunnel is assumed to act in the same direction to the ring. This pressure acts on the tunnel when rhe major portion of the soil is gravel or sand (Yukinori, 2003).

- Surcharge pressure is assumed to be a uniform load, and the pressure will decrease with ground depth levels. Therefore, the surcharge increases earth pressure on shallow levels which affect shallow tunnels. For example, a surcharge source which acts on a lining is road traffic and building weights. There are a number of formulas to calculate these pressures.

- Sub-grade reaction is based on assumptions based on the proportion between ground displacement and pressure loading at a single point. However, sub-grade

reaction is difficult to determine because soil behavior is nonlinear inelastic and depends on the loading rate and magnitude of displacement. Therefore, engineers should predict displacement and the time to disturb the soil that will occur to complete a lining. Because of soil plasticity, it is difficult to use to estimate sub-grade reaction with a linear, bilinear or multi-linear equation. In most practical cases, the reaction model will be assumed to be ground springs located along the whole periphery of the tunnel in a perpendicular direction. Table 3.2 shows the approximated coefficient of soil reaction.

- Dead load is the gravity load acting along the centroid of the cross section of a tunnel. It is calculated by the volume of lining multiplied by unit weight of construction material.

- Internal loads caused by facilities suspended from the ceiling of a tunnel or by inner water pressure should be investigated.

- Loads during construction such as shield jacks thrust force , load during transportation and handling of segments, backfill grouting pressure, and equipment operation load should be carefully considered because of their effect on lining stability. Some important loads, like ingredient lining, must be examined to confirm the limit of tolerance.

- Earthquake load and other loads should be investigated if the load effects structure safety or recommended code specifications.

However, at both tunnel ends, earth pressure gradually changes over the long term. This is thought to result from changes in atmospheric temperature (Ariizumi et al., 1998)

3.4 Subgrade reaction

Subgrade reaction is a main factor of underground tunnel design that does not have a constant value. It depends on many parameters of soil and underground structure. When engineers attempt to calculate member force in the lining, they must determine the acting range, magnitude and direction of the subgrade reaction. The subgrade reaction is divided into

- the reaction independent of ground displacement, and
- the reaction dependent on ground displacement

It is assumed that the latter subgrade reaction is proportional to the ground displacement, and its factor of proportionality is defined as the coefficient of subgrade reaction. The value of this factor depends on ground stiffness and the dimension of the lining (radius of lining). The subgrade reaction is the product of the coefficient of subgrade reaction and the displacement of the lining which is decided by ground stiffness and rigidity of the segmental lining. The rigidity of the segmental lining depends on the segment rigidity and number and type of joints.

3.5 Ideal design of underground tunnel lining and segmental joint

After acquiring all primary information for a lining design, a numerical model should be created to compute structural forces. The structure model should closely represent the real behavior of the lining. However, in-situ stress and displacement of soil in the long term are difficult to predict because of the time dependent effect of soil, which is the result of inconsistent behavior with the circumstantial environment. Therefore, information based on experiment or filed measurements are important to set up some assumptions. The existing

loads and underground structure based on the assumption will be simplified attain a practical design formula. For example, the concept of a competence factor (Muir Wood, 1972), which shows the ratio of ground strength in simple compression to the vertical overburden pressure, is one indicator for assessing whether the assumption of linearity is likely to be acceptable within the limitations of any two dimensional tunnel analyses. Peck (1969) stated that a liner is said to be flexible if it interacts with the surrounding ground in such a way that the pressure distribution on the liner and the corresponding deflected shape result in the lining, and a liner is said to be rigid if it deflects insignificantly under the loads imposed by the ground with very little ground-structure interaction. Whether a liner is flexible or rigid depends on the relative stiffness between ground and liner and the tunnel diameter. For example, a liner may be flexible with a stiff surrounding ground and a large diameter, but the same liner may be rigid with a soft surrounding ground and a small diameter.

Moreover, as underground tunnels are located at different ground levels depending on project objectives, economic issues, and available space, the circumferential environment, like a retaining wall and existing lining, is one factor that should be considered when evaluating lining behavior because of soil resistance in each direction. The lateral soil resistance pressure is only considered when significant tunnel deformation (squash) is induced by the soil-structure interaction effect of subsequent construction activities. However, this value can be ignored for a tunnel lining constructed in compressible soft clay when only long-term equilibrium conditions are considered. . Engineering judgments, therefore, must be exercised to decide which tunnel displacement direction should be adopted as the matching criterion. Figure 3.3 shows some related problems and the suggested matching directions of the displacement.

In general, if the subsequent construction activities or the existence of a relatively high vertical overburden pressure are causing the tunnel to "squash" significantly in the lateral direction, the matching scheme should be conducted in the horizontal direction

(Δ_h). The additional lateral soil resistance pressure imposed on the springline of the lining should then be considered by the effect of lateral soil resistance pressure. On the other hand, if the subsequent construction activities are causing release of earth pressure in the vertical direction, the matching scheme should be conducted in the vertical direction (Δ_v). The effect of lateral soil resistance pressure on the springline of the tunnel can be ignored. The resulting oval shape of the tunnel lining may result in an increase of soil resistance in the vertical direction across the top and bottom levels of the lining system. However, such an effect should be very small for shallow tunnels, as the soil cover above the tunnel crown cannot generate significant vertical soil resistance.

Based on Peck's and Wood's assumption, one important parameter is the segmental joint of a lining, which is not focused on presently. Therefore, this parameter will be considered in this research. First, because lining segments are connected by steel bolts, its actual flexural rigidity at the joint is smaller than the flexural rigidity of the segment. The segmental joint rigidity varies between a perfectly uniform rigid ring and a multiple hinge ring. If the segments are staggered, the moment at the joint is smaller than the moment of the adjacent segment. The actual effect of the joint should be evaluated in the design.

3.6 Conceptual numerical modeling of shield tunnel lining

In this work, the SAP2000 finite element program is used to solve three-dimensional behavior of tunnel problems. Circular tunnels and steel bolts are modeled to shell elements and rigid beam elements, respectively, shown in Figure 3.4. The deformation of the tunnel structure is limited because the structures are made from reinforced concrete, which is brittle. Additionally, soil behavior and water pressure around are the tunnel over the long term have changed when compared to before excavation. Therefore, soil strength can be considered as an elastic material, with properties based on subgrade modulus. Hence, the

main analysis focuses on the elastic behavior of both the tunnel structure and soil structure. Furthermore, this problem analysis focuses on a no-slip surface between soil and tunnel surface. In this analysis, lining parameters and soil properties are adopted in the modeling as summarized in Table 3.3 and Table 3.4 respectively. However, the evaluation of the earth pressure loads that may act on a buried pipe is based on the total weight of the backfill at the center of the circular lining and the load acting on the lining is uniform in both horizontal and vertical direction.

As most segmental concrete lining systems adopted for tunnels in soft ground are waterproofed using rubber gaskets at the joints, the lining structures are subjected to both earth and water pressures. Thus, the earth pressure acting on the segmental circular tunnel lining is total stress. Assuming , for simplicity, the groundwater level to be at the surface of the ground, the total pressures acting around a jointed lining structure are assumed to be those shown in Figure 3.5. The assumption is based on the projected pressure distribution along the vertical and horizontal directions around the tunnel ring, which are based on field-observed earth pressure distribution patterns as described in the following section. The assumed total pressure as shown in Figure 3.5 is defined as follows:

Vertical overburden earth pressure at the tunnel crown, p_1:

$$p_1 = q_1 + q_2$$

where q_1 is the total earth pressure developed above the tunnel level, i.e.,

$$q_1 = \sum_{i=1}^{n} \gamma_i h_i$$

where γ_i is the total unit weight of the soil layer i; h_i is the thickness of the soil layer i; n is total number of soil layers above tunnel crown; and q_2 is the total earth pressure developed at the shoulder regions, which can be approximated by

$$q_2 = \frac{2\left(1 - \frac{\pi}{4}\right)R^2\gamma_{as}}{2R} = 0.215R\gamma_{as}$$

where R is the calculation tunnel radius, defined as the average of the outer and inner radii; and γ_{as} is the average total unit weight of soil at the shoulder regions;

Reaction pressure p_2 generated at the bottom of the tunnel lining and calculated by taking p_1 and the self-weight of the tunnel lining:

$$p_2 = p_1 + \frac{2\pi R t \gamma_c}{2R} = p_1 + \pi t \gamma_c$$

where t is the thickness of the tunnel lining, and γ_c is the average unit weight of the lining material;

Total lateral earth pressure at the crown level of the tunnel lining, p_3:

$$p_3 = K_0 \gamma' h + \gamma_w h$$

where K_0 is the coefficient of earth pressure at rest, γ' is the average effective unit weight of soils, γ_w is the unit weight of water, and h is the total thickness of the soil layer above the tunnel crown;

Additional earth pressure developed at the tunnel invert level, p_4:

$$p_4 = 2K_0 \gamma' R + 2\gamma_w R$$

3.7 Flowchart for the proposed research methodology

This study tests plastic structure tunnel models under vertical load to determine the behavior of segmental joints of a shield tunnel structure under vertical loading response. Figure 3.6 presents the overall methodology used in this work. Each process is explained in the next section.

Table 3.1: Coefficient (λ) of lateral earth pressure in full-circumferential spring model (RTRI, 1997)

Type of soil			λ	N value guideline
Soil-water separated	Sandy soil	Very dense	0.45	$30 \leqq N$
		Dense	0.45-0.50	$15 \leqq N < 30$
		Medium, Loose	0.50-0.60	$N < 15$
Soil-water integrated	Clayey soil	Hard	0.40-0.50	$8 \leqq N \leqq 25$
		Medium, stiff	0.50-0.60	$4 \leqq N < 8$
		Soft	0.60-0.70	$2 \leqq N \leqq 4$
		Very soft	0.70-0.80	$N < 2$

Table 3.2: Coefficient (k) of ground reaction* tunnel diameter (D) in full-circumferential spring model (RTRI, 1997)

Type of soil		During grouted material hardening (N/mm2)	After grouted material hardening (N/mm2)	N valuve guideline
Sandy soil	Very dense	35.0-47.0	55.0-90.0	$30 \leqq N$
	Dense	21.5-35.0	28.0-55.0	$15 \leqq N < 30$
	Medium, loose	-21.5	-28.0	$N \leqq 15$
Clayey soil	Hard	31.5-	46.0-	$25 \leqq N$
	Medium	13.0-31.5	15.0-46.0	$8 \leqq N < 25$
	Stiff	7.0-13.0	7.5-15.0	$4 \leqq N < 8$
	Soft	3.5-7.0	3.8-7.5	$2 \leqq N < 4$
	Very soft	-3.5	-3.8	$N < 2$

Table 3.3: Properties of Elastic Tunnel Ling and soil strength

Parameter	Value	Unit
Diameter of tunnel	vary	m
Lining thickness	0.3	m
Young's modulus	25000	MN/m^2
Poisson's ration	0.2	-
Angular joint stiffness	vary	kN/m

Table 3.4: Properties of Elastic Tunnel Ling and soil strength

Parameter	Value	Unit
Subgrade modulus	vary	kN/m^3
Unit weight	20	kN/m^3
Coefficient of earth pressure at rest	0.5	-

```
                          ┌─────────────────────────────┐
                          │ Planning of Tunnel Project  │
                          └─────────────────────────────┘

  ┌──────────────┐    ┌──────────────┐              ┌──────────────────┐
  │ Alignment    │◄──►│ Survey/      │              │ Function/ Capacity│
  │ Plan/Profile │    │              │              │ to be given to   │
  │              │    └──────────────┘              └──────────────────┘
  └──────────────┘
                    ┌────────────────────────────────┐     ┌──────────┐
                    │ Specification/ Code/ Standard to be │  │ Inner    │
                    └────────────────────────────────┘     │ Diameter │
                                                           └──────────┘
  ┌──────────┐                              ┌─────────────────────────┐
  │ Load     │◄────────────────────────────►│ Assumption of Lining    │
  └──────────┘                              │ Condition (Thickness,   │
                                            └─────────────────────────┘
                    ┌────────────────────────────┐
                    │ Model to Compute Member Forces │◄──
                    └────────────────────────────┘

                    ┌────────────────────────────┐
                    │ Computation of Member Forces │
                    └────────────────────────────┘

                    ┌────────────────────────────┐
                    │ Check  of  Safety  of       │
                    └────────────────────────────┘

                           ◇ Safe and ◇ ──── No
                               │ Yes
                           ◇ Approval ◇ ──── No
                               │ Yes
                    ┌────────────────────────────┐
                    │ Execution of Construction   │
                    └────────────────────────────┘
```
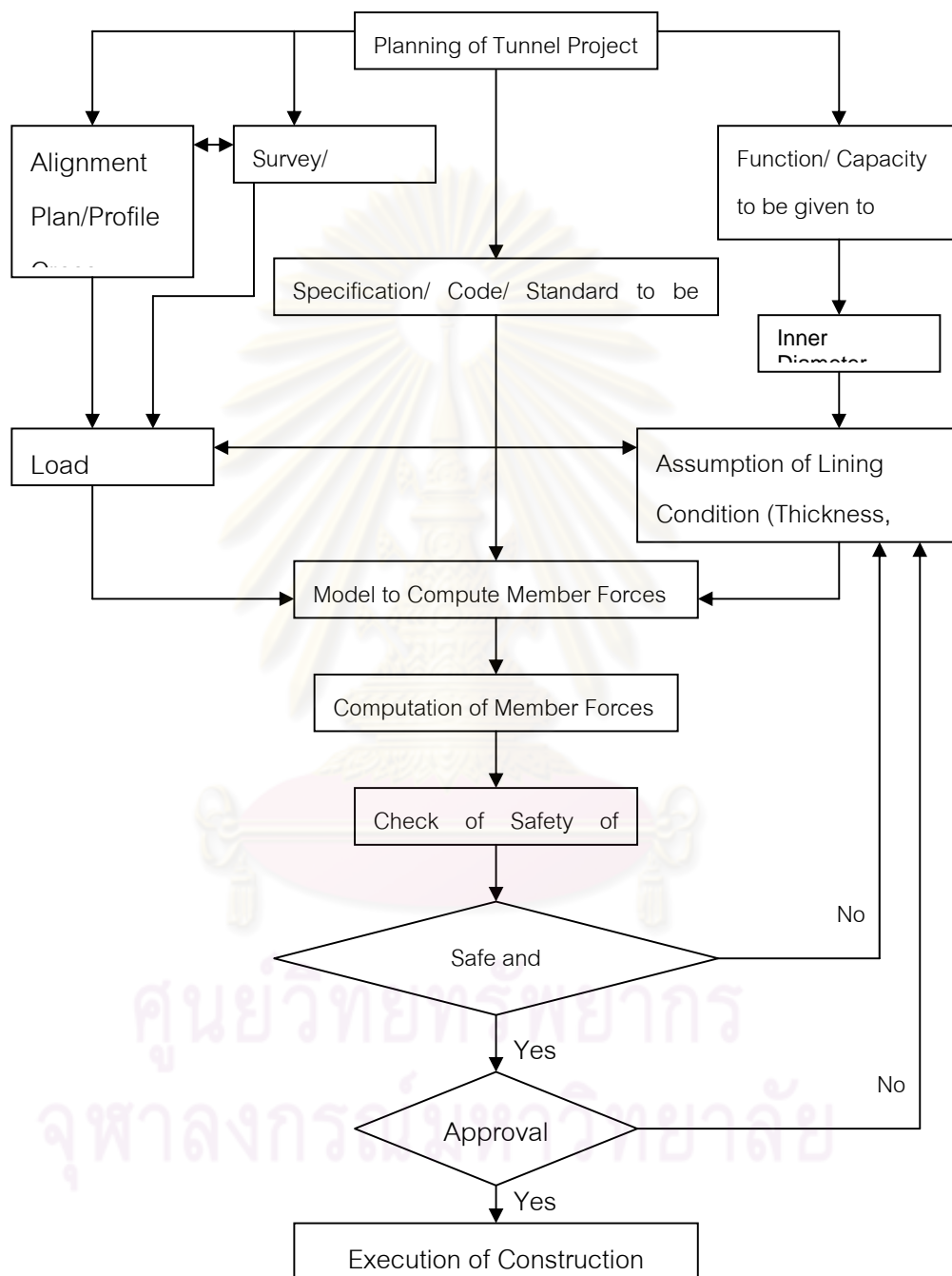
Figure 3.1: Presents the overall guideline used in analysis and designing tunnel lining.
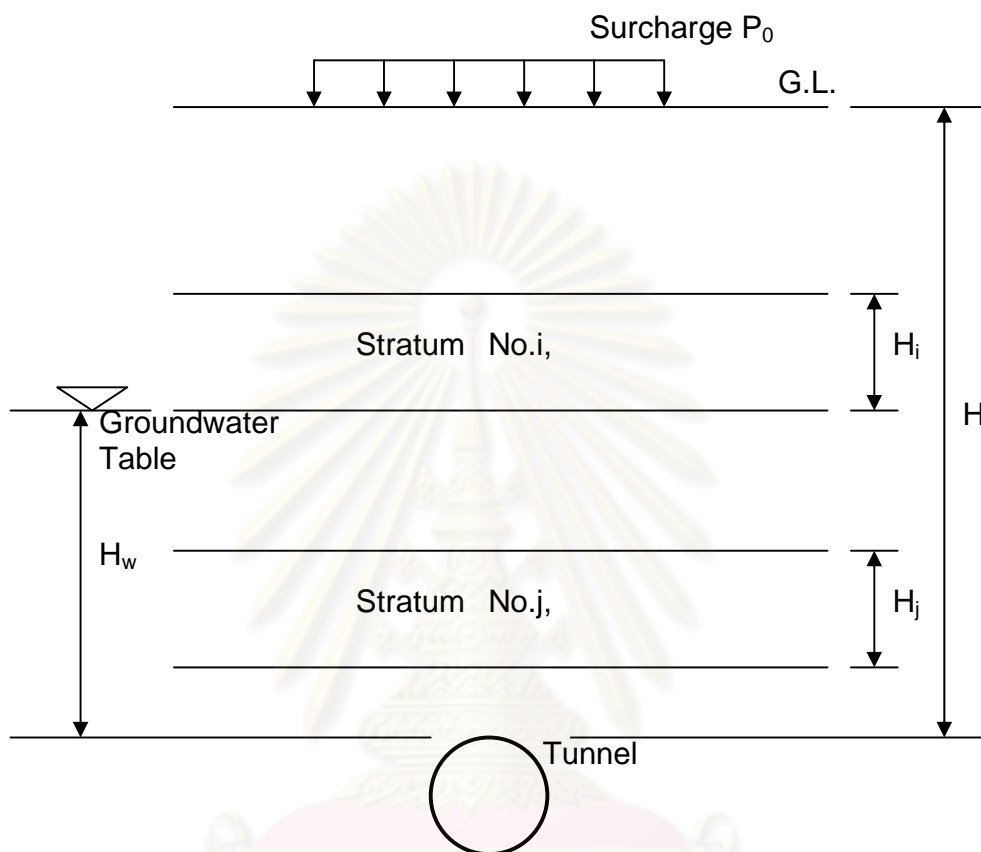
Figure 3.2: Section of tunnel and surrounding ground

a) Prediction of ground surface
   settlement (matching Δ_h)

b) The influence of subsequent surcharge
   loading on ground surface (matching Δ_h)

c) The influence of excavation directly
above an existing tunnel (matching Δ_v)

d) The influence of excavation
adjacent to an existing tunnel (matching Δ_h)

e) The construction of a new tunnel adjacent to an existing tunnel (matching Δ_h)
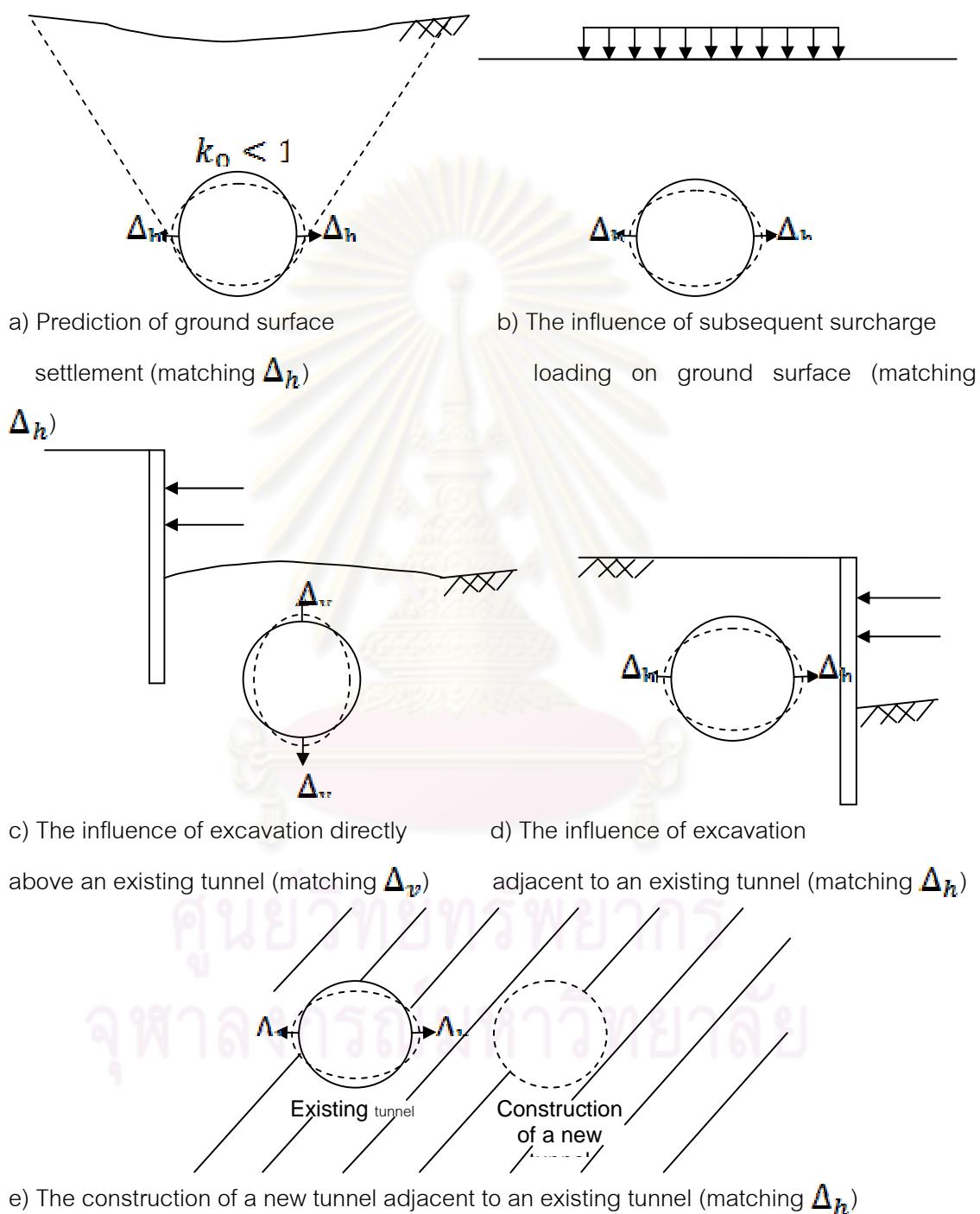
Figure 3.3: Different types of tunneling-related problems and associated matching criteria
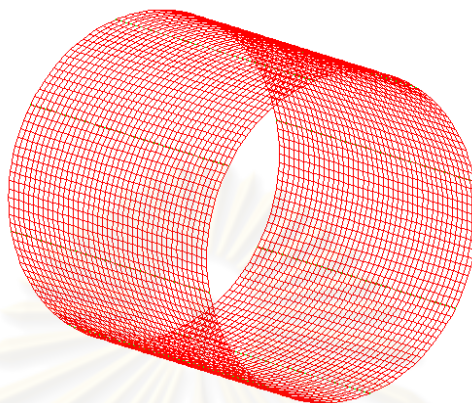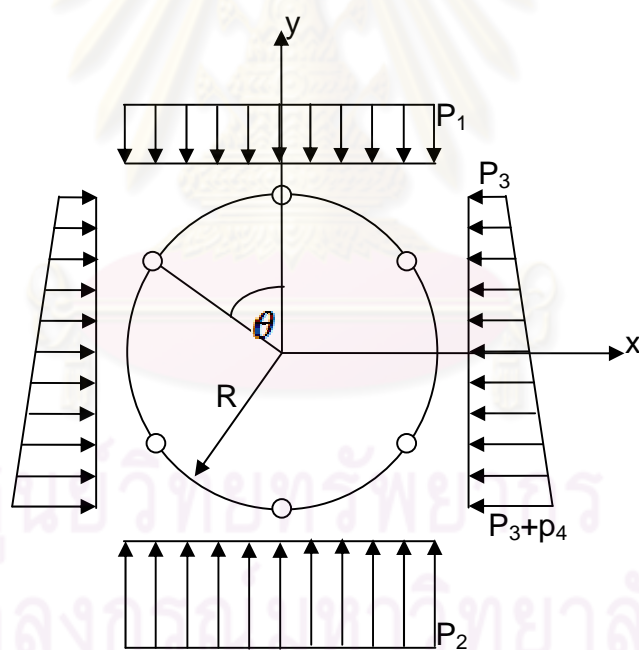
Figure 3.4: Cross section of segment model

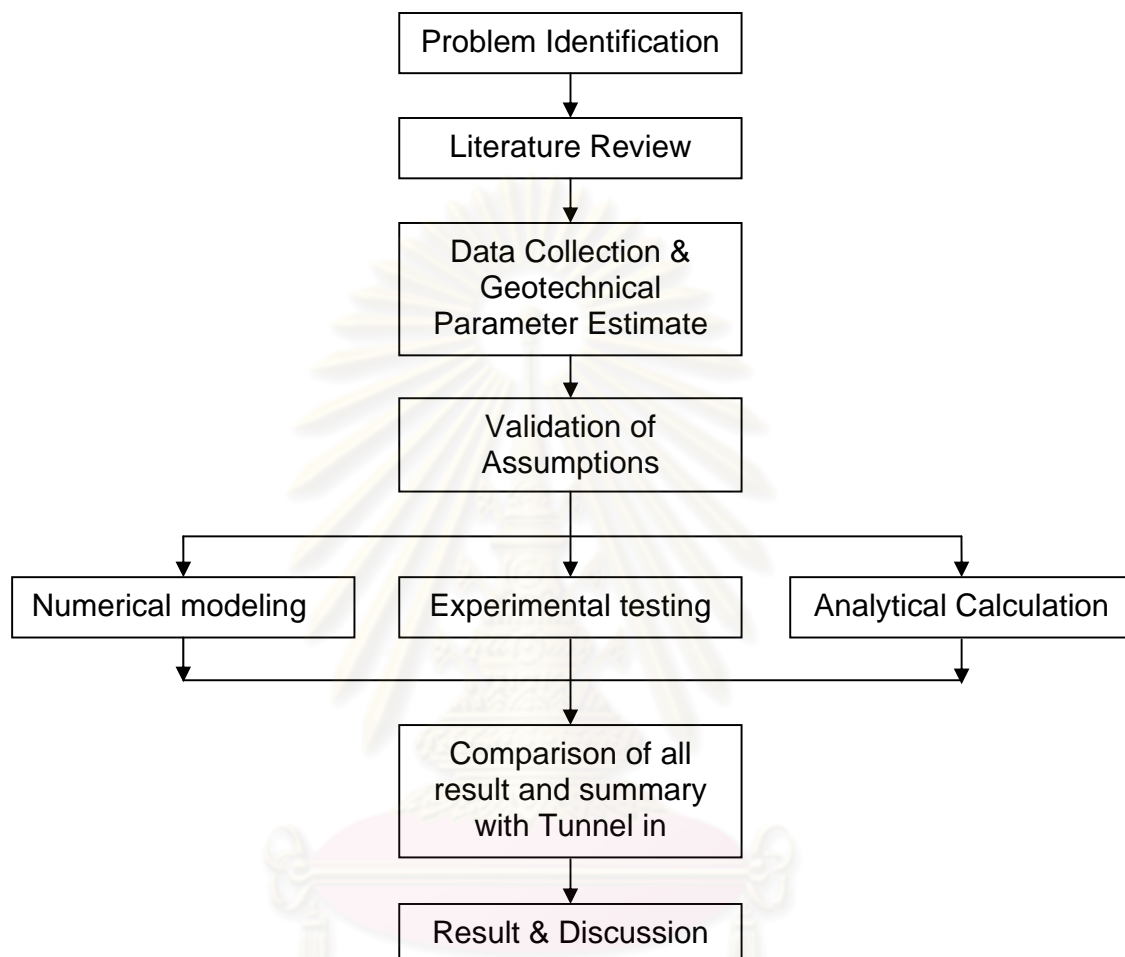Figure 3.5: Model diagram of a jointed tunnel lining

```
┌─────────────────────────┐
│  Problem Identification  │
└─────────────────────────┘
            │
            ▼
┌─────────────────────────┐
│    Literature Review     │
└─────────────────────────┘
            │
            ▼
┌─────────────────────────┐
│    Data Collection &     │
│      Geotechnical        │
│   Parameter Estimate     │
└─────────────────────────┘
            │
            ▼
┌─────────────────────────┐
│      Validation of       │
│       Assumptions        │
└─────────────────────────┘
```

Numerical modeling	Experimental testing	Analytical Calculation

```
┌─────────────────────────┐
│     Comparison of all    │
│    result and summary    │
│      with Tunnel in      │
└─────────────────────────┘
            │
            ▼
┌─────────────────────────┐
│    Result & Discussion   │
└─────────────────────────┘
```

Figure 3.6: The overall methodology of the proposed study

CHAPTER IV

TEST SPECIMEN AND EXPERIMENTAL SETUP

4.1 Overview

A tunnel is an underground structure widely used for transportation transfer, water passage as well as electrical and communication cable installation. With the development and upgrade of infrastructures, tunnel construction is increasing all over the world, and tunnel engineers must be more aware of the importance of the safety and economics of tunnel construction. In relation to tunnel construction, Peck (1969) stated three issues: first, maintaining stability and safety during construction, second, minimizing unfavorable impact on 3rd parties, and finally performing intended function over the life of a project. Among the issues, the first issue is directly related to the appropriate design of tunnel support system.

The construction operation for shield tunneling consists of excavation of a tunnel face using miners and machinery protected by a shield. A permanent tunneling lining is erected within the tail-skin as the shield advances. Grout is usually placed between the lining and surrounding soil. Because the process is very complicated, it is obviously impossible to duplicate all of the details of the tunneling process within a small-scale centrifuge model. Approximations need to be made in the model so that key features in engineering practice can be easily investigated.

The aim of this study is to suggest advances in the design concept of segmental joints in shield tunnels, which directly affect the behavior of the whole structure. Plastic pipe lining specimens and half sections of reinforced concrete full-scale specimens were constructed in this experimental study. However, the plastic model was rescaled to one-

fortieth of full-scale. Because of its small size, the model can explain only elastic behavior of segmental joints in a tunnel lining (Harry, 1999).

The segmental joints in the plastic model are plastic pieces of polyvinyl chloride (PVC) of varied thicknesses and sizes to represent changes in material properties of the joint. The specimens were constructed to create representative behavior of segmental joints of an underground circular tunnel lining. In general, the underground lining is composed of many segments, depending on project criteria, tunnel boring mechanics, and designers. However, this experimental study focuses on just four to eight segments in each lining ring.

4.2 Test Specimen Modeling

The purpose of this experimental study is to investigate the behavior of a typical segmental joint of a tunnel lining subjected to earth pressure and other loading. Because of the many patterns and locations of segmental joints in a real tunnel structure, it is difficult to specifically construct a model very similar to a structure. The practical structure is composed of two main parts. First, a piece of a segment is made from reinforced concrete, or steel which is strong enough to resist any loading. The second part is the segmental joint that is normally made from high strength steel bar. Therefore, this study tries to simplify the structure to a simple pattern similar to a conceptual design where every piece of the segmental lining is made to equal size. Furthermore, because the whole small models are made from plastic, which is not close to real structure material, location and material type of the segmental joints is this study must be simplified. The segmental joints in this study are made from a piece of plastic and vary thickness and then stuck into the lining's inner circumference. In this study, the lining model is 4 to 8 tunnel lining segments. However, to increase the reliability of the results, a full-scale test should be investigated and compared

with half sections of the plastic model, but due to a limitation of funds and construction time, a half-space scale lining is investigated in this research.

There is a good deal of past experience and analytical research to validate this method of modeling for segmental joint connections. Lee and Ge (2001), using elastic analyses on steel model lining, indicate that the position of the segmental joint model would change behavior of the whole structure by just a few percent. Cracking around the edge of a segment will make stiffness even less sensitive to the experimental boundary conditions. Zhong and Zhu (2006) show that extrapolating the behavior of a half space of lining sub-assemblage to the behavior of the complete lining system is a realistic procedure.

4.3 Design and Description of specimen

Until now, there are very few studies on the behavior of segmental joints. The only attempt was to implement existing evaluation procedures and adjust some specific parts using available information such as sealing cushion, transmission cushion, and connection surface (Zhong, 2006). To obtain reliable results, it is clearly seen that each evaluation method should be based on real behavior that is easy to predict. It should be noted that a segmental joint evaluation procedure is intended for general patterns of tunnel structure, not specific ones. Therefore, testing methods that can impose real pressure are not necessary. The test specimen is designed to represent the real behavior of typical segmental joint connections under excited loading. An attempt to achieve this concept was conducted by selecting the specimen in a way that processes the value of structural indices in the range of mean value. The main structure of the tunnel lining is real input as much as possible.

The plastic test specimen designed for this study is one fortieth of full-scale. It should be noted that specimen is scaled down this amount due to economic sample size and laboratory area limitations. At this scale, the 4.50 m diameter of the full-scale prototype structure is scaled down to 0.15 m, the 9.00 m length of the lining is scaled down to 0.30 m,

and the 26 cm lining thickness is scaled down to 0.85 cm. One advantage of the scale chosen for the test specimen is it can meet a limited budget and it is easy assembly. The samples in this test are mainly composed of two types of specimen. One is a half structure of the lining. This model is set up to evaluate angular stiffness of the lining's segmental joints. The second specimen type is the lining's whole structure. This model is set up to evaluate segmental joint behavior and the effects because of the number of joints in the complete structure. Drawings of the plastic model specimen used in this test is shown in Figure 4.1 and Figure 4.2. To accommodate the installation of the segmental joints in the lining model, two screws must be assembled in the model and each segmental joint. As a result, the overall stiffness of the structure should be stronger than the design and failure of the structure must be occur only at the hole. However, this study focuses on the elastic behavior and limits in service load interval. For comparison and results reliability, a second full-scale testing should conducted.

The full-scale specimen is reinforced-concrete and includes two segments of a water drainage tunnel project in Bangkok, Thailand. The outside diameter of the structure is 4.50 m, the lining thickness is 0.26 m, and each segment has a width of1.00 m. The concrete segments are assembled with a high-strength steel bar. A drawing of the full-scale structure specimen used in this test is shown in Figure 4.3. This test is designed as a part of the complete lining which is constructed underground. In the model test, the the plastic's specified yield strength for the segment and joint is 24 MPa and the modulus of elasticity is 2400 MPa. For full scale test, the concrete's specified yield strength segment is 40 MPa and the modulus of elasticity is 3040 MPa. The steel bar used to connect each segment has a specified yield strength of 480 MPa and the modulus of elasticity is 2.04×10^{6} MPa.

The objectives of this study are to carry out a structural examination of a tunnel's segmental joint behavior obtain the various physical properties of the segmental joints and segmental lining. Information on segmental joint behavior for tunnel structure numerical

models found in journals, text books and international proceedings was collected and reviewed.

4.4 Preparation of Test Specimen

The plastic model lining specimen should be prepared to represent the segmental joints which influence the whole lining structure.This study focuses on only radial segmental joints which connect each segment to form a ring. Therefore, a plastic model specimen is only connected in radial direction. Before the test is started, material properties should be investigated, including modulus of elasticity, specimen's physical properties as shown in Figure 4.5, Figure 4.6 and Figure 4.9 respectively.

This experiment is based on a plain strain assumption. Hence, longitudinal strain is not considered. Another test is conducted on the two full-scale reinforced concrete segments once connected. Emphasis is placed on reproducing actual construction procedures to minimize error that will cause differences in behavior between the specimen and prototype. For the full-scale test, the sspecimen must be prepared by the manufacturer of the segments on site.

4.5 Fabrication of specimen

The plastic lining model was made from PVC pipe cut to equal lengths. Every segment is connected, or installed, by a small plastic pieces in a circumferential direction with varying thicknesses and then assembled with steel bolts in a longitudinal direction as shown in Figure 4.1 and Figure 4.7. This is done to reproduce actual segmental joint behavior as much as possible. In the model tests, the segmental lining is constructed from PVC pipe with a Young's modulus E of 2400 MPa. The lining ring is composed of four and

six segments. The outer diameter is 150 mm and thickness of the lining is 8.5 mm. The width of each segmental ring is 300 mm, which is long enough to avoid edge effects. The four plastic segmental joints are 3 mm × 25 mm, 8.5 mm × 25 mm, and 8.5 mm × 300 mm respectively. The joints of the plastic lining model are located at θ = 45, 135, 225, 315 respectively for four segmental linings, and ω = 30, 90 150, 210, 270, 330 for six segmental lining respectively. In the plastic lining model, strain gauges were attached on the outer and inner surface of the lining and displacement transducers were set up in the vertical and horizontal directions to measure the lining deformation during testing. Before attaching the strain gauge to plastic specimens, the area of interest must be selected by engineering justice and preparation of specimen surface had to be completed. To avoid the edge effect, strain gauges were attached at the midpoint of the surface. Then, strain gauges were attached to transverse the specimen by a chemical adhesive. To prevent short circuits, strain gauge wires were protected with normal paper tape and strain readings by a data logger were carried out throughout the attachment, procedure that proved to be effective in this study.

The model for the full-scale test sincludes segments of a prefabricated reinforced concrete underground water drainage tunnel. Model tests were conducted using two connected segments. The test arrangement is depicted in Figure 4.3 and Figure 4.4. Tested segments were connected by 2M22 curved bolts of grade 6.8 (f_y = 480 MPa) and supports were connected at the same bolts.

4.6 Testing setup

Figures 4.1 to 4.3 show the overall test setup. The test plastic specimen is supported by two 12 mm diameter steel bars which have the same interval as line loading at the lining crown. The support is used to restrict movement in a transverse direction and determine the model tunnel lining joint stiffness. A full-scale model test for loading

conditions was conducted by two line loadings applied on the tunnel crown by a hydraulic actuator with a capacity of 10 kN force. The loading and support structure were insprepared with pre-bored holes produced by an actuator machine using four 12 mm (5/8 inch) diameter bolts. The bolts were fastened as tight as possible to create pre-stress force in the bolts, to minimize slippage.

Each support segment is also connected with a steel frame by 2M22 curved bolts of grade 6.8. These steel frame assemblies transfer the reaction force to the strong floor and are fixed on both ends. Vertical loading from the actuator is transferred to two steel H sections to represent two lines, the same as the for the plastic model. Maximum capacity of the hydraulic actuator for this test is 120 kN. A designed deflection at the tip of reaction frame for static force of 120 kN is 0.3 mm.

4.7 Instrumentation and Data Recording

The test plastic specimen is designed as shown Figure 4.7 and Figure 4.8 to obtain data on excited loading, vertical displacement, and member strains. Vertical load applied to the top of the specimen was measured by load cells attached to the actuators. The vertical displacement of the specimen was measured using LVDT installed outside the specimen as shown in Figure 4.1and Figure 4.8. The LVDT was placed on a magnetic stand attached to a reference based frame. In another full-scale test, a dial gauge placed by a magnetic stand attached to a reference frame was used to measure displacement In addition, vertical load applied to the crown of the specimens was measured by load cells attached to actuators. Prior to testing, this load cell was calibrated by standard proving ring (Clockhouse Engineering Ltd., England). Three instruments were also used for data acquisition: a data logger model, automatic switching box model, and personal computer. The data logger and automatic switching box read the data from each instrument and transferred the data to the personal computer in text format.

4.8 Testing Procedures

When considering the experimental simulation of exited loading on a structure to study segmental joint behavior, it often happens that a distinction is made between tests conducted to improve the understanding of material or structural behavior and tests intended for the verification of response. The first type of tests is conceived as an aid in the development of numerical models for materials or structural elements. The objectives of the second type of test is considered to be the verification of the response of structural elements, or an entire structure subjected to excited loading as predicted by a previously developed model, or to verify the performance of a structural system designed according to specific methodology (Calvi and Kingley, 1996).

The specimen setup for testing is to facilitate monitoring of deformation during testing. The basement frame is attached with a measurement meter and grid lines spaced at 10 mm. The vertical actuator is attached to the crown of the specimen in all experimental cases. After preparing the specimen, instrumentation that measures the response of the specimen is wired, calibrated, checked and installed onto the test specimen. Next is the testing. Before beginning, all instrumentation and data acquisition are rechecked and zeroed. The testing begins with the pumping of the vertical actuators to apply vertical loading. During testing, data is collected at appropriate intervals (2 seconds). The fifty-two loading steps (applied vertical load P) are carried out to a maximum load of 10 kN for the plastic model test and 120 kN for the full-scale segment test to determine the joint stiffness of the model tunnel. When the test is completed, equipment is once more checked and corrected. Then, after the instrumentation is removed, the plastic models are discarded and the full-scale specimen cut into small parts for removal.
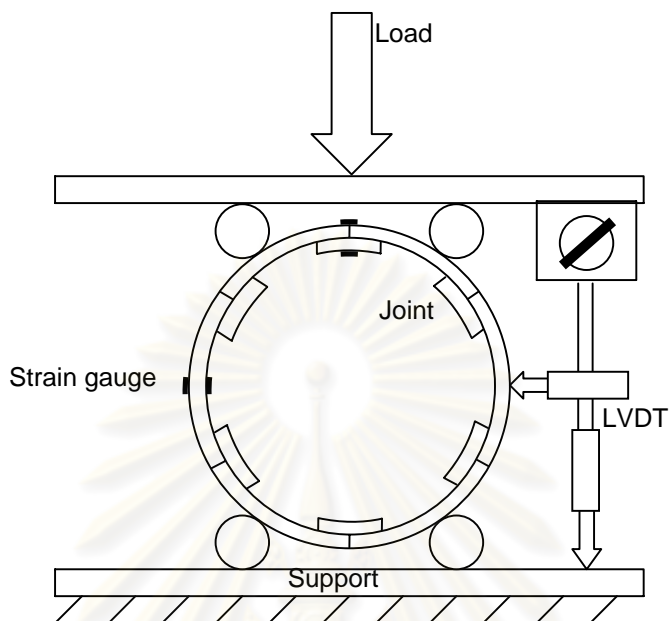
Figure 4.1: The full section plastic model test set up
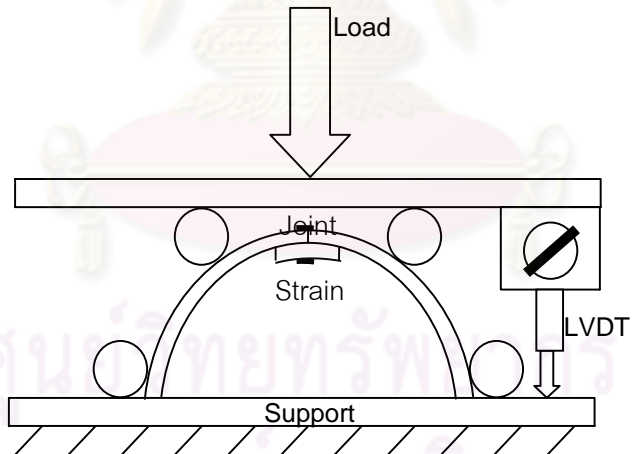

Figure 4.2: The half section plastic model test set up
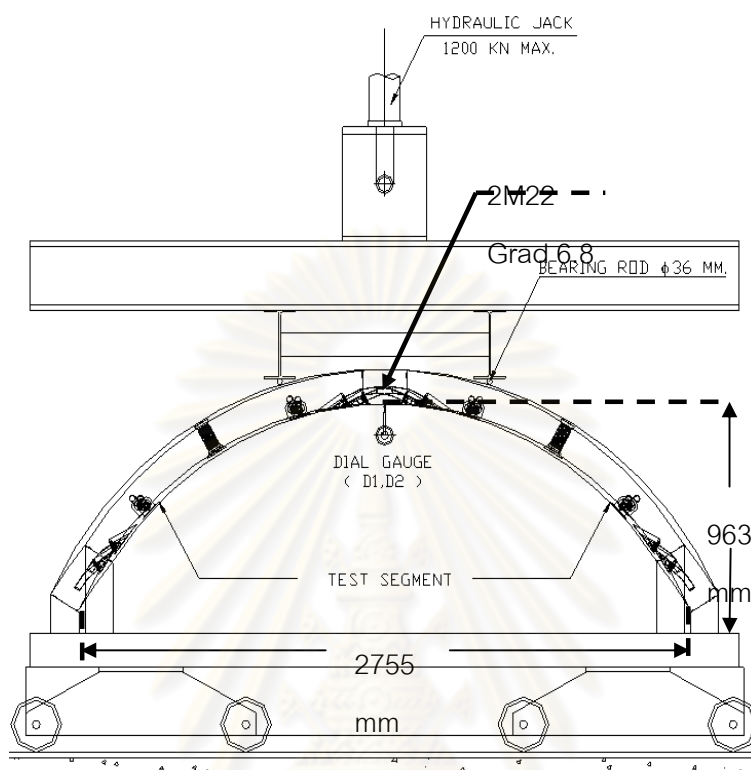
Figure 4.3: Full scale test set up
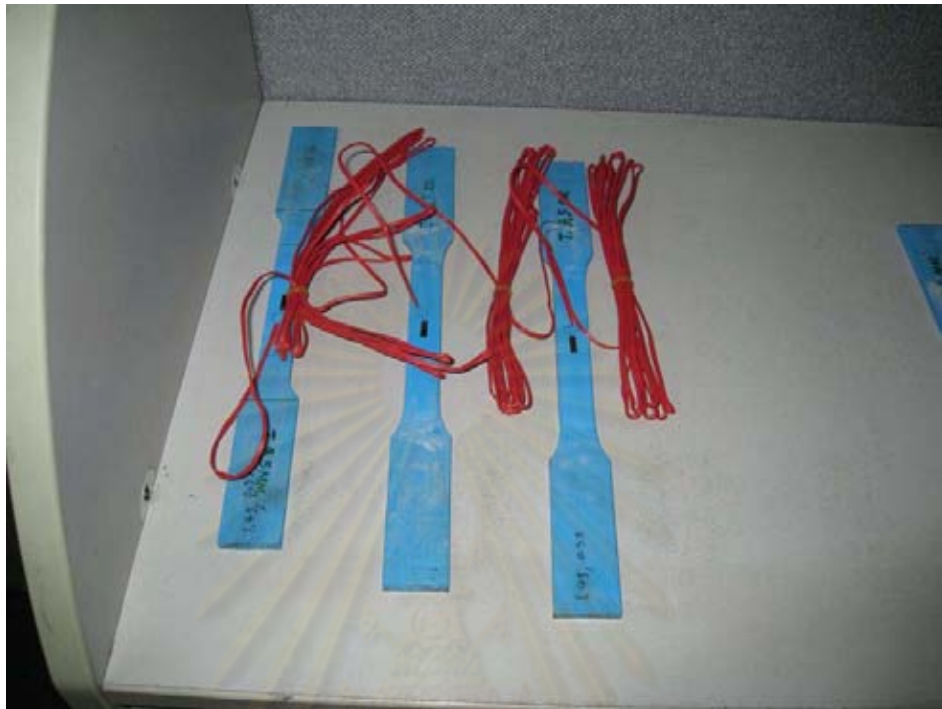

Figure 4.4: Photo of full scale test specimen

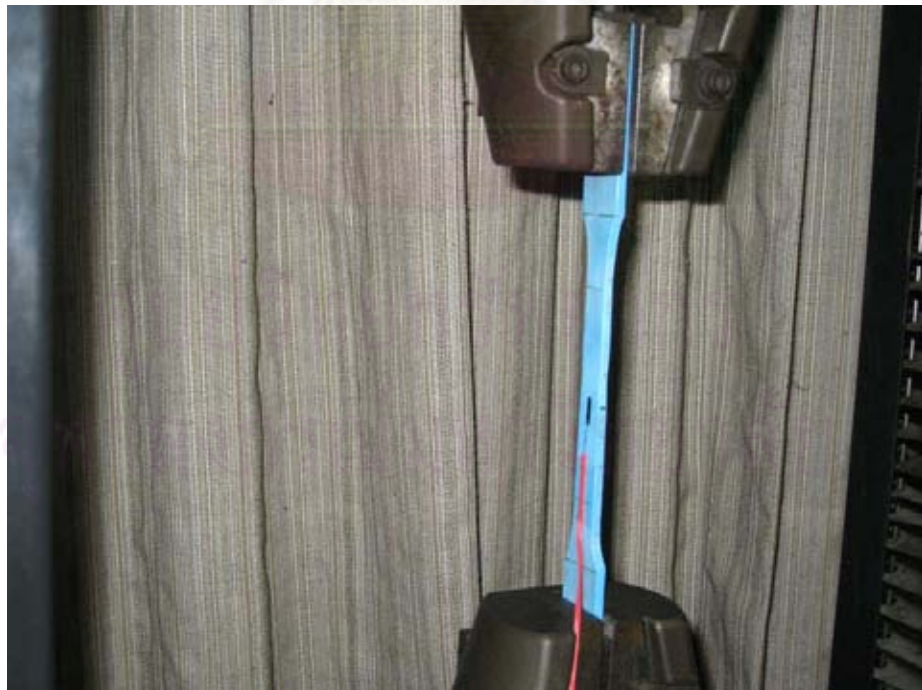Figure 4.5: Prepare material testing

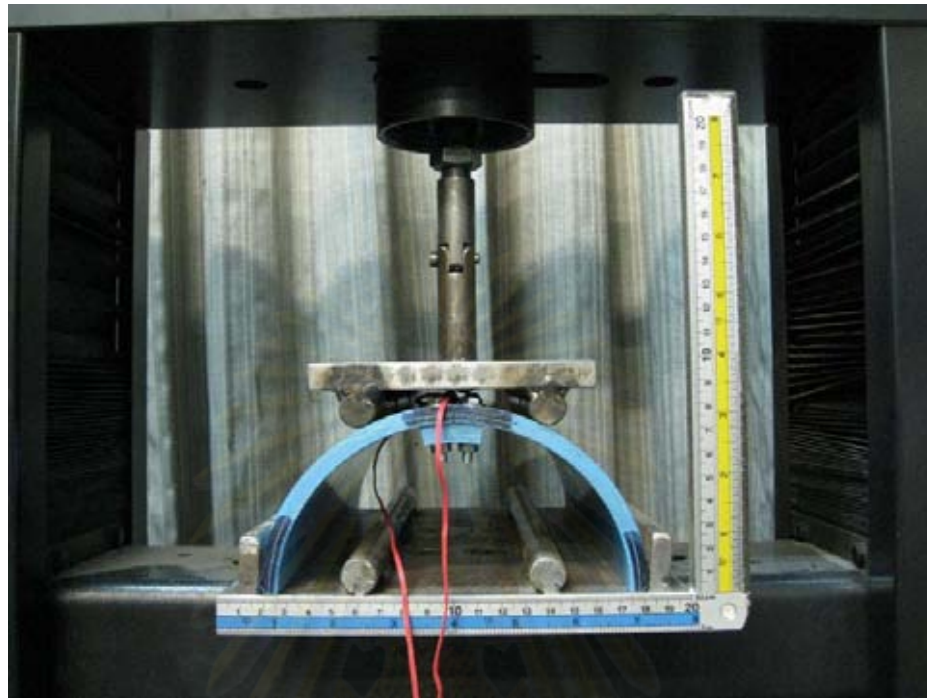
Figure 4.6: Testing material property
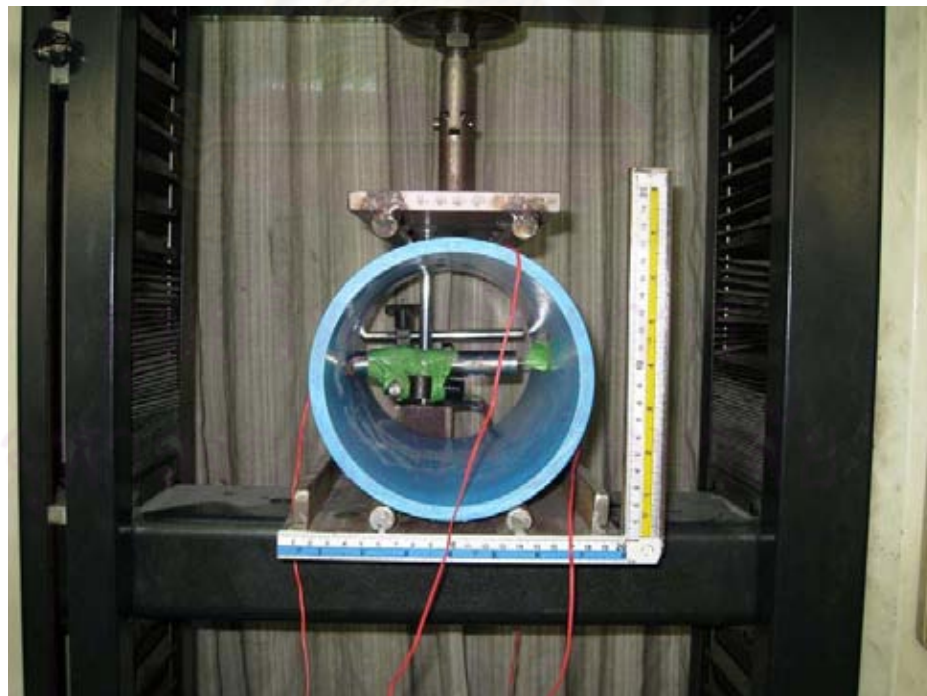
Figure 4.7: Photo of half section plastic test specimen

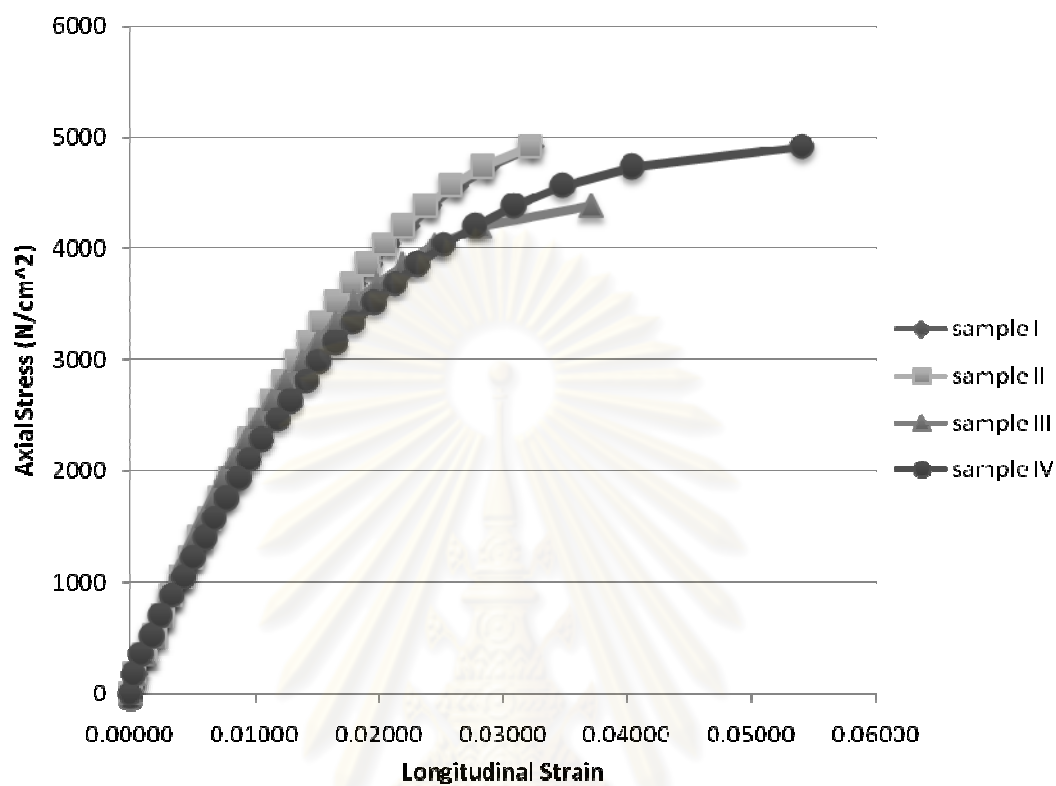Figure 4.8: Photo of full section plastic test specimen

Figure 4.9: Material property of plastic lining model.

CHAPTER V

Numerical Result, Experimental Results,
and Discussions

5.1 Overview

The shield-driven tunneling method has been widely adopted for construction of urban underground tunnels in soft ground. Joined segmental precast concrete linings connected by steel bolts are commonly used in most shield-driven tunnels. As the lining of a shield-driven tunnel is not a continuous ring structure due to the existence of joints, the effects of the joints on internal forces and structure deformation should be taken into consideration in the design of a tunnel lining. In numerical analyses of underground shield-driven tunnel problems, one of the major difficulties lies with the proper simulation of the structural behavior of the segmental joint in a tunnel. A way to deal with this issue is to consider the tunnel lining as a continuous ring with a discounted rigidity by applying a reduction factor, n, to the bending rigidity (EI) of the tunnel lining. The value of the reduction factor adopted in the tunnel project is later verified by tests on a full-scale prototype segmental lining.

The experimental results obtained from the static loading test of a one-fortieth plastic model are presented. The specimen performance was evaluated on the basic of moment capacity and deformation behavior. Bending moment at any section of a specimen was calculated based on static equilibrium. A comparison between the numerical and experimental results was carried out to investigate the behavior of segmental joint structure in whole tunnel.

5.2 Numerical and full scale test Result

In this work, SAP2000, a finite element program, is used to solve three-dimensional behavior of the tunnel problem. To simulate underground behavior, circumferential soil around the tunnel is simulated by soil spring stiffness, which is generated from subgrade modulus. However, this study does not focus on behavior of the soil which is not considered a yield failure surface. Therefore, soil spring stiffness is constant and stays on a linear elastic zone. The circular tunnels and steel bolts are modeled to shell and rigid beam elements respectively. This research focused on segmental joints in a tunnel lining. However, each tunnel project does not use the same criteria to design the lining. Therefore, this research should be studied on affected segmental parameters as follows:

5.2.1 Effect of number and orientation of joints

First of all, joint orientation effect is investigated by rotating the joints and increasing the number of joints along the tunnel's circumference to find the absolute maximum moment in the structures. From the results, joint orientation is found to greatly affect the amount of maximum bending moment acting on the lining. Every joint orientation pattern has a maximum moment in the circular structure as shown in Figure 5.1. A reference joint is defined as the joint located closest to the tunnel crown in clockwise direction from the tunnel crown. The variation of maximum bending moment against joint location is sinusoidal in nature at which frequency increases according to the number of joints.

The maximum bending moment, which is generally used in the design of aa lining structure, therefore varies within the boundary of oscillation of the sinusoidal curve, which gives the upper and lower values of maximum bending moment. The variation can be generally represented as a function as shown below:

$$M_N = \left(M_{nonjo\,int} - 5N\right) + A\sin\left(N\theta - 90\right)$$

(5.1)

where N = Number of joints in the lining,

θ = Angle of rotation (Figure 5.5)

A = Amplitude of the sinusoidal curve = $f(N, K_\omega, k)$

k = Subgrade modulus

This empirical equation is difficult to normalize to provide a dimensionless representation. Further detail investigation into the analytical results as described in the following paragraphs leads to a more practical representation.

Figure 5.1 clearly explains the influence of number and orientation of joints on the maximum bending moment induced in the tunnel lining. If the number of joints is increased in the lining structure, the maximum bending moment diagram will be reduced in the lining. On another hand, minimum moment on the lining structure does not show the same pattern as the maximum bending moment, which can be classified into two groups. The minimum bending moment of an even number of joints increases joint numbers, while the minimum bending moment of an odd number of joints decreases with joint number. Additionally, the bending moment of even joint number has only a maximum peak, but the bending moment of an odd joint number has two maximum peaks. Moreover, it should be noted that 4 joints induced the highest and lowest maximum bending moments as compared to other joint numbers, and maximum bending moment of 4 joints is higher than no joint at all. Furthermore, the interval value between maximum and minimum bending moment will decrease when the joint number is increased. The different value of bending moment is lower than 10 percent when the joint number is more than 7, which achieves maximum bending moment when joint orientation becomes insignificant for cases involved with a greater number of joints. This reflects the behavior of rigidity structure distribution and can be explained by the fact that

for tunnel rings with greater more segments, the span of each segment becomes shorter. These observations are important in the design of segmental tunnel rings as the location of each segmental tunnel ring joint varies along the tunnel alignment. The bending moment is directly related to stress induced in each segmental tunnel ring. Hence, the stress induced in each segmental tunnel ring of different joint orientation is different for the same ground conditions and tunnel depth.

5.2.2 Effect of angular joint stiffness

Not only the number and orientation of joints but also joint stiffness is a factor that directly affect stress distribution of a segmental ring. Therefore, joint stiffness is studied in this research by varying stiffness values in the tunnel modeling. It is assumed that the segmental ring is deformed but ignored in the mechanical analysis of the joint. Hence, the concrete surface at the joint is considered as a rigid surface. Additionally, each segmental ring is connected by an arc steel bolt. The result is that each segment can not freely translate in x, y, and z directions, but it can rotate slightly in a longitudinal direction when enough force acts on the structure. Hence, the assumption that joint stiffness of a segment ring is considered only for angular joint stiffness. The calculation thus varies for angular joint stiffness and the number of joints in a reinforced concrete tunnel model.

Figure 5.2 and Figure 5.3 show the plots between the upper and lower values of the maximum bending moment against the angular joint stiffness, K_ω. The results are obtained from a case where the diameter of the tunnel and subgrade modulus of surrounding soil are 4 m and 15,000 kN/m^3 respectively. When joints are rigid (high value of K_ω), the maximum bending moment, both upper and lower values, of the jointed lining becomes natural, approaching the non-jointed one. However, within the recommended range of the angular joint

stiffness for design ($\approx$ 1,000 – 3,000 kN/rad), the maximum bending moment decreases to about 0.50 – 0.95 (for upper value of maximum bending moment) and 0.3 – 0.90 (for lower value of maximum bending moment) of that obtained from the non-jointed lining, which varies according to the number of joints in the structure. Maximum bending moment with angular joint stiffness becomes insignificant for cases involving high angular joint stiffness. This lining behavior could be explained by the fact that for a tunnel ring with greater angular joint stiffness, the stress can be dispersed throughout the entire segmental lining.

However, the actual angular joint stiffness is very difficult to fit a value for use in design because it has many parameters that affect it such as type of steel joint, position of steel bolt in the segmental ring, pre-tension applied to the steel bolt, and transmission cushion. To obtain a value for the angular joint stiffness, the load deformation relationship of segmental lining must be determined by assembling the two actual segmental linings as in the actual construction of the water supply network in Bangkok. Tested segments were connected by 2 M22 curved bolts of grade 6.8 (f_y=480 MPa). The testing method is to determine two point loads which eliminate the effect of shear force on a joint structure as shown in Figure 5.4. To estimate the practical range of the angular joint stiffness, K_ω, simple FEM analysis using a similar configuration as the main analysis is conducted to simulate the test results. The relationships between the vertical load and deformation obtained from testing and analytical results are plotted together in Figure 5.5.

The results show the relation of load and displacement in nonlinear characteristics. The fitted formula for load-displacement of segments test is

$$D = 0.006F^2 + 0.0407F \qquad\qquad (5.2)$$

where, D is the vertical deformation and mid curve of segments (mm)

F is the two point load on the structure (kN)

Nonlinear behavior of load-displacement can be explained by the segment joint which is connected by a steel bolt with the cross section area of the bolt being smaller than the cross section of the segment area. Although stiffness of the steel bolt is higher than stiffness of the concrete segment, it is not enough to represent all concrete segments. Second, the two segments are not completely connected to each other; therefore, distribution of stress and stress transfer are not complete. The behavior is explicitly explained when the applied load is very high. The lower positions of segments are separate to each other. In this stage, the force and moment of the steel bolt increase rapidly, which is the trend of angular rotation. These will all directly affect the behavior of load-displacement. In addition, angular stiffness is dependant on many factors that are difficult to clearly explain. However, if the load deformation relationship in testing is compared with computer simulation, the possible range of the angular joint stiffness for a design should be 1650 kN/m to 2550 kN/m. These angular stiffness values develop over 80% of maximum bending moment of a no-joint tunnel structure as shown in Figure 5.5.

The reduction in maximum bending moment, called herein moment reduction factor, η, is also strongly dependent on the number of joints in the lining. A lining with a larger number of joints exhibits larger value of η. The values of η obtained from other analytical cases are summarized in Table 5.1.

5.2.3 Effect of lining flexibility

The number of joints does not only directly influence the maximum bending moment induced in a tunnel structure but also affects the bending moment of all segments in a segmental ring tunnel as shown in Figure 5.6. This

behavior comes from the flexibility of the lining effect. Ashraf investigated behavior of lining flexibility with flexibility ratio, F, defined by Peck (1972) in Equation 5.2.

$$F = \frac{\dfrac{E_s}{(1+\upsilon_s)}}{\dfrac{6E_l I_l}{(1-\upsilon_l^2)R^3}} \tag{5.3}$$

where, E_s is the young's modulus of the ground

υ_s is the Poisson's ratio of the ground

E_l is the Young's modulus of the lining

υ_l is the Poisson's ratio of lining

I_l is the moment of inertia of the lining of the cross

section per unit length

R is radius of the lining

Flexibility ratio is the flexural stiffness ratio between the ground and the liner, with flexural stiffness defined as the resistance of change in shape under a state of pure shear (Son, 2007). Ashraf found that the number of joints directly influences the rigidity of a tunnel structure. From the flexibility ratio equation, inverse lining flexibility relates to the stiffness of the soil. Figure 5.7 expresses the influence of the subgrade modulus of surrounding soil on the upper value of maximum bending moment. When a lining is simulated in a stiffer soil (higher value of subgrade modulus), the maximum bending moment acting on the lining decreases. The increase in tunnel diameter also results in increasing the maximum bending moment as shown Figure 5.8. Fortunately, the influences of the subgrade modulus and tunnel diameter are equally applied to both jointed and non-jointed cases. As a consequence, the relationship between $\eta \sim K_\omega$ is not affected by the change in stiffness of soil and diameter of tunnel. Similar

$\sim K_{\omega}$ curves, as those shown in Figure 5.2, can be obtained from other analytical cases with different values of subgrade modulus and tunnel diameter.

Since installation of segmental lining during tunnel construction is random in process, the upper value of maximum bending moment (Figure 5.2) should be selected in practice to provide safe lining design. In the present study, an empirical correlation that best fits the $\eta \sim K_{\omega}$ curves in Figure 5.2 is proposed as:

$$\eta = \frac{(4/N)^2}{1+K_{\omega}} + \frac{K_{\omega}}{1+K_{\omega}}$$

(5.4)

where N is the number of joints in the lining. When K_{ω} is equal to zero, the joint becomes perfectly hinged and $\eta = \left(\dfrac{4}{N}\right)^2$ is attained as recommended by Wood (1975). Therefore, the effective moment of inertia of a segmental tunnel ring with a number of equal segments can be expressed as

$$I_e = I_j + \eta I \qquad I_e \leq I, \, n>4$$

(5.5)

5.3 Study of experimental result

The experimental results obtained from static loading test of a plastic lining model specimen are presented. The specimen performance was evaluated on the basis of stress-strain behavior, deformation and moment capacity. Bending moment at any section of a specimen was calculated based on static equilibrium and based on plain strain conditions. A comparison between the predicted and experimental results was also carried out to investigate the performance of those formulas in predicting the behavior of the specimens.

To study the structural performance of the multi-joint lining system, the relationship between deformation of a tunnel section and vertical load must be

investigated in a laboratory. The overall behavior of the specimen is represented by the force-displacement relationship at the crown of the lining specimen. In the experimental data, some information of the specimen behavior can be qualitatively indicated. First, the overall load resistance of the specimens is directly dependant on the performance of segment-joint connections. When the connection failed prematurely in bending moment, the segmental joint could not develop its full flexural capacity and the observed strength of the specimen was lower than expected.

The test is conducted in the same way as full-scale testing. The tests started with determining joint stiffness by comparing results of a half-section test and numerical results. After that, the calculated segmental joint stiffness is used to calculated η factor to predict inertia of the lining section that will be used in lining design method.

For the purpose of optimizing the design of a segmental joint in a circular lining, the experimental tests were conducted on two test groups according the above details. The first group was used to determine the angular stiffness of a half section of lining with varied physical properties of the segmental joint. Results of first group are then compared with numerical results to find angular joint stiffness in each test. In this study, numerical studies using the computer program SAP2000 are also conducted using the material properties according to experimental tests. The angular stiffness of the tests are shown in Table 5.3 and Fig. 5.19 to Fig. 5.22. The analyses of flexible rigidity (EI) of joints and main segments showed predominant angular stiffness of joint lining which directly affects the behavior of the whole lining structure. In addition, other segmental joint components such as sealing cushion and surface of connection showed minor effects of angular joint stiffness. From the experiment, carrying maximum moment of the multi segment lining structure should be discounted 50 – 90 % when compared with a continuous ring as shown in Fig. 5. In lining design, tunnel lining as a multi-segment ring should discount the bending rigidity factor with a continuous ring.

The plastic specimen was loaded with uni-axial testing mechanic increased to 10000 Newtons in 200 Newtons increments. At each increment, the data accusation mechanic records vertical displacement and strain at the surface of the plastic

specimen. Figure 5.9 indicates the relationship between vertical load and vertical displacement. From the relationships, a non-joint lining section has the straightest structure when compared with other tests. This test confirms the numerical results that non-joint lining stiffness is highest, and the summaries of the tests show that the number of segmental joints mainly affects lining behavior. In addition, the deformation of a lining section increases as the number of segmental joints is increased while the strength of segmental joints decreases. However, the weakest segmental joint stiffness in this test is not a clear behavior because the model failed before full developed loading was achieved.

Figure 5.10 and 5.11 show a plot of the bending moment on the crown of tunnel lining against vertical displacement and vertical loading respectively. The results are in line with numerical results of bending moment that show four segmental joints in a lining case are higher than non-joint lining. Moreover, the bending moment in a six segmental joint case must be lower than the bending moment in a non-joint lining section case. However, one case of the bending moment of four segmental joints in a lining is lower than the bending moment in non-joint section because of the stiffness of the bolt connection. Furthermore, the weakest segmental joint stiffness is not clear because the model structure failed before full developed loading.

Figure 5.12 and 5.13 show the relationship between displacement of a homogeneous section and a multi-section tunnel. This strongly confirms the numerical results and assumption that number and strength of segmental joints affect strength and stability of a whole tunnel structure. In additional, Figure 5.14 and Figure 5.15 show the plot between vertical displacement and vertical loading of a half section. This test uses the two-point load method. The results as agree with the above graph. However, Figure 5.16 does not demonstrate clear behavior because the strain gauge is not in good condition and thus, the data is questionable. In addition, results from the plastic model testing show that segmental joint angular stiffness is mainly affected by the flexibility of the lining structure. Figure 5.30 to Figure 5.34 show the relationship between segmental joint stiffness and bending moment. The graph shows that resistant bending moment will

increase when segmental joint stiffness is increased. As a result, the structure can increasingly afford stress when the segmental joint strength of a structure is increased. Despite the strength and area of inertia of a segmental joint being equal to the main segment of the lining, deformation of a multi-segment structure is still higher than deformation of a homogenous lining structure because of the connectivity of the structures.

5.4 Comparison between predicted and experimental results

Figure 5.17 and 5.18 show the simulation model using the SAP2000. This model compares results with experiment testing. Therefore, the loading pattern of the testing and the numerical model try act the same based on the two-point load method. This method tries to reduce the effects of shear and considers bending moment, deformation and rotation of the segmental joint. From the numerical model and half-section specimens, angular stiffness of a segmental joint in an 8.5 mm thickness along the tunnel structure should be 7500 N-rad. Angular stiffness of a segmental joint in N 8.5 mm thickness at some part of the tunnel structure should be 5000 N-rad. Lastly, angular stiffness of the segmental joint in 3.5 mm thickness at some part of the tunnel structure should be 500 N-rad. The matching solution is shown in Figures 5.19 to 5.22. Although different types of segmental joints for the plastic specimen and full-scale concrete are not the same, the pattern of relationship between vertical load and vertical deformation is the same foe full-scale concrete testing as shown in Figure 5.5 and Figures 5.19 to 5.22.

This numerical method is based on a linear elastic model which displays opposite behavior to real behavior of a plastic material. The plastic specimens tested are not perfectly linear elastic as assumed. For small and slow rate loading, the plastic behavior should be linear elastic, while with large and high rate loading, the plastic behavior will be shown as non-linear elastic when combined with plastic behavior.

Therefore, loading of the specimen should be done as slow as the testing machine can do because of the reduced effect of plasticity behavior (Harry, 1999). Finally, the results in the testing have shown some non-linear plastic behavior because the machine can operate not slow enough, and the maximum load of the test is over linear behavior interval. Hence, the results of numerical model and experimental testing should be slightly different as shown in comparisons in Figure 5.19 to Figure 5.29. However, the results of the 3.5 mm segmental joint is different than the numerical results because of segmental joint failure before the structure has been fully loaded. Figure 5.30 to Figure 5.34 shows the effects of angular stiffness with bending moment of a tunnel structure. Compared with the numerical results, the trend of the graphs in Figure 5.30 to Figure 5.34 is close to that in Figure 5.2. This means the strength of the whole structure as well as stress transfer must be developed when angular stiffness of the segmental joint is increased according to the first assumption. However, it is very difficult to develop the real segmental joint strength to be close to the strength of the lining segment because of the stress concentration and weakness of the joint hole in the segment.

5.5 Designed simulation

In this work, it is assumed that the soil pressure is based only on the soil weight and water level being lower than lining location. The basic soil profile is stiff clay as shown in Figure 5.35, where H is the tunnel depth, γ is the unit weight of soil, D is the external diameter of tunnel, λ is the lateral coefficient of soil, and k is the soil resistance coefficient. Additionally, structure parameters of the segment are as follows: calculation diameter of segment is 4 meter, elastic modulus of concrete is 2.482×10^{7} kN/m^{2}, and block partition of the segment is 5, 6, 7 respectively. The segmental joint stiffness determined by experimental testing is 2100 kN/m^{2}.

Table 5.2 shows the effect on the joint according to the maximum bending moment in the lining calculated by many design methods such as Muir Wood, Einstein, JSCE, and Finite Element. There is no joint maximum bending moment by a finite

element method because of a resemble assumption. Moreover, the results of the joint effect from a Finite Element method is lower than with the other methods. Maximum bending moment with 4 joints using a Finite Element method is over the maximum bending moment with a non-joint lining because of the structure of the lining. With different model assumptions, the results of calculation are greatly different. However, when the number of joints is increased, the percentage of maximum moment reduction increases as well. The main reason is that, because of flexibility of tunnel structure, the pressure on the lining is reduced with the increased number of joints, which is to say that the moment is reducing. According to the results, the stiffness of the lining is dependant on the number of joints.

Table 5.1 Moment reduction factors from some analytical cases

General Description	No. of joints	η [1]	η ($K_\omega = 750$ kN/rad [2])		η ($K_\omega = 2,550$ kN/rad [2])	
			Upper value	Lower value	Upper value	Lower value
Soft soil k [3] $= 3,750$ kN/m^3 Diameter = 4 m	4	1	1.08	0.7	1.04	0.88
	5	0.64	0.96	0.86	1	0.95
	6	0.44	0.88	0.79	0.96	0.93
	7	0.33	0.52	0.82	0.94	0.93
	8	0.25	0.49	0.79	0.93	0.92
Soft soil k [3] $= 3,750$ kN/m^3 Diameter = 6 m	4	1	1.1	0.47	1.05	0.75
	5	0.64	0.88	0.73	0.96	0.88
	6	0.44	0.79	0.54	0.91	0.8
	7	0.33	0.68	0.63	0.86	0.84
	8	0.25	0.63	0.56	0.83	0.8
Stiff soil k [3] $= 45,000$ kN/m^3 Diameter = 4 m	4	1	1.12	0.4	1.06	0.69
	5	0.64	0.93	0.73	0.97	0.86
	6	0.44	0.84	0.43	0.92	0.72
	7	0.33	0.7	0.61	0.84	0.8
	8	0.25	0.63	0.54	0.81	0.77
Stiff soil k [3] $= 45,000$ kN/m^3 Diameter = 6 m	4	1	1.09	0.32	1.05	0.62
	5	0.64	1.07	0.81	1.04	0.89
	6	0.44	1.05	0.42	1.03	0.61
	7	0.33	0.91	0.69	0.94	0.81
	8	0.25	0.8	0.37	0.88	0.66

1) According to Wood (1975), 2) Angular joint stiffness, 3) Soil subgrade modulus

Table 5.2: Number of joint effect to maximum bending moment in lining in many design methods

Calculation method	Muir Wood (kN-m/m)	Eintein (kN-m/m)	JSCE (kN-m/m)	Finite Element (kN-m/m)
No joint	189.63	189.48	175.78	178.13
4 joint	189.63 (0%)	189.48 (0%)	175.78 (0%)	187.39 (5.2%)
5 joint	166.87 (12%)	170.91 (9.8%)	163.65 (6.9%)	169.94 (4.6%)
6 joint	145.64 (23.2%)	152.34 (19.6%)	151.17 (14%)	159.96 (10.2%)
7 joint	126.67 (33.2%)	135.1 (28.7%)	139.04 (20.9%)	150.34 (15.6%)
8 joint	109.99 (42%)	119.56 (36.9%)	127.79 (27.3%)	145.71 (18.2%)

Table 5.3: Angular joint stiffness in each test

Size of segmental joint	Angular joint stiffness
3 mm × 25 mm	500
8.5 mm × 25 mm	5000
8.5 mm × 300 mm	6000
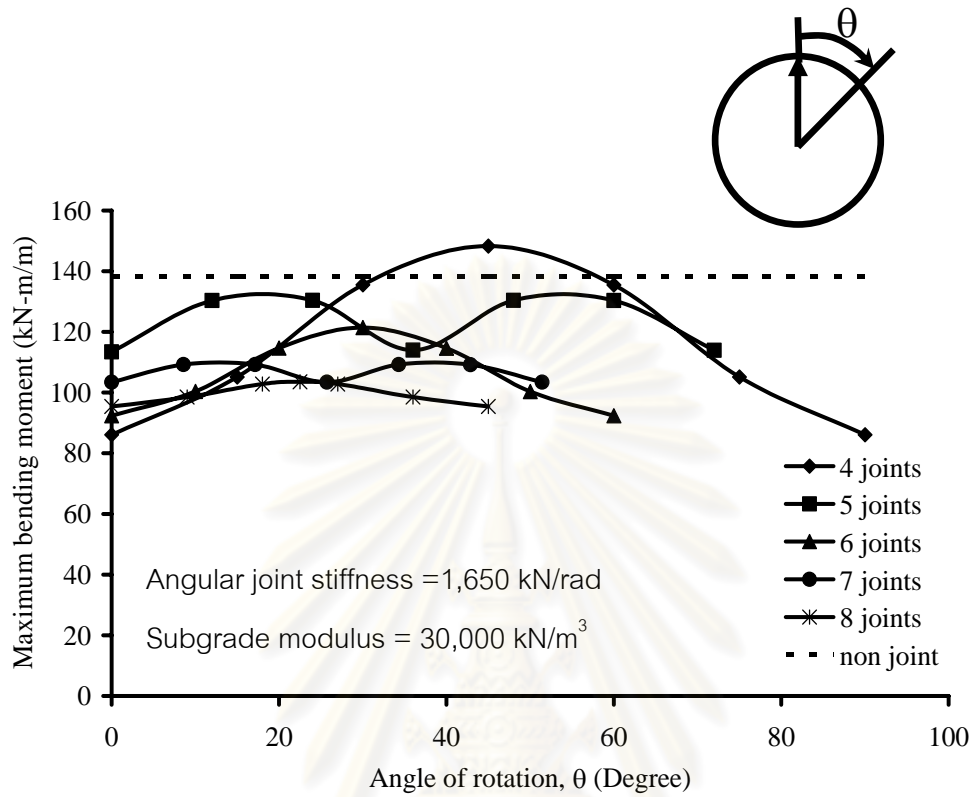
Figure 5.1: Variation of Maximum Bending Moment with Number and Orientation of joints.
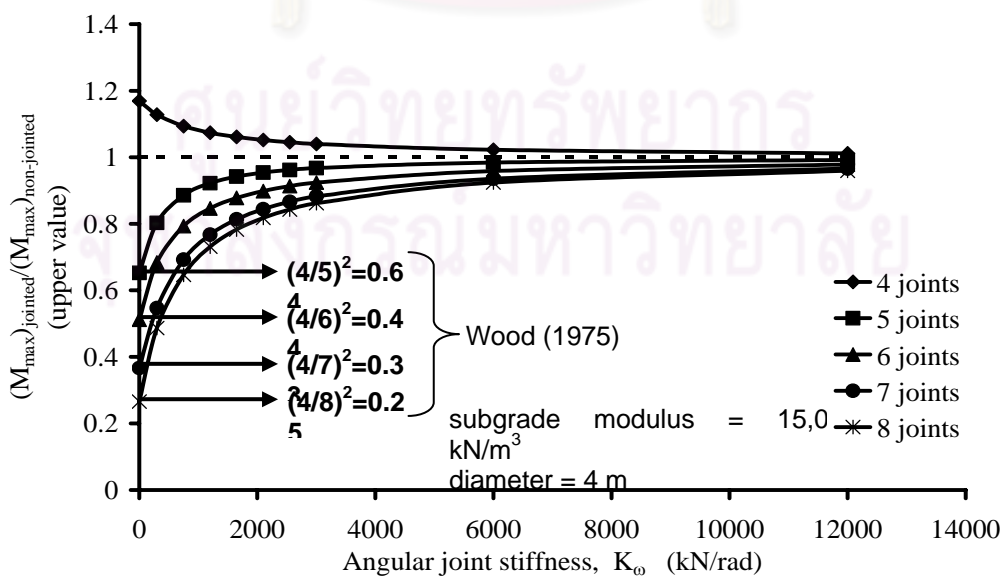
Figure 5.2: Normalize of Maximum Bending Moment with angular joint stiffness.
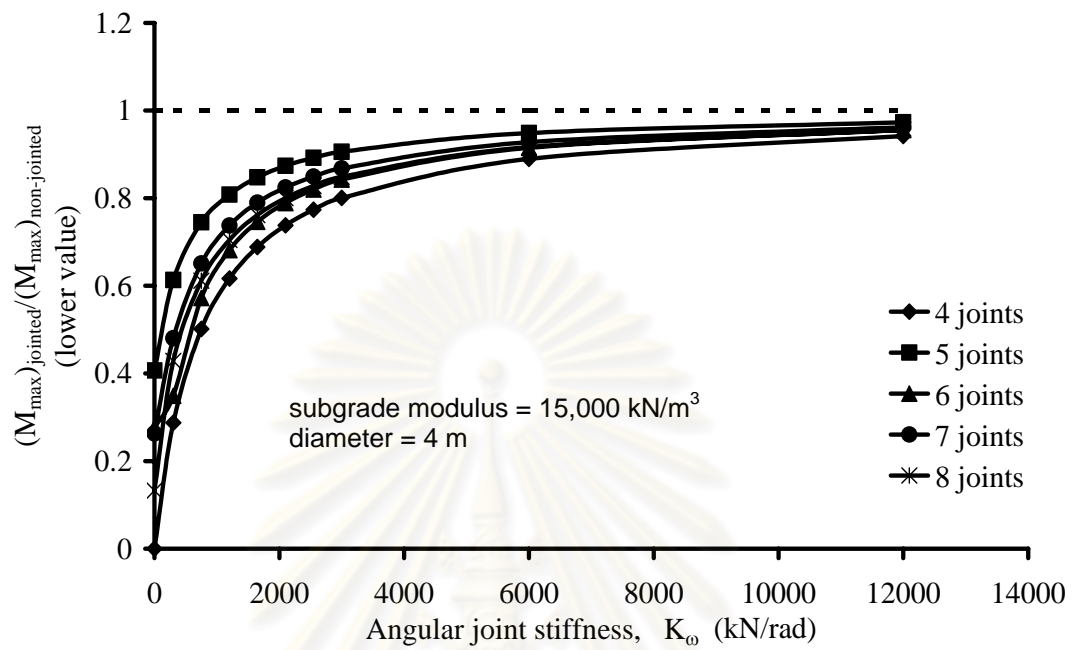
Figure 5.3: Normalize of Minimum Bending Moment with angular joint stiffness.
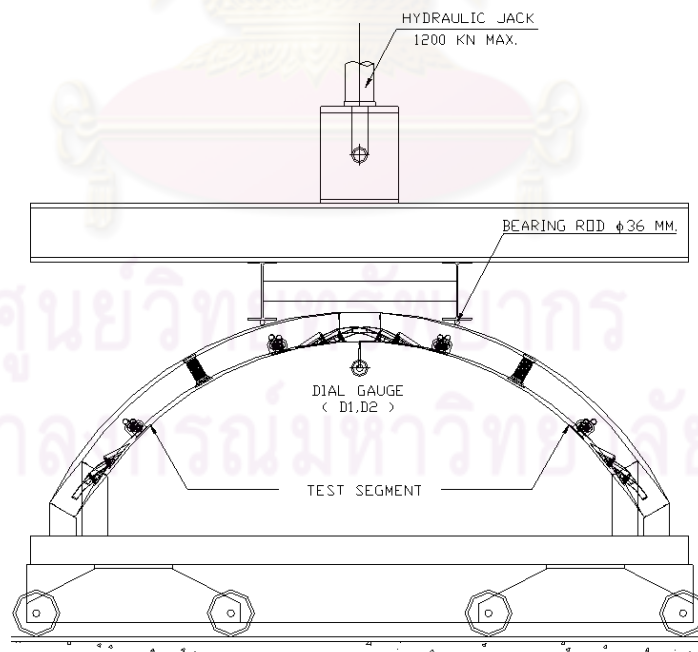
Figure 5.4: Angular Joint Stiffness Testing Equipment.
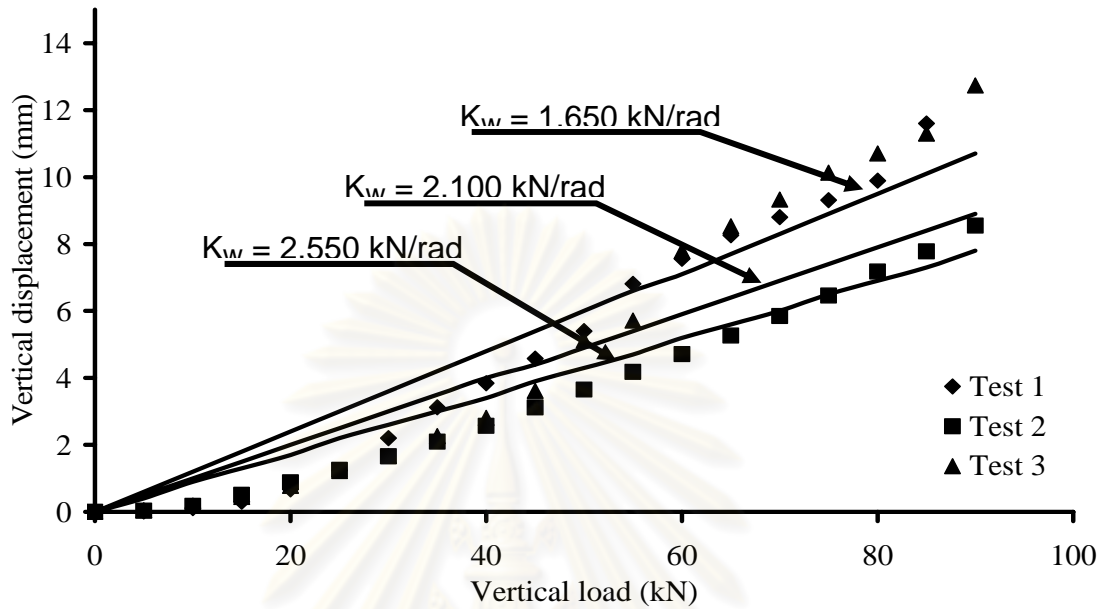
Figure 5.5: Relationship of load with displacement in segments testing
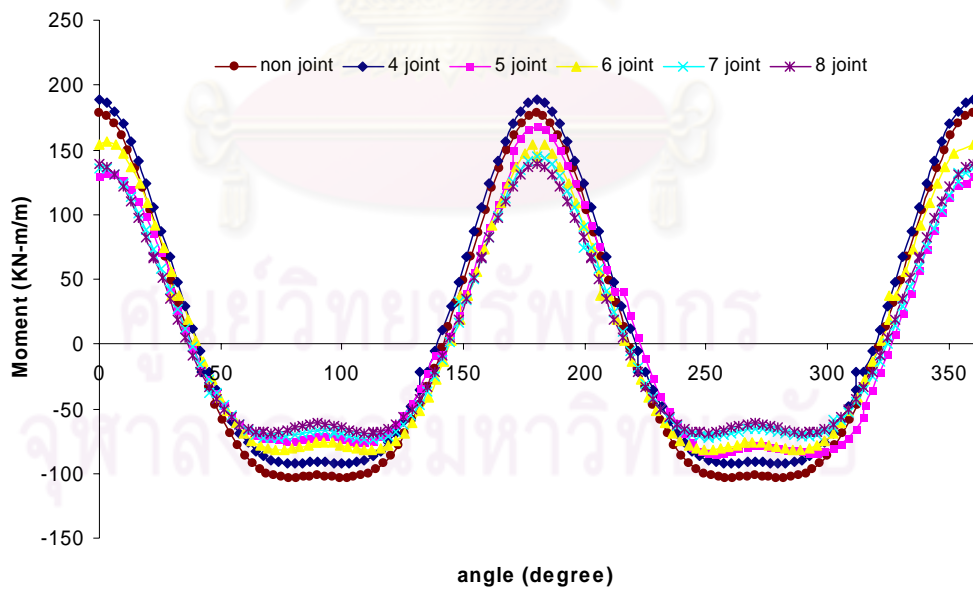
Figure 5.6: Variation of Moment distribution in Lining Structure with Number of joints
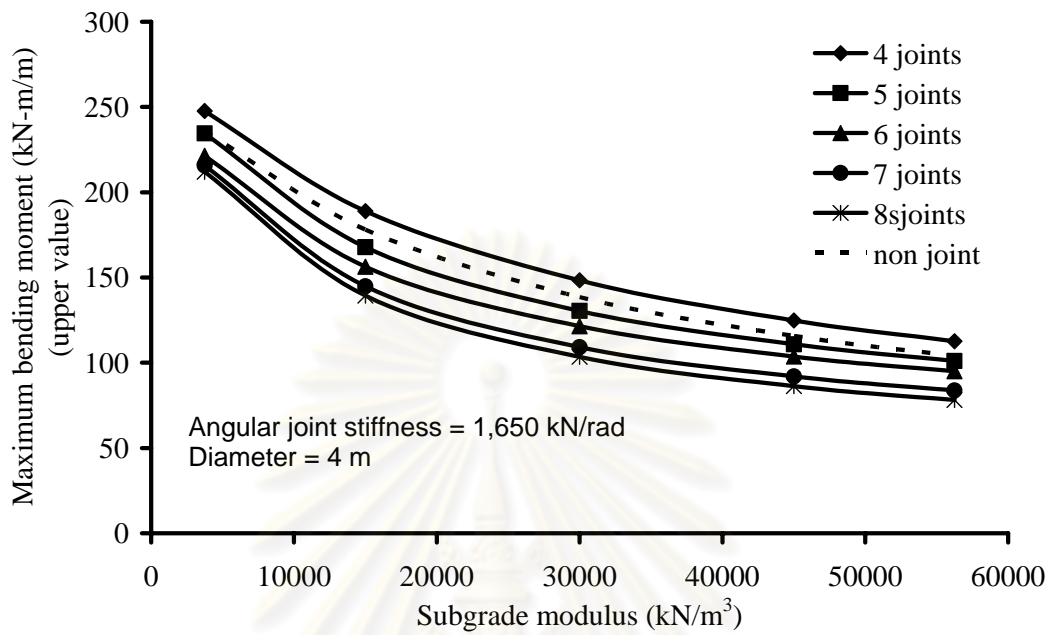
Figure 5.7: Variation of Maximum Bending Moment with soil spring stiffness
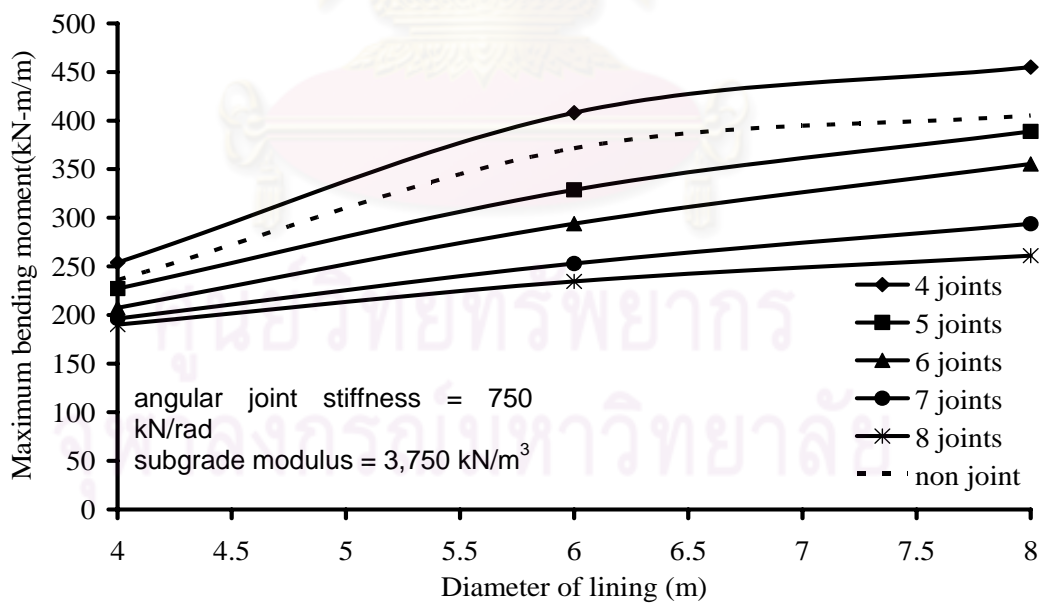
Figure 5.8: Variation of Maximum Bending Moment with diameter of lining
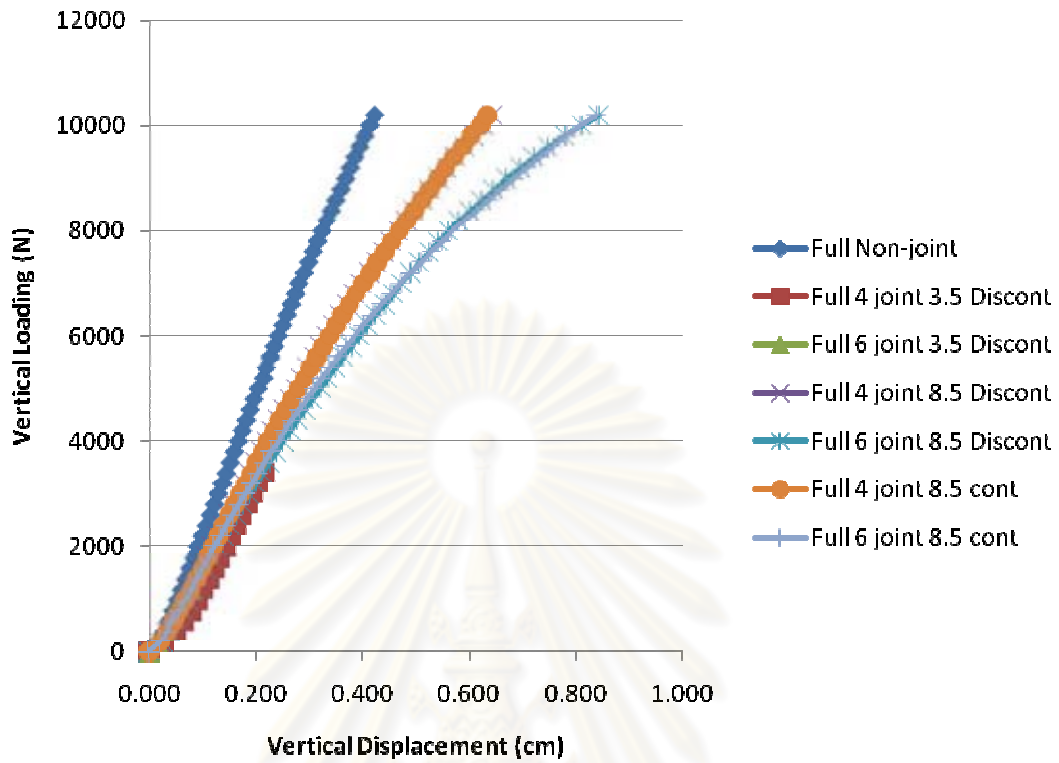
Figure 5.9: Vertical Displacement and vertical Loading of full section
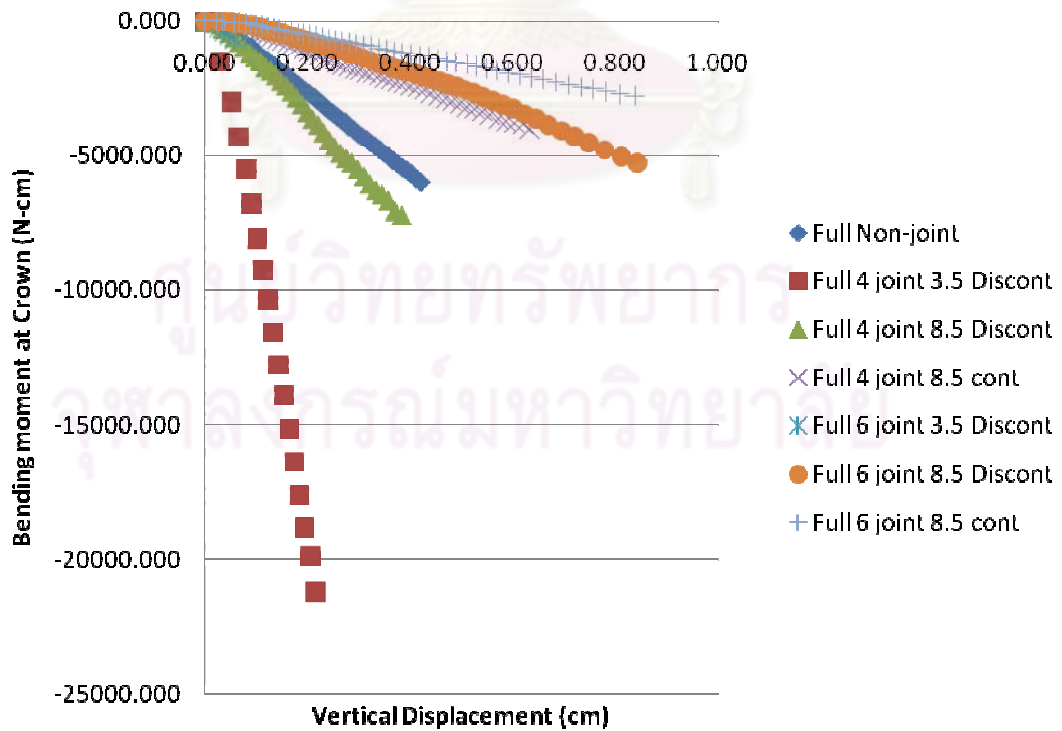
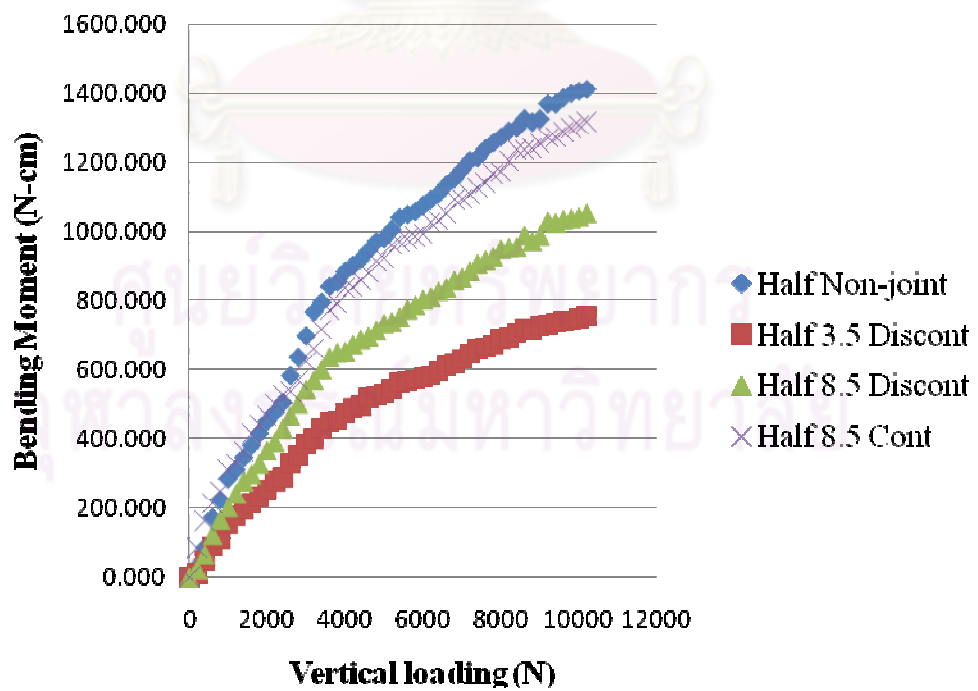Figure 5.10: Vertical Displacement VS Moment at crown of full section
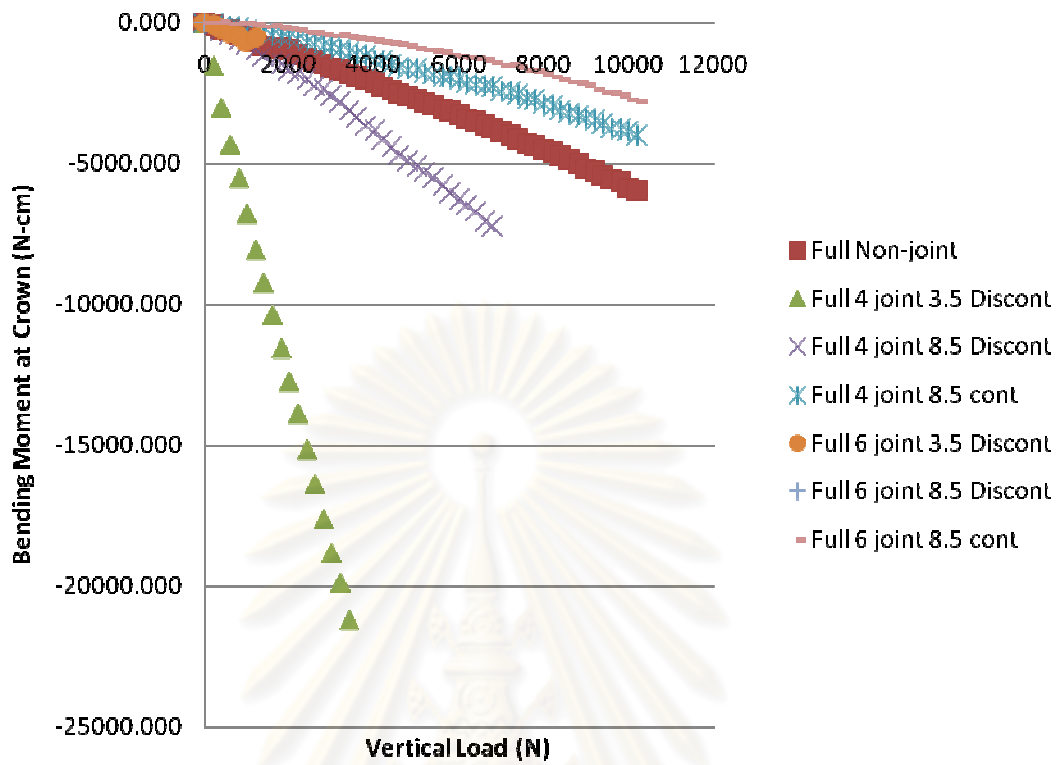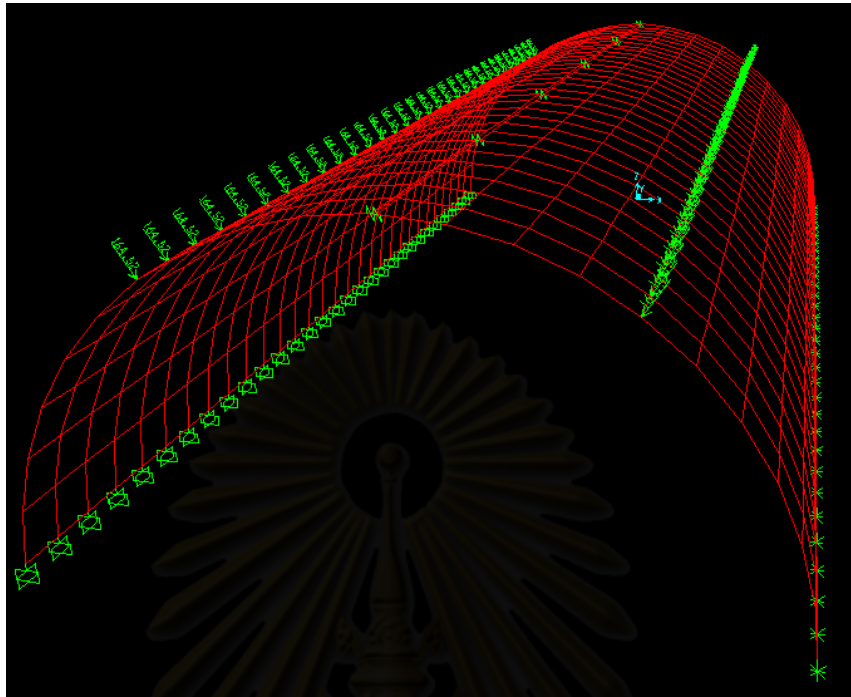
Figure 5.11: Vertical loading VS Moment at crown of full section
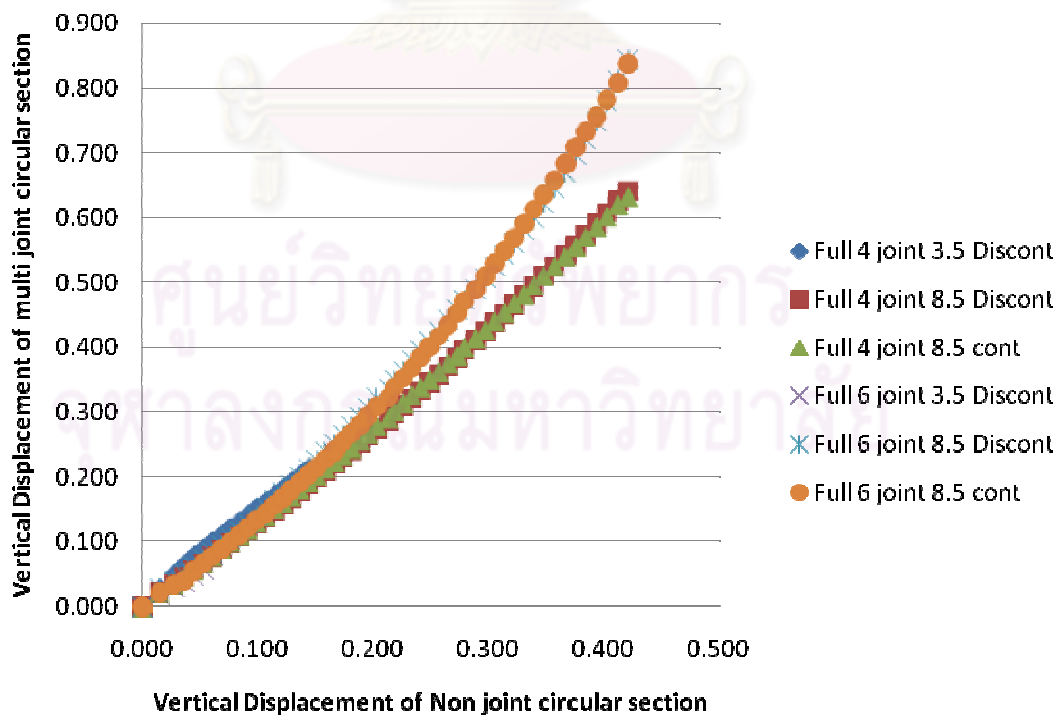
Figure 5.12: Relationship of displacement in difference full section
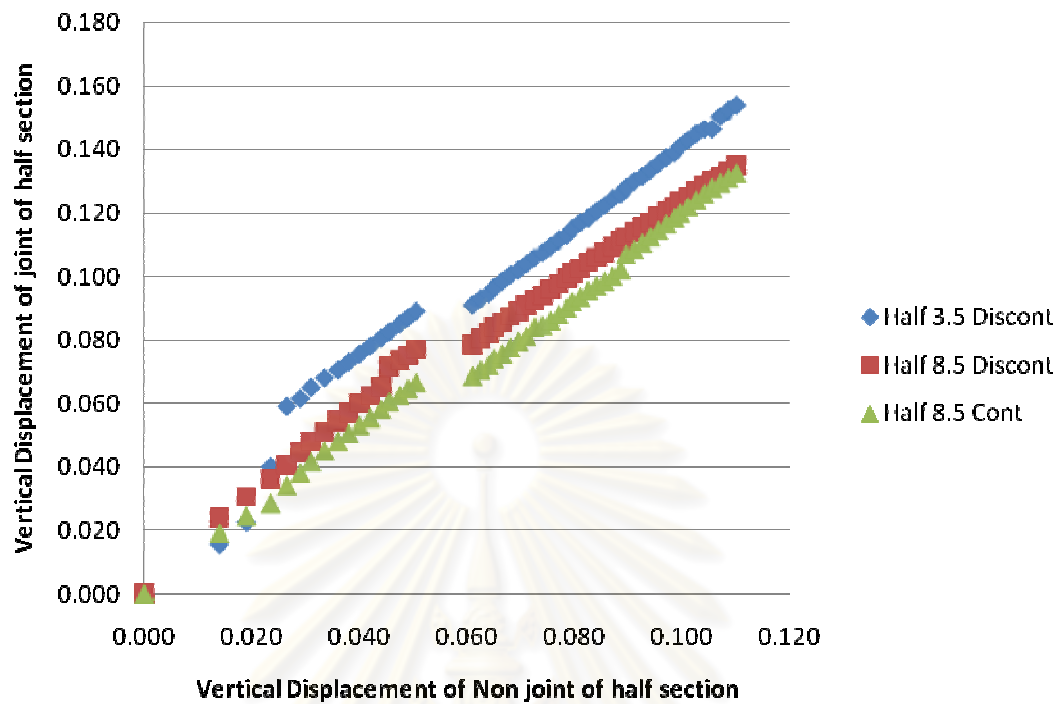
Figure 5.13: Relationship of displacment in difference half section
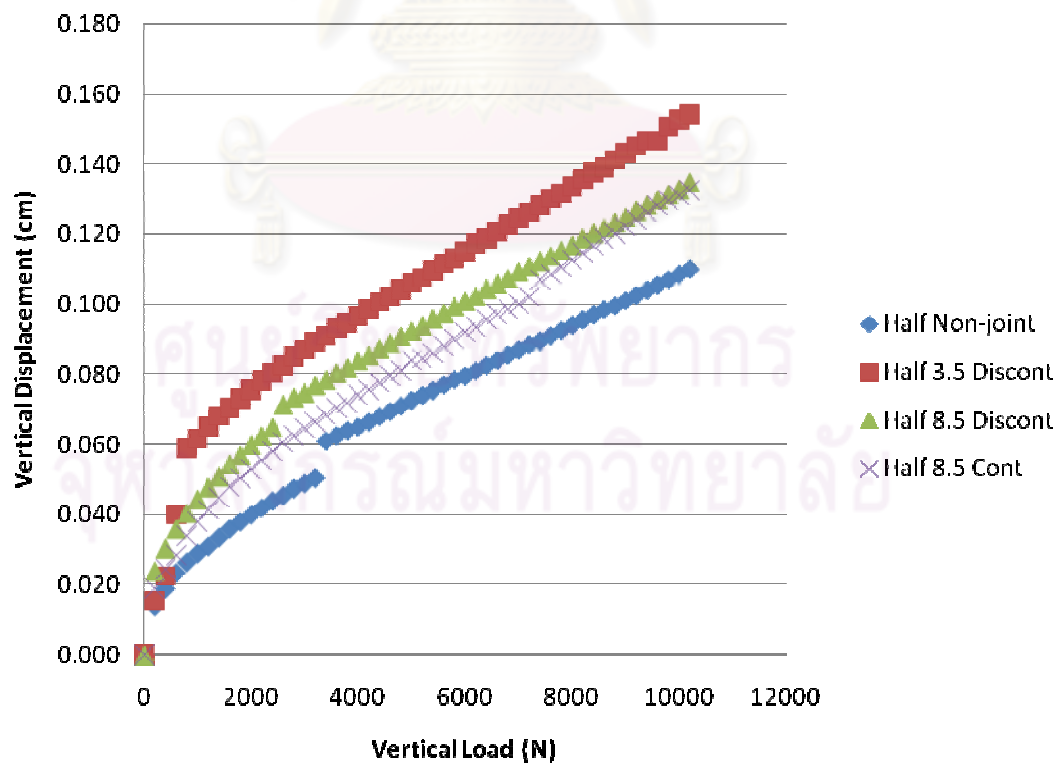
Figure 5.14: Vertical Displacement and Vertical Loading of half section
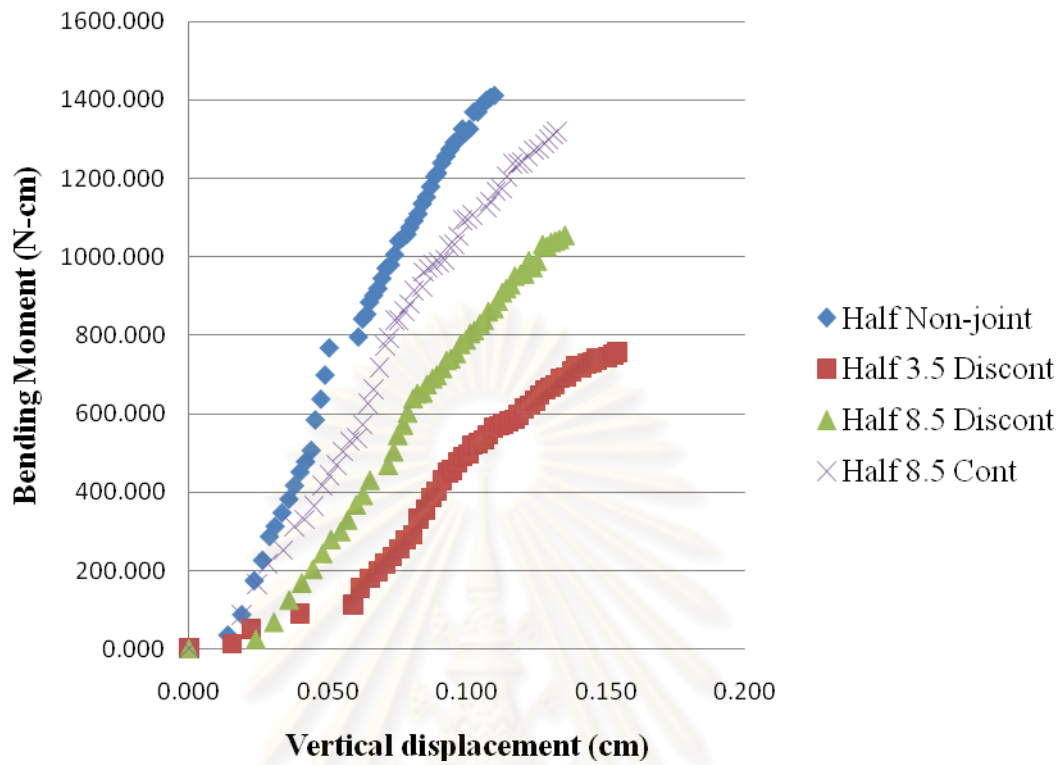
Figure 5.15: Displacement VS Moment at crown of half section

Figure 5.16: Vertical loading VS Moment at crown of half section

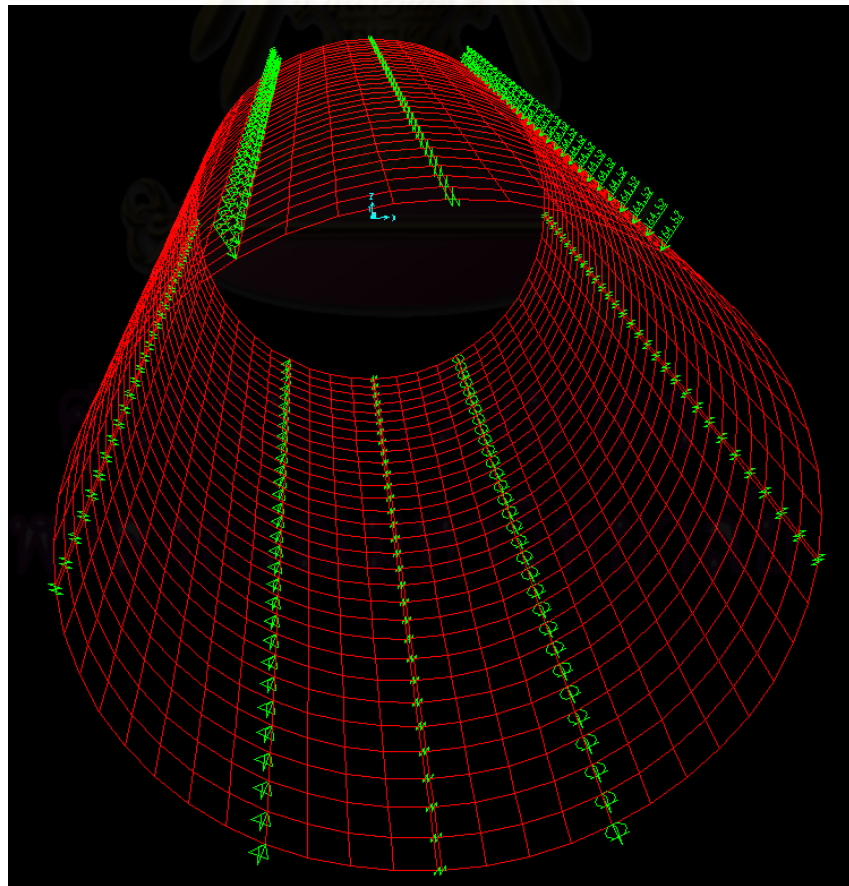Figure 5.17: Numerical model for half section of plastic model

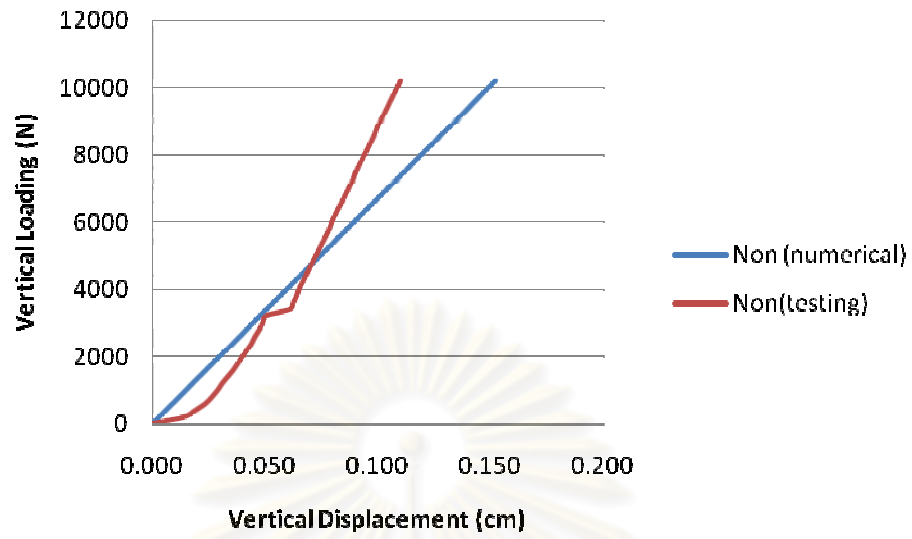Figure 5.18: Numerical model for full section of plastic model

Figure 5.19: Vertical Displacement VS Vertical loading at crown of half section
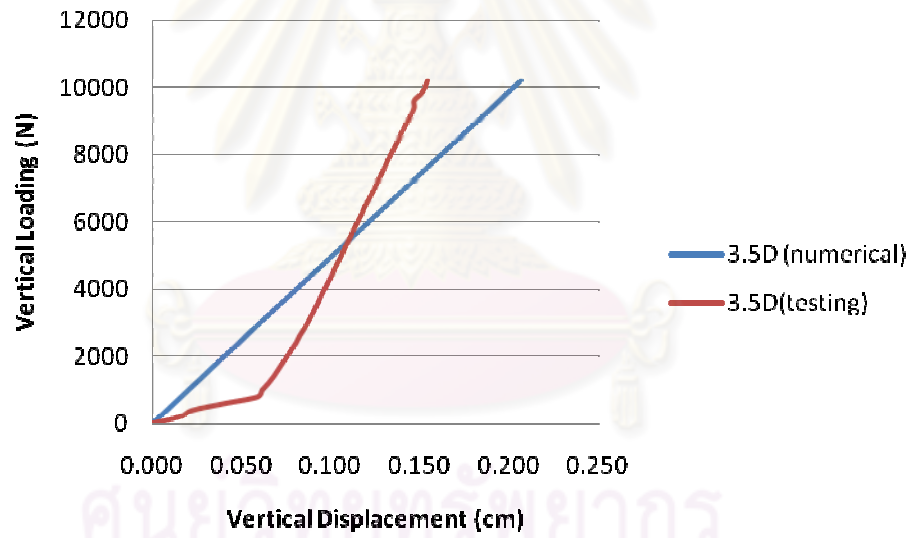

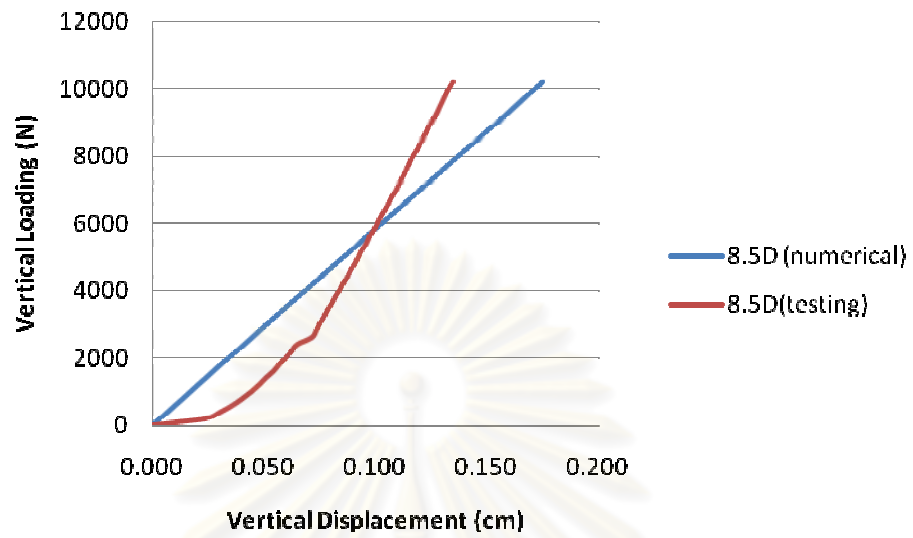Figure 5.20: Vertical Displacement VS Vertical loading at crown of half section

Figure 5.21: Vertical Displacement VS Vertical loading at crown of half section

Figure 5.22: Vertical Displacement VS Vertical loading at crown of half section

Figure 5.23: Vertical Displacement VS Vertical loading at crown of full section
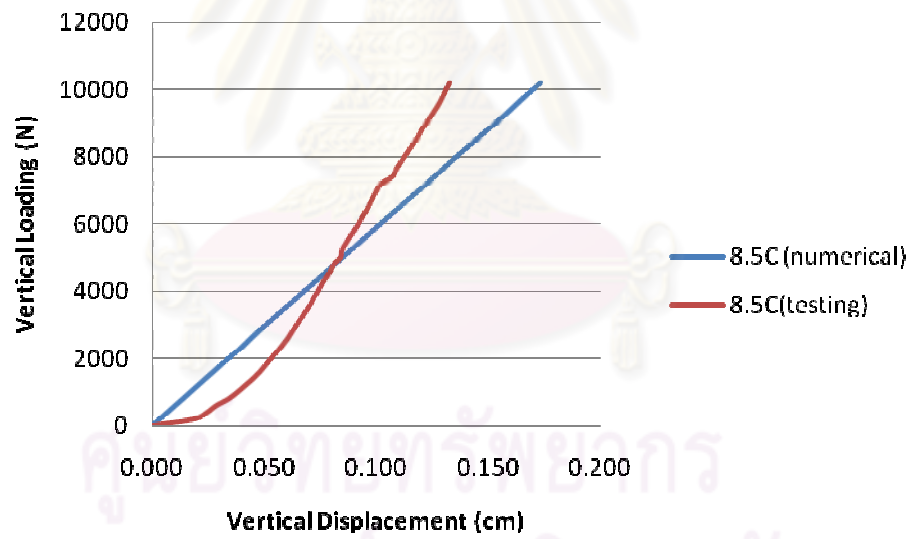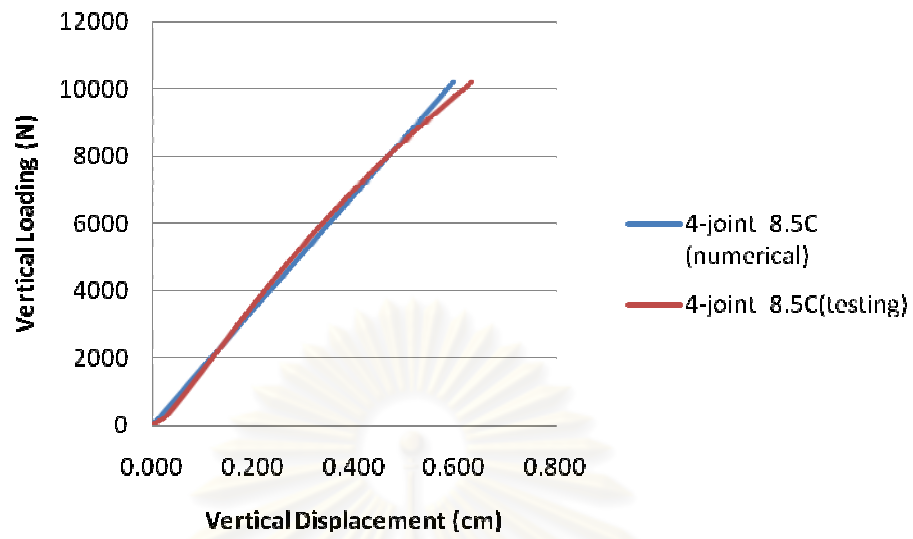

Figure 5.24: Vertical Displacement VS Vertical loading at crown of full section

Figure 5.25: Vertical Displacement VS Vertical loading at crown of full section
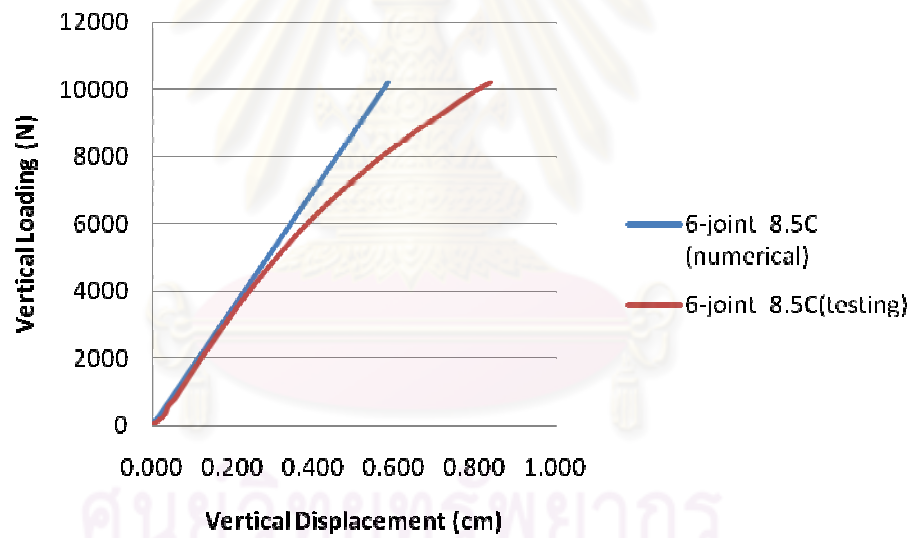
Figure 5.26: Vertical Displacement VS Vertical loading at crown of full section

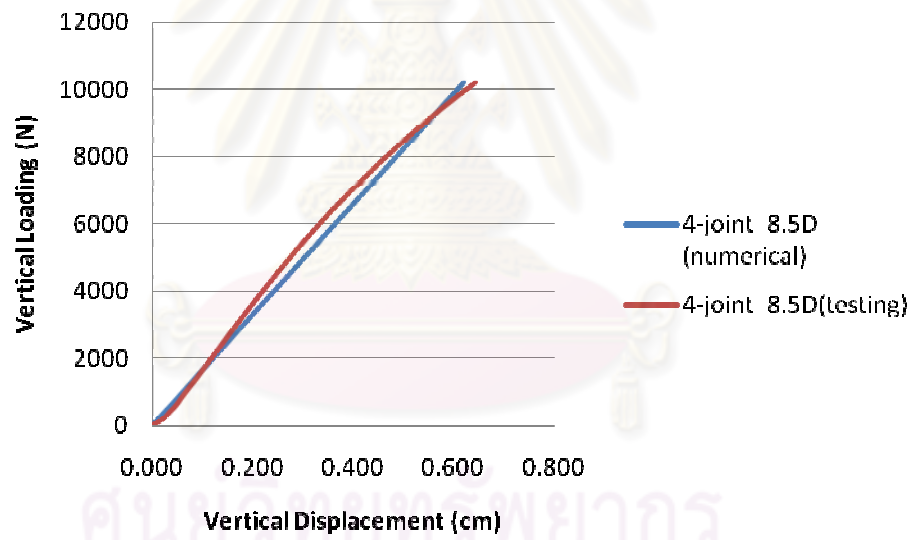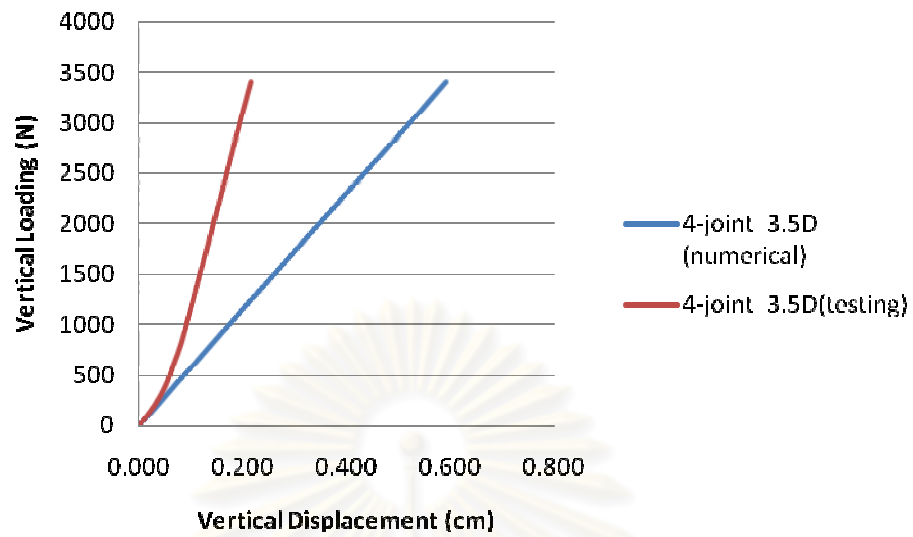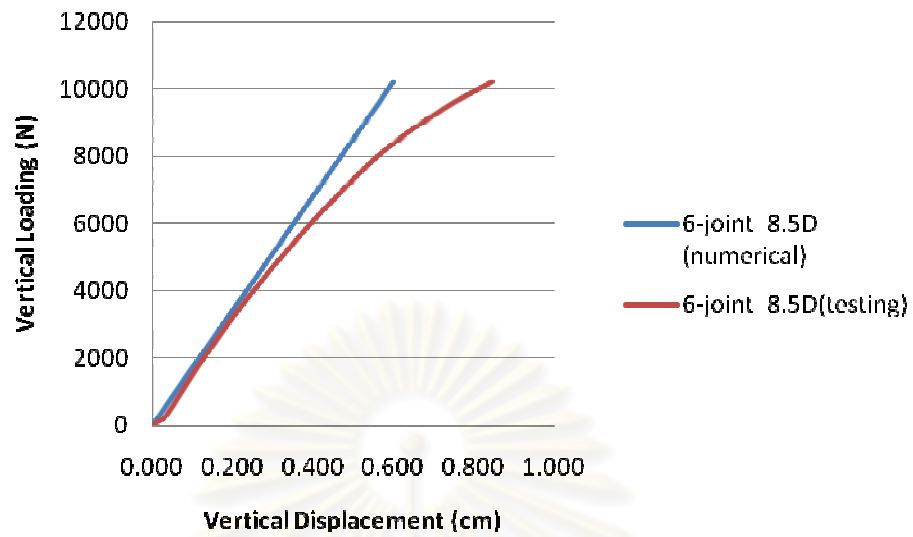Figure 5.27: Vertical Displacement VS Vertical loading at crown of full section
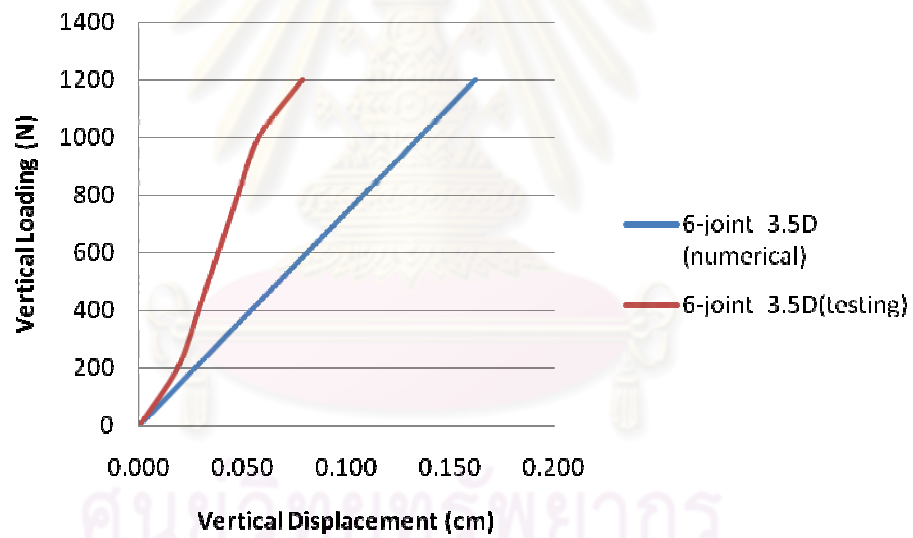
Figure 5.28: Vertical Displacement VS Vertical loading at crown of full section
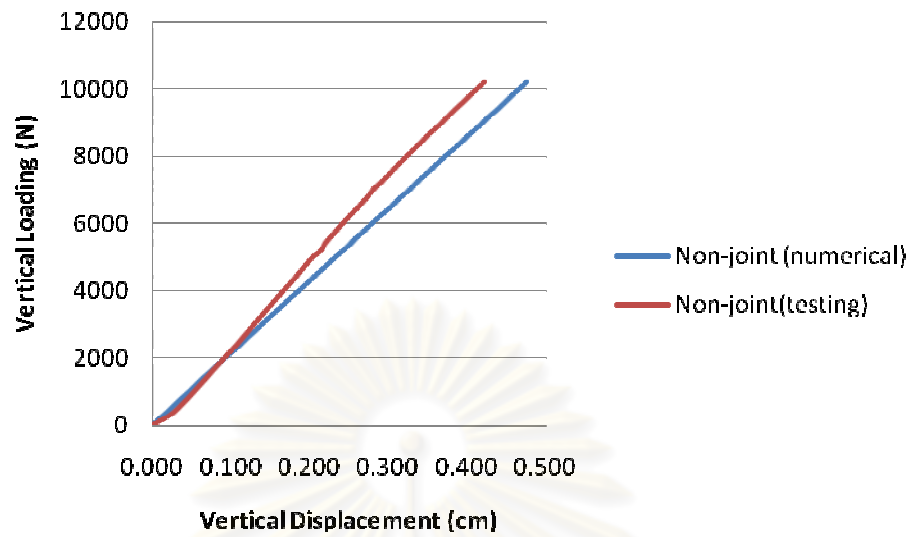
Figure 5.29: Vertical Displacement VS Vertical loading at crown of full section
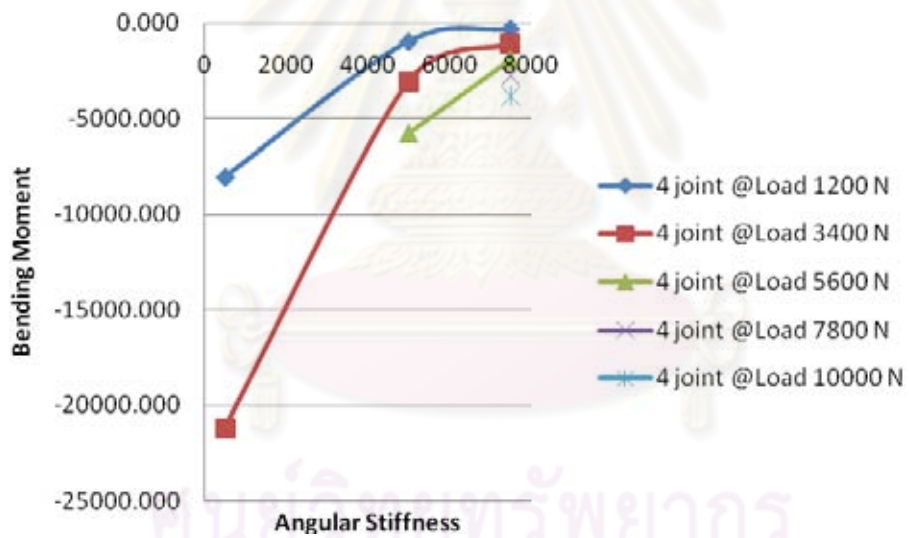
Figure 5.30: Angular Stiffness VS Bending Moment at crown of full section
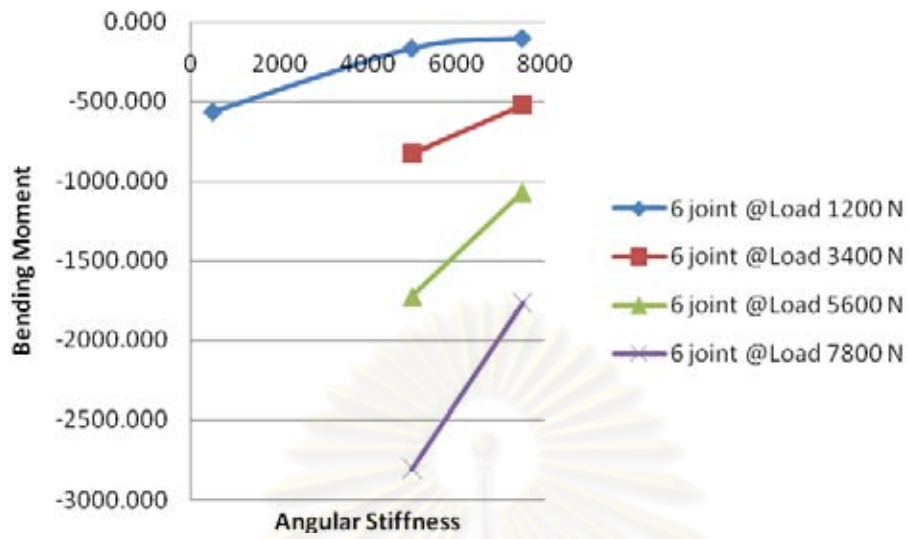
Figure 5.31: Angular Stiffness VS Bending Moment at crown of full section
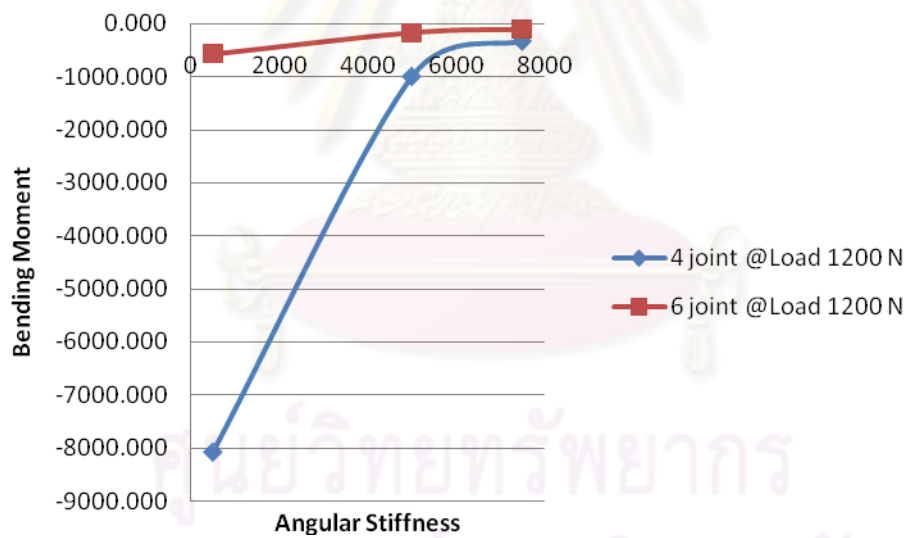
Figure 5.32: Angular Stiffness VS Bending Moment at crown of full section
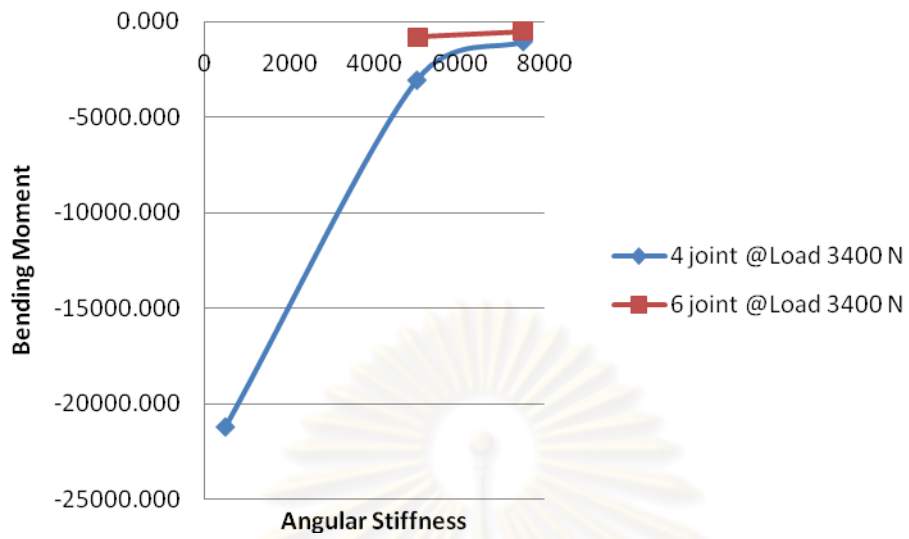
Figure 5.33: Angular Stiffness VS Bending Moment at crown of full section

Figure 5.34: Angular Stiffness VS Bending Moment at crown of full section

$\gamma = 25 \, KN/m^3$
$D = 4 \, m$
$\lambda = 0.5$
$k = 20000 \, KN/m^3$

$H = 20 \, m$
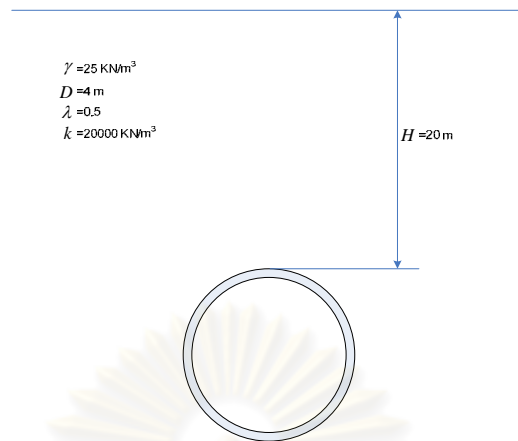
Figure 5.35: The basis stratum conditions of calculation

CHAPTER VI

CONCLUSIONS AND RECOMMENDATIONS

6.1 Conclusions

This study presents behavior of a segmental joint tunnel in radius direction that should affect the whole tunnel structure's behavior. The behavior is determined by the number of segments, segmental joint strength, and soil subgrade modulus that carry characteristics of a seg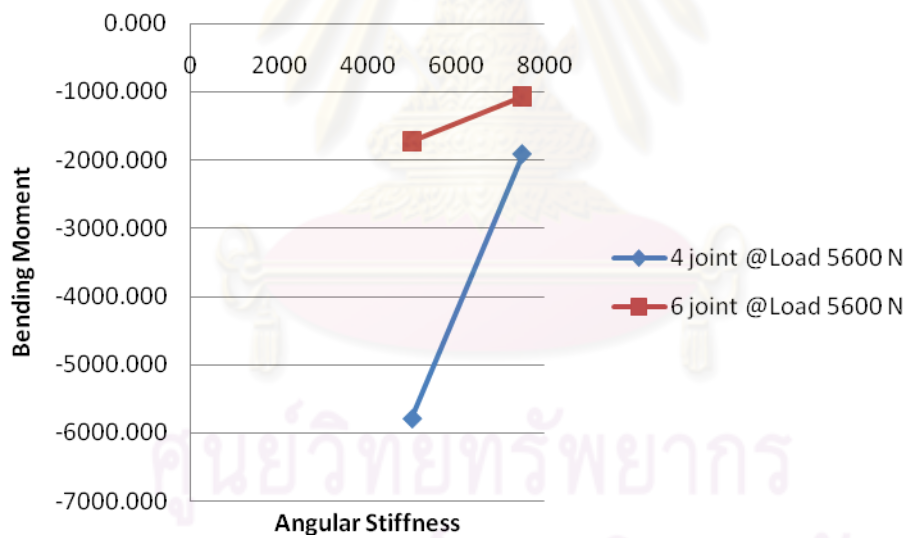mental tunnel. The proposed behavior employs numerical analysis, half-section and full-scale tunnel testing, and full section of a one-fortieth plastic specimen tested to study the mechanism. From observing behavior of a segmental joint on experimental testing, each joint can be rotated but translation of each segment is minimal. Therefore, a joint should be represented by an angular spring with an angular joint stiffness that allows each joint to be rotated with no translation. Henceforth, the results are compared for experimental and numerical methods to verify the assumption. Moreover, the numerical results suggest a tendency of reduced segmental joint factor that affects the whole tunnel structure. The following conclusions can thus be drawn based on the results of these analyses.

- The present solution method is based on linear elastic material which is dominates the design assumption. In additional, this method can fix unpredictable underground behavior.
- Segmental joint strength and tunnel size are mainly affected by bending moment transfer between joints and segments. Additionally, maximum bending moment of a lining is affected by these properties, or lining behavior flexibility of lining depending on lining stiffness.
- Based on a set of numerical and experimental tests, it was found that the practical range of angular joint stiffness was between 1,000 - 3,000 kN/rad.

However, this experiment used a curved bolt for the segmental joint, which does not represent all types of segmental joints in underground lining.

- Jointed lining carried smaller value of maximum bending moment than the non-jointed lining because jointed lining is more flexible than non-jointed lining. However, the effect of a flexible structure shows that jointed lining has more deformation than non-jointed lining, which should be considered as a design limitation.

- Orientation of joints in a lining affects the bending moment of a lining. Hence, designs should consider the position of joints for maximum bending moment. However, real construction does not locate the maximum moment position.

- The reduction in bending moment, represented by the parameter called moment reduction factor, can be simply expressed as a function of angular joint stiffness and segment number. The reduction factor should be higher than the reduction factor of Muir Wood because Wood's reduction is based on a hinge structure.

- From full-scale testing, a segmental joint hole in a segment is a weak point of the tunnel structure and a first part of structure failure that can lead to other problems such as water leakage and instability of whole tunnel structure.

- Finite element method results shows a lower reduced maximum bending moment than other design methods.

6.2 Recommendations

- This study focused on the segmental joint, which exhibits simple behavior of a multi-segment tunnel. Further research should be conducted to evaluate the specific type of each segmental joint connection.

- In this research, full-scale testing of a full tunnel section is not considered because of budget limitations. Therefore, further studies should focus on behavior in real soil conditions.

- The plastic specimen is very small and so test connections can be not interpret the real failure behavior of a segmental joint. Therefore, new research of a full-scale tunnel section should be considered.

One shortcoming of the plastic model and two-point loading method is an unexplained real mechanism of the segmental joint which occurs underground because of different assembly methods.

REFERENCES

A. A. Stamos, D. E. Beskos, 3-D seismic response analysis of long lined tunnels in half-space, **Soil Dynamics and Earthquake Engineering**, 1996 15, pp. 111-118.

Ariiumi, T., Okadome, K., Nagaya, J., 1998. Results and analysis on site measurement of load acting on the shield tunnel (in Japanese). **Proc. Tunnel Engineering JSCE 8**, pp 367-372.

Balvant Rajani and Solomon Tesfamariam, Uncoupled axial, flexural, and circumferential pipe-soil interaction analyses of partially supported jointed water mains, **Canadian Geotechnical Journal**, 2004 41, pp 997-1010.

Burns, J.Q., Richard, R.M., Attenuation of stresses for buried cylinders. In: Proceedings, **Symposium on Soil-Structure Interaction**, Tucson, 1964, pp. 833-858.

Burns, J.Q., Richard, R.M., Attenuation of stresses for buried cylinders. In: Proceedins, **Symposium on Soil-Structure Interaction**, Tucson, 1964, pp. 833-858.

Engelbreth, K., Correspondence on morgan, **Geotechnique 11**, 1961, No. 3, pp. 246-248.

George P. Kouretizs, George D. Bouckovalas, Charis J. Gantes, 3-D shell analysis of cylindrical underground structures under seismic shear (S) wave action, **Soil Dynamics and Earthquake Engineering**, 2006 26, pp 909-921.

Guidelines for the design of shield tunnel lining, **Tunnelling and Underground Space Technology**, Volume 15, No 3, pp 303-331.

Harry G. Harris, Gajanan M. Sabnis, **Structural modeling and experimental techniques**, CRC Press, New York, 1999.

Hoeg, K., Stresses against underground structural cylinders. **Journal of the Soil Mechanics and Foundation Division**, 1968, 94 (4), pp 833-858.

Hoeg, K., Stresses against underground structural cylinders. **Journal of the Soil Mechanics and Foundation Division**, 1968, 94 (4), pp 833-858.

Iftimie, T. 1994. Prefabricated lining, conceptional analysis and comparative studies for optimal solution. **Proc. of the ITA International Congress "Tunnelling and Ground Conditions"**, April 1994, Cairo, Egypt, pp 339-346. Rotterdam: Balkema.

Japanese Society of Civil Engineers., The design and construction of underground structures, **Japanese Society of Civil Engineers**, Tokyo, 1977. (In Japanese.)

Joseph W. Tedesco, William G. McDougal, C. Allen Ross, **Structural dynamics: theory and applications**, Addison Wesley Longman, Inc, 1999.

Kazuo Konagai, Dae-Sang Kim, Simple evaluation of the effect of seismic isolation by covering a tunnel with a thin flexible material, **Soil Dynamics and Earthquake Engineering**, 2001, 21, pp 287-295.

Koyama, Y., 2000. Study on the improvement of design method of segments for shield-driven tunnels (in Japanese). **RTRI Report: Special No. 33**. RTRI.

Koyama, Y., and Nishimura, T., Design of lining segment of shield tunnel using a beam-spring model. **Quarterly Report of RTRI (Railway Technical Research Institute, Japan)**, 39(1), 1998, pp 23-27.

Liu, J.H., and Hou, X.Y., **Shield-driven tunnels**., China Railway press, Beijing, China, 1991, pp 152-303. (In Chinese)

Mohammad C. Pakbaz, Akbar Yareevand, 2-D analysis of circular tunnel against earthquake loading, **Tunnelling and Underground Space Technology**, 2005, 20, pp 411-417.

Morgan, H.D., A contribution to the analysis of stress in a circular tunnel. **Geotechnique**, 1961, No 11, pp 37-46.

Muir Wood, A. M., Proc. VIIth Conference of Int. Soc. Of soil Mechanics and Foundation Engineering, Mexico 3, pp. 363-365, 1969.

Muir Wood, A. M., Soft ground tunneling. **Technology and Potential of tunnelling**, Jahannesburg, 1970, 1, pp167-174, and 2, pp72-75.

Muir Wood, A. M., The circular tunnel in elastic ground. **Geotechnique**, 1975, No. 1, pp. 115-127.

Muir Wood, A. M., Tunnels for roads and motorways. **Q. Jnl Engng Geol**. 5, 1972, pp 111-126.

Muir Wood, A.M., The circular tunnel in elastic ground. **Geotechnique**, 25(1), 1975, pp 115-127.

Okamoto, S., **Introduction to Earthquake Engineering**, University of Tokyo Press, Tokyo, Japan, 1973.

P.Warnitchai, "Lessening the Vulnerability of structures in Bangkok to Impacts of Distance large earthquakes", **Asian Infrastructure Research review**, Jan 2004.

Peck, R.B. Hendron, A.J., Mohraz, B., State of the art of soft-ground tunneling. **In: Proceedings of the North American Rapid Excavation and Tunneling Conference**, Chicago, IL, 1972, pp. 259-286.

Peck, R.B., Deep excavations and tunneling in soft ground. In : **Proceedings of the Seventh International Conference on Soil Mechanics and Foundation Engineering**, Mexico City, State-of-the-Art, 1969, pp.225-290.

Peck, R.B., Deep excavations and tunneling in soft ground. In: **Proceedings of the Seventh International Conference on Soil Mechanics and Foundation Engineering**, Mexico City, State-of-the-Art, 1969, pp. 225-290.

Peck, R.B., Hendron, A.J., Mohraz, B., State of the art of soft-ground tunneling. **In: Proceedings of the North American Rapid Excavation and Tunneling Conference**, Chicago, IL, 1972, pp. 259-286.

Railway Technical Research Institute (RTRI), Design Standard for Railway Structures (Shield-Driven Tunnel) (in Japanese). Maruzen, 1997, pp. 47-61.

Reynold King Watkins, Loren Runar Anderson, **Structural mechanics of buried pipes**, CRC Press, New York, 2000.

Schmid, H., **Statische problem des Tunnel-und Druckstollenbaues**. Berlin: Springer., 1926, (Engl. Trans. US Bureau of Reclamn. Tech. Memo. 262, 1931).

Steven L. Kramer, **Geotechnical Earthquake Engineering**, Prentice-Hall,Inc, 1996.

Wang, J.-N., Seismic **Design of tunnels: A state-of-the-Art Approach, Monograph**, monograph 7. Parsons, Brinckerhoff, Quade and Douglas Inc, New York, 1993.

Wang, J.-N., **Seismic Design of tunnels: A state-of-the-Art Approach**, Monograph, monograph 7. Parsons, Brinckerhoff, Quade and Douglas Inc, New York., 1993.

Yokinori Koyama, Present status and technology of shield tunneling method in Japan, **Tunnelling and Underground Space Technology**, 2003, No 18, pp 145-159.

Youssef M.A. Hashash, Duhee Park, John I.-Chiang Yao, Ovaling deformations of circular tunnels under seismic loading, an update on seismic design and analysis of underground structures. **Tunnelling and Underground Space Technology**, 2005, 20, pp 435-441.

Zhoung Xiaochun, Zhu Wei, Huang Zhengrong, Han Yuewang, Effect of joint structure on joint stiffness for shield tunnel lining. **Tunneling and Underground Space Technology**, 2006, 21, pp.406-407.

APPENDIX

Appendix

Compare result between laboratory testing and numerical testing to find angular stiffness

Load (N)	Half Non-joint		Half 3.5 Discont		Half 8.5 Discont		Half 8.5 Cont	
	Virtical displacement(cm)	Angular Stiffness (N-cm)	Virtical displacement(cm)	Angular Stiffness = 500 (N-rad)	Virtical displacement(cm)	Angular Stiffness = 5000 (N-rad)	Virtical displacement(cm)	Angular Stiffness = 7500 (N-rad)
0	0.000	inf	0.000	0	0.000	0	0.000	0
1000	0.029	inf	0.062	0.014	0.045	0.015	0.038	0.013
2000	0.040	inf	0.076	0.032	0.060	0.025	0.053	0.026
3000	0.049	inf	0.087	0.046	0.075	0.041	0.065	0.039
4000	0.065	inf	0.097	0.06	0.084	0.055	0.074	0.052
5000	0.073	inf	0.106	0.074	0.093	0.068	0.084	0.066
6000	0.080	inf	0.115	0.092	0.101	0.082	0.092	0.079
7000	0.087	inf	0.125	0.11	0.110	0.096	0.100	0.092
8000	0.094	inf	0.134	0.124	0.117	0.115	0.113	0.105
9000	0.101	inf	0.143	0.14	0.125	0.122	0.122	0.118
10000	0.109	Inf	0.153	0.154	0.133	0.133	0.131	0.131

Compare result between laboratory testing and numerical testing. (1/3)

	Vertical Displacement (linear elastic model)						Vertical Displacement (plastic model testing)						
Load	Non joint	4j_8.5C	4j_8.5D	4j_3.5D	6j_8.5C	6j_8.5D	6j_3.5D	Non joint	4j_8.5C	4j_8.5D	4j_3.5D	6j_8.5C	6j_8.5D	6j_3.5D
0	0.000	0.000	0.000	0.000	0.000	0.000	0.000	0.000	0.000	0.000	0.000	0.000	0.000	0.000
200	0.009	0.012	0.012	0.035	0.011	0.012	0.027	0.016	0.023	0.022	0.030	0.022	0.029	0.019
400	0.019	0.023	0.024	0.069	0.023	0.024	0.054	0.028	0.035	0.034	0.052	0.034	0.041	0.029
600	0.028	0.035	0.037	0.104	0.034	0.035	0.081	0.037	0.046	0.047	0.066	0.040	0.052	0.038
800	0.037	0.047	0.049	0.139	0.046	0.047	0.108	0.045	0.057	0.057	0.080	0.056	0.063	0.048
1000	0.047	0.059	0.061	0.174	0.057	0.059	0.135	0.053	0.068	0.067	0.091	0.067	0.074	0.058
1200	0.056	0.070	0.073	0.208	0.069	0.071	0.162	0.061	0.079	0.077	0.102	0.078	0.085	0.079
1400	0.065	0.082	0.085	0.243	0.080	0.082	0.189	0.069	0.089	0.088	0.113	0.089	0.096	
1600	0.075	0.094	0.097	0.278	0.091	0.094	0.216	0.077	0.100	0.098	0.123	0.100	0.107	
1800	0.084	0.105	0.110	0.312	0.103	0.106	0.244	0.085	0.110	0.108	0.134	0.111	0.118	
2000	0.093	0.117	0.122	0.347	0.114	0.118	0.271	0.092	0.120	0.118	0.144	0.123	0.129	
2200	0.103	0.129	0.134	0.382	0.126	0.129	0.298	0.100	0.130	0.128	0.154	0.134	0.141	
2400	0.112	0.140	0.146	0.416	0.137	0.141	0.325	0.108	0.140	0.138	0.164	0.145	0.152	
2600	0.121	0.152	0.158	0.451	0.149	0.153	0.352	0.115	0.151	0.148	0.174	0.157	0.164	
2800	0.131	0.164	0.170	0.486	0.160	0.165	0.379	0.123	0.161	0.158	0.184	0.169	0.176	
3000	0.140	0.176	0.183	0.521	0.171	0.176	0.406	0.130	0.171	0.169	0.195	0.181	0.188	
3200	0.149	0.187	0.195	0.555	0.183	0.188	0.433	0.137	0.181	0.179	0.205	0.192	0.201	

Compare result between laboratory testing and numerical testing. (Continuous)(2/3)

Load	Vertical Displacement (linear elastic model)							Vertical Displacement (plastic model testing)						
	Non joint	4j_8.5C	4j_8.5D	4j_3.5D	6j_8.5C	6j_8.5D	6j_3.5D	Non joint	4j_8.5C	4j_8.5D	4j_3.5D	6j_8.5C	6j_8.5D	6j_3.5D
3400	0.159	0.199	0.207	0.590	0.194	0.200	0.460	0.145	0.192	0.189	0.216	0.204	0.214	
3600	0.168	0.211	0.219	0.625	0.206	0.212	0.487	0.152	0.202	0.200		0.216	0.227	
3800	0.177	0.222	0.231	0.659	0.217	0.224	0.514	0.160	0.213	0.210		0.229	0.239	
4000	0.187	0.234	0.244	0.694	0.229	0.235	0.541	0.167	0.224	0.221		0.242	0.253	
4200	0.196	0.246	0.256	0.729	0.240	0.247	0.568	0.175	0.234	0.231		0.255	0.266	
4400	0.205	0.258	0.268	0.764	0.251	0.259	0.595	0.182	0.245	0.242		0.268	0.279	
4600	0.215	0.269	0.280	0.798	0.263	0.271	0.622	0.190	0.257	0.253		0.281	0.293	
4800	0.224	0.281	0.292	0.833	0.274	0.282	0.649	0.197	0.268	0.264		0.295	0.307	
5000	0.233	0.293	0.304	0.868	0.286	0.294	0.676	0.204	0.280	0.275		0.310	0.322	
5200	0.243	0.304	0.317	0.902	0.297	0.306	0.704	0.215	0.291	0.286		0.323	0.336	
5400	0.252	0.316	0.329	0.937	0.309	0.318	0.731	0.219	0.303	0.298		0.338	0.350	
5600	0.261	0.328	0.341	0.972	0.320	0.329	0.758	0.227	0.314	0.310		0.353	0.365	
5800	0.271	0.339	0.353	1.006	0.332	0.341	0.785	0.235	0.326	0.322		0.369	0.380	
6000	0.280	0.351	0.365	1.041	0.343	0.353	0.812	0.242	0.339	0.334		0.385	0.395	
6200	0.289	0.363	0.377	1.076	0.354	0.365	0.839	0.250	0.351	0.346		0.401	0.410	
6400	0.299	0.375	0.390	1.111	0.366	0.376	0.866	0.258	0.363	0.358		0.418	0.425	
6600	0.308	0.386	0.402	1.145	0.377	0.388	0.893	0.266	0.375	0.371		0.435	0.443	

Compare result between laboratory testing and numerical testing. (Continuous)(3/3)

Load	Vertical Displacement (linear elastic model)							Vertical Displacement (plastic model testing)						
	Non joint	4j_8.5C	4j_8.5D	4j_3.5D	6j_8.5C	6j_8.5D	6j_3.5D	Non joint	4j_8.5C	4j_8.5D	4j_3.5D	6j_8.5C	6j_8.5D	6j_3.5D
6800	0.317	0.398	0.414	1.180	0.389	0.400	0.920	0.274	0.388	0.384		0.453	0.459	
7000	0.327	0.410	0.426	1.215	0.400	0.412	0.947	0.280	0.401	0.396		0.471	0.474	
7200	0.336	0.421	0.438	1.249	0.412	0.424	0.974	0.290	0.414	0.412		0.489	0.491	
7400	0.345	0.433	0.451	1.284	0.423	0.435	1.001	0.299	0.427	0.425		0.510	0.507	
7600	0.355	0.445	0.463	1.319	0.434	0.447	1.028	0.307	0.441	0.439		0.529	0.525	
7800	0.364	0.457	0.475	1.354	0.446	0.459	1.055	0.315	0.454	0.452		0.549	0.543	
8000	0.373	0.468	0.487	1.388	0.457	0.471	1.082	0.324	0.469	0.466		0.569	0.561	
8200	0.383	0.480	0.499	1.423	0.469	0.482	1.109	0.332	0.482	0.481		0.591	0.581	
8400	0.392	0.492	0.511	1.458	0.480	0.494	1.136	0.341	0.496	0.495		0.614	0.601	
8600	0.401	0.503	0.524	1.492	0.492	0.506	1.164	0.349	0.511	0.511		0.636	0.623	
8800	0.411	0.515	0.536	1.527	0.503	0.518	1.191	0.359	0.525	0.525		0.658	0.646	
9000	0.420	0.527	0.548	1.562	0.514	0.529	1.218	0.368	0.540	0.542		0.683	0.670	
9200	0.429	0.538	0.560	1.596	0.526	0.541	1.245	0.376	0.555	0.558		0.709	0.697	
9400	0.439	0.550	0.572	1.631	0.537	0.553	1.272	0.385	0.571	0.573		0.733	0.722	
9600	0.448	0.562	0.584	1.666	0.549	0.565	1.299	0.394	0.587	0.591		0.757	0.749	
9800	0.457	0.574	0.597	1.701	0.560	0.576	1.326	0.403	0.603	0.608		0.782	0.780	
10000	0.467	0.585	0.609	1.735	0.572	0.588	1.353	0.413	0.620	0.626		0.808	0.813	
10200	0.476	0.597	0.621	1.770	0.583	0.600	1.380	0.422	0.633	0.643		0.838	0.844	

Load (N)	Number of joint	Angular Stiffness	Vertical displacement	Moment Crown	Moment Springline
1200	Non-joint	inf	0.061	-693.525	797.554
3400			0.145	-1820.503	2132.589
5600			0.227	-3042.840	3623.667
7800			0.315	-4377.876	5314.134
10000			0.413	-5860.285	7316.687
1200	4	500	0.102	-8079.565	1072.004
3400			0.216	-21204.523	3441.387
5600					
7800					
10000					
1200		5000	0.077	-988.273	1092.302
3400			0.189	-3094.855	3207.552
5600			0.310	-5790.933	5981.652
7800					
10000					
1200		7500	0.079	-320.755	572.158
3400			0.192	-1083.633	1837.841
5600			0.314	-1907.193	3138.200
7800			0.454	-2765.430	4395.214
10000			0.620	-3831.725	6068.343
1200	6	500	0.079	-565.399	398.777
3400					
5600					
7800					
10000					
1200		5000	0.085	-167.602	866.906
3400			0.214	-826.450	2566.042
5600			0.365	-1722.253	4143.811
7800			0.543	-2808.776	5137.863
10000			0.813	-5039.614	7172.203
1200		7500	0.078	-104.029	1022.949
3400			0.204	-520.144	3207.552
5600			0.353	-1066.294	5574.206
7800			0.549	-1759.819	8070.896
10000			0.808	-2722.085	9735.355

Plastic modeling testing result

Physical property of Plastic Material Testing. (1/4)

Load(N)	stress(N/cm2)	Elongation(mm)	strain(calculation)	strain(measurment)
0	0	0	0.00000	0
100	175	0.08	0.00053	0.00017
200	351	0.18	0.00120	0.00048
300	526	0.28	0.00187	0.00093
400	702	0.39	0.00260	0.00152
500	877	0.5	0.00333	0.00199
600	1053	0.62	0.00413	0.00259
700	1228	0.73	0.00487	0.00305
800	1404	0.85	0.00567	0.00367
900	1579	0.97	0.00647	0.00413
1000	1754	1.09	0.00727	0.00477
1100	1930	1.21	0.00807	0.00526
1200	2105	1.34	0.00893	0.0059
1300	2281	1.47	0.00980	0.00655
1400	2456	1.61	0.01073	0.0072
1500	2632	1.75	0.01167	0.00803
1600	2807	1.89	0.01260	0.00868
1700	2982	2.04	0.01360	0.00936
1800	3158	2.2	0.01467	0.0102
1900	3333	2.36	0.01573	0.01105
2000	3509	2.54	0.01693	0.01194
2100	3684	2.72	0.01813	0.01301
2200	3860	2.9	0.01933	0.01393
2300	4035	3.12	0.02080	0.01525
2400	4211	3.36	0.02240	0.01659
2500	4386	3.63	0.02420	0.01817
2600	4561	3.94	0.02627	0.01979
2700	4737	4.32	0.02880	0.02249
2800	4912	4.86	0.03240	0.02587
2880	5053			

Physical property of Plastic Material Testing. (Continuous)(2/4)

Load(N)	stress(N/cm2)	Elongation(mm)	strain(calculation)	strain(measurment)
0	0	0	0.00000	0
100	175	0.05	0.00033	0.00019
200	351	0.18	0.00120	0.00072
300	526	0.3	0.00200	0.0012
400	702	0.4	0.00267	0.00168
500	877	0.5	0.00333	0.00217
600	1053	0.62	0.00413	0.00265
700	1228	0.73	0.00487	0.0033
800	1404	0.84	0.00560	0.0038
900	1579	0.96	0.00640	0.00447
1000	1754	1.08	0.00720	0.00498
1100	1930	1.22	0.00813	0.00569
1200	2105	1.33	0.00887	0.0062
1300	2281	1.44	0.00960	0.00691
1400	2456	1.58	0.01053	0.00761
1500	2632	1.72	0.01147	0.00832
1600	2807	1.86	0.01240	0.00904
1700	2982	2.01	0.01340	0.00976
1800	3158	2.16	0.01440	0.01068
1900	3333	2.32	0.01547	0.01162
2000	3509	2.49	0.01660	0.01279
2100	3684	2.67	0.01780	0.01381
2200	3860	2.87	0.01913	0.01527
2300	4035	3.07	0.02047	0.01634
2400	4211	3.3	0.02200	0.01789
2500	4386	3.57	0.02380	0.01975
2600	4561	3.87	0.02580	0.02195
2700	4737	4.25	0.02833	0.02477
2800	4912	4.83	0.03220	0.02971
2885	5061			

Physical property of Plastic Material Testing. (Continuous)(3/4)

Load(N)	stress(N/cm2)	Elongation(mm)	strain(calculation)	strain(measurment)
0	0	0	0.00000	0
100	175	0.05	0.00033	0.00015
200	351	0.17	0.00113	0.00065
300	526	0.27	0.00179	0.0011
400	702	0.37	0.00245	0.00157
500	877	0.47	0.00311	0.00206
600	1053	0.57	0.00377	0.00254
700	1228	0.68	0.00450	0.00302
800	1404	0.78	0.00517	0.00351
900	1579	0.89	0.00589	0.00419
1000	1754	1.01	0.00669	0.00471
1100	1930	1.14	0.00755	0.00541
1200	2105	1.27	0.00841	0.00615
1300	2281	1.41	0.00934	0.00691
1400	2456	1.56	0.01033	0.00733
1500	2632	1.72	0.01139	0.00868
1600	2807	1.89	0.01252	0.00968
1700	2982	2.09	0.01384	0.01088
1800	3158	2.28	0.01510	0.0121
1900	3333	2.49	0.01649	0.01337
2000	3509	2.73	0.01808	0.01508
2100	3684	3	0.01987	0.01685
2200	3860	3.31	0.02192	0.01892
2300	4035	3.7	0.02450	0.02184
2400	4211	4.26	0.02821	0.02599
2500	4386	5.6	0.03709	0.03884
2600	4561			0.06665

Physical property of Plastic Material Testing. (Continuous)(4/4)

Load(N)	stress(N/cm2)	Elongation(mm)	strain(calculation)	strain(measurment)
0	0	0	0.00000	0
100	175	0.07	0.00046	0.00022
200	351	0.19	0.00126	0.00059
300	526	0.31	0.00205	0.00118
400	702	0.43	0.00285	0.00163
500	877	0.54	0.00358	0.00228
600	1053	0.66	0.00437	0.00291
700	1228	0.77	0.00510	0.00338
800	1404	0.89	0.00589	0.00404
900	1579	1.01	0.00669	0.00452
1000	1754	1.13	0.00748	0.00519
1100	1930	1.26	0.00834	0.00587
1200	2105	1.39	0.00921	0.00637
1300	2281	1.53	0.01013	0.00704
1400	2456	1.67	0.01106	0.00789
1500	2632	1.81	0.01199	0.00856
1600	2807	1.96	0.01298	0.00943
1700	2982	2.11	0.01397	0.01013
1800	3158	2.27	0.01503	0.011
1900	3333	2.45	0.01623	0.01191
2000	3509	2.63	0.01742	0.01303
2100	3684	2.83	0.01874	0.01416
2200	3860	3.04	0.02013	0.01534
2300	4035	3.27	0.02166	0.01675
2400	4211	3.54	0.02344	0.01843
2500	4386	3.85	0.02550	0.02038
2600	4561	4.23	0.02801	0.02309
2700	4737	4.78	0.03166	0.02681
2800	4912	6.19	0.04099	0.03575

Biography

Author's Name: Mr. Tanan Chub-uppakarn

Birth Data: 12 August 1979   **Birth Place:** Hatyai, Songkla, Thailand

Education:

1997-2001:   Bachelor degree,B.Eng, Faculty of Civil Engineering, Prince of Songkla University, GPA 2.98

2001-2003:   Master Degree , M. Eng, Field of Structural Engineering, School of Civil Engineering, Asian Institute of Technology, GPA 3.05

2003-2004:   Intensive English Program and Non-degree program at University of Missouri – Columbia, GPA 3.33

2006-2008:   Doctor of Philosophy Degree, Ph.D Eng, Field of Geotechnical Engineering, School of Civil Engineering, Chulalongkorn University, GPA 3.64

Working Experiences:

2007:   Research in the study of number of curve bolt and curve bolt properties which effect to main structure of tunnel.

2007:   Analysis soil strength and structure of sky train parking station of addition part MRTA (Blue line).

2007: Estimation and Designed Private Home (3 stories) at Nakonsretommakat province.

2007:   Safety Inspection of Human safety in Luvata Hitachi Cable Factory, Thailand.

2005:   Designer Engineer at CEDA Co, LTD Company, Working on estimation and Designed 70th floor Condominium.

2005:   Project Engineer in a studying Rama 9 Bridge Pendel Project, IMMS Company.

2005:   Engineer at IMMS Company, LTD. Studied, checked and repaired RC-Bridge of Department of rural roads, Working on making Bridge models and analysis them.

Award and Scholarship:

2006-2008:   AUN/SEED-Net Doctoral Degree Program Scholarship.

2001-2003:   Partial Scholarship of Royal Thai Government.